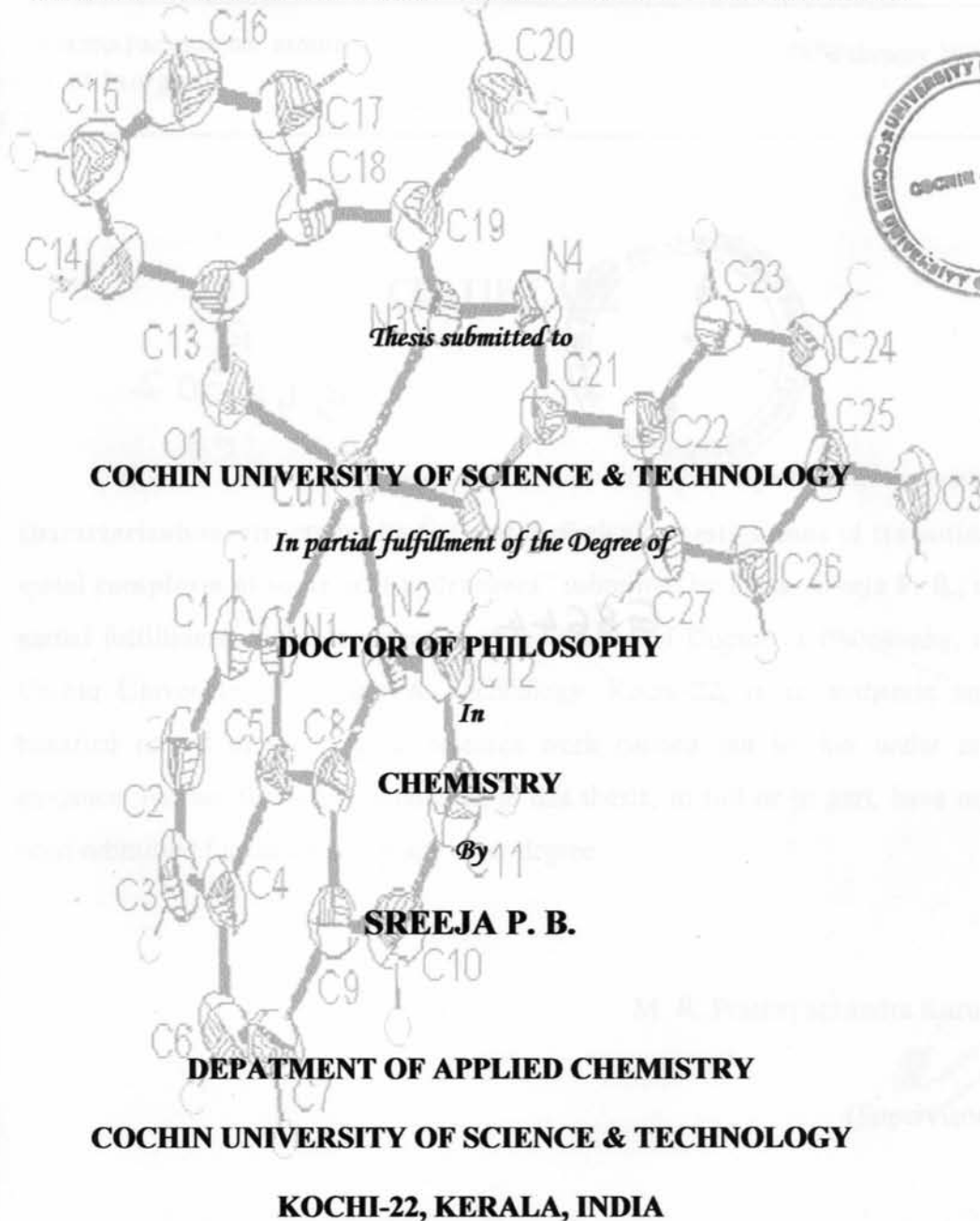


**SYNTHESIS, SPECTRAL CHARACTERIZATION, STRUCTURAL
STUDIES AND BIOLOGICAL INVESTIGATIONS OF TRANSITION
METAL COMPLEXES OF SOME ACID HYDRAZONES**



FEBRUARY 2004

Phone Off. 0484-2575804
Phone Res. 0484-2576904
Telex: 885-5019 CUIIN
Fax: 0484-2577595
Email: mrp@cusat.ac.in
mrp_k@yahoo.com

DEPARTMENT OF APPLIED CHEMISTRY
COCHIN UNIVERSITY OF SCIENCE AND TECHNOLOGY
KOCHI - 682 022, INDIA

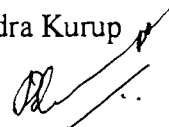
Dr. M.R. PRATHAPACHANDRA KURUP
Professor of Inorganic
Chemistry

16th February 2004

CERTIFICATE

This is to certify that the thesis entitled **“Synthesis, spectral characterization, structural studies and biological investigations of transition metal complexes of some acid hydrazones”** submitted by **Miss. Sreeja P. B.**, in partial fulfillment of the requirement of the degree of Doctor of Philosophy, to Cochin University of Science & Technology, Kochi-22, is an authentic and bonafied record of the original research work carried out by her under my guidance. Further the results embodied in this thesis, in full or in part, have not been submitted for the award of any other degree.

M. R. Prathapachandra Kurup


(Supervisor)

Chapter 1

A BRIEF INTRODUCTION TO ACID HYDRAZONES AND THEIR STRUCTURE AND BONDING NATURE TO TRANSITION METALS

| | Page No. |
|--|----------|
| 1.1 Introduction | 1 |
| 1.2 Structure, bonding and stereochemistry of the acid hydrazones | 3 |
| 1.3 Objectives and scope of the work | 6 |
| 1.4 Structural characterization techniques | 6 |
| 1.4.1. <i>Magnetic measurement</i> | 7 |
| 1.4.2. <i>Electronic spectroscopy</i> | 8 |
| 1.4.3. <i>Infrared spectroscopy</i> | 8 |
| 1.4.4. <i>EPR spectroscopy</i> | 9 |
| 1.4.5. <i>X-Ray crystallography</i> | 10 |
| 1.4.6. <i>NMR techniques</i> | 10 |
| 1.4.7. <i>Cyclic voltammetry</i> | 11 |
| 1.4.8. <i>Biological studies</i> | 12 |
| References | 14 |

Chapter 2

SYNTHESIS, SPECTRAL CHARACTERIZATION AND X-RAY STRUCTURE OF SOME ACID HYDRAZONES

| | Page No. |
|--|----------|
| 2.1 Introduction | 19 |
| 2.2 Experimental | 20 |
| 2.2.1. <i>Materials</i> | 20 |
| 2.2.2. <i>Physical measurements</i> | 20 |
| 2.2.3. <i>Syntheses</i> | 21 |
| 2.3. Result and discussion | 22 |
| 2.3.1. <i>Syntheses of the hydrazones</i> | 22 |
| 2.3.2. <i>Electronic spectral studies</i> | 23 |
| 2.3.3. <i>IR spectral studies</i> | 24 |
| 2.3.3. <i>¹H NMR spectral studies</i> | 27 |
| 2.3.5. <i>¹³C NMR and ¹H-¹³C correlation spectral studies of H₂L²</i> | 35 |
| 2.3.6. <i>X-Ray data collection, structure solution and refinement</i> | 38 |
| Concluding remarks | 42 |
| References | 43 |

Chapter 3

SYNTHESES, SPECTRAL CHARACTERIZATION, X-RAY STRUCTURE, ELECTROCHEMICAL STUDIES AND BIOLOGICAL INVESTIGATIONS OF COPPER(II) TERNARY COMPLEXES 2-HYDROXYACETOPHENONE 4-HYDROXYBENZOIC ACID HYDRAZONE AND HETEROCYCLIC BASES

| | Page No. |
|--|----------|
| 3.1 Introduction | 46 |
| 3.2 Experimental | 48 |
| 3.2.1. <i>Materials</i> | 48 |
| 3.2.2. <i>Syntheses of the complexes</i> | 48 |
| 3.2.3. <i>Physical measurements and instrumentation</i> | 49 |
| 3.2.4. <i>X-Ray data collection, structure solution and refinement</i> | 49 |
| 3.3. Results and discussion | 49 |
| 3.3.1. <i>Synthesis of copper(II) complexes</i> | 49 |
| 3.3.2. <i>EPR spectral studies</i> | 50 |
| 3.3.3. <i>Electronic spectral studies</i> | 55 |
| 3.3.4. <i>IR spectral studies</i> | 57 |
| 3.3.5. <i>Crystal structure of CuL⁴phen</i> | 62 |
| 3.3.6. <i>Biological activity studies</i> | 67 |
| 3.3.7. <i>Electrochemical studies</i> | 69 |
| Concluding remarks | 70 |
| References | 71 |

Chapter 4

SYNTHESIS, SPECTRAL CHARACTERIZATION, AND BIOLOGICAL INVESTIGATIONS OF TERNARY OXOVANADIUM(IV) COMPLEXES OF SOME ACID HYDRAZONES AND 2, 2'- BIPYRIDINE

| | Page No. | |
|-------------|--|----|
| 4.1 | Introduction | 74 |
| 4.2 | Experimental | 75 |
| | <i>4.2.1. Materials</i> | 75 |
| | <i>4.2.2. Syntheses of the complexes</i> | 75 |
| 4.3. | Results and discussion | 76 |
| | <i>4.3.1. Synthesis of oxovanadium(IV) complexes</i> | 76 |
| | <i>4.3.2. Magnetic measurements</i> | 77 |
| | <i>4.3.3. Electronic spectral analysis</i> | 77 |
| | <i>4.3.4. Electron paramagnetic resonance spectral studies</i> | 79 |
| | <i>4.3.5. Infrared spectral studies</i> | 84 |
| | <i>4.3.6. Biological activity studies</i> | 87 |
| | Concluding remarks | 88 |
| | References | 89 |

Chapter 5

SYNTHESES AND SPECTRAL CHARACTERIZATION OF MANGANESE(II) COMPLEXES OF SOME ACID HYDRAZONES

| | Page No. |
|--|----------|
| 5.1 Introduction | 91 |
| 5.2 Experimental | 92 |
| 5.2.1. <i>Materials</i> | 92 |
| 5.2.2. <i>Synthesis of Mn(HL²)₂</i> | 92 |
| 5.2.3. <i>Synthesis of MnL³₂</i> | 93 |
| 5.2.4. <i>Syntheses of Mn(HL⁵)₂ and Mn(HL⁶)₂</i> | 94 |
| 5.3. Results and discussion | 94 |
| 5.3.1. <i>Synthesis of manganese(II) complexes</i> | 94 |
| 5.3.2. <i>Magnetic moment measurements</i> | 95 |
| 5.3.3. <i>Electron paramagnetic resonance spectral studies</i> | 96 |
| 5.3.4. <i>Infrared spectral studies</i> | 98 |
| 5.3.5. <i>Electronic spectral analyses</i> | 101 |
| 5.3.6. <i>Biological activity studies</i> | 102 |
| Concluding remarks | 102 |
| References | 103 |

Chapter 6

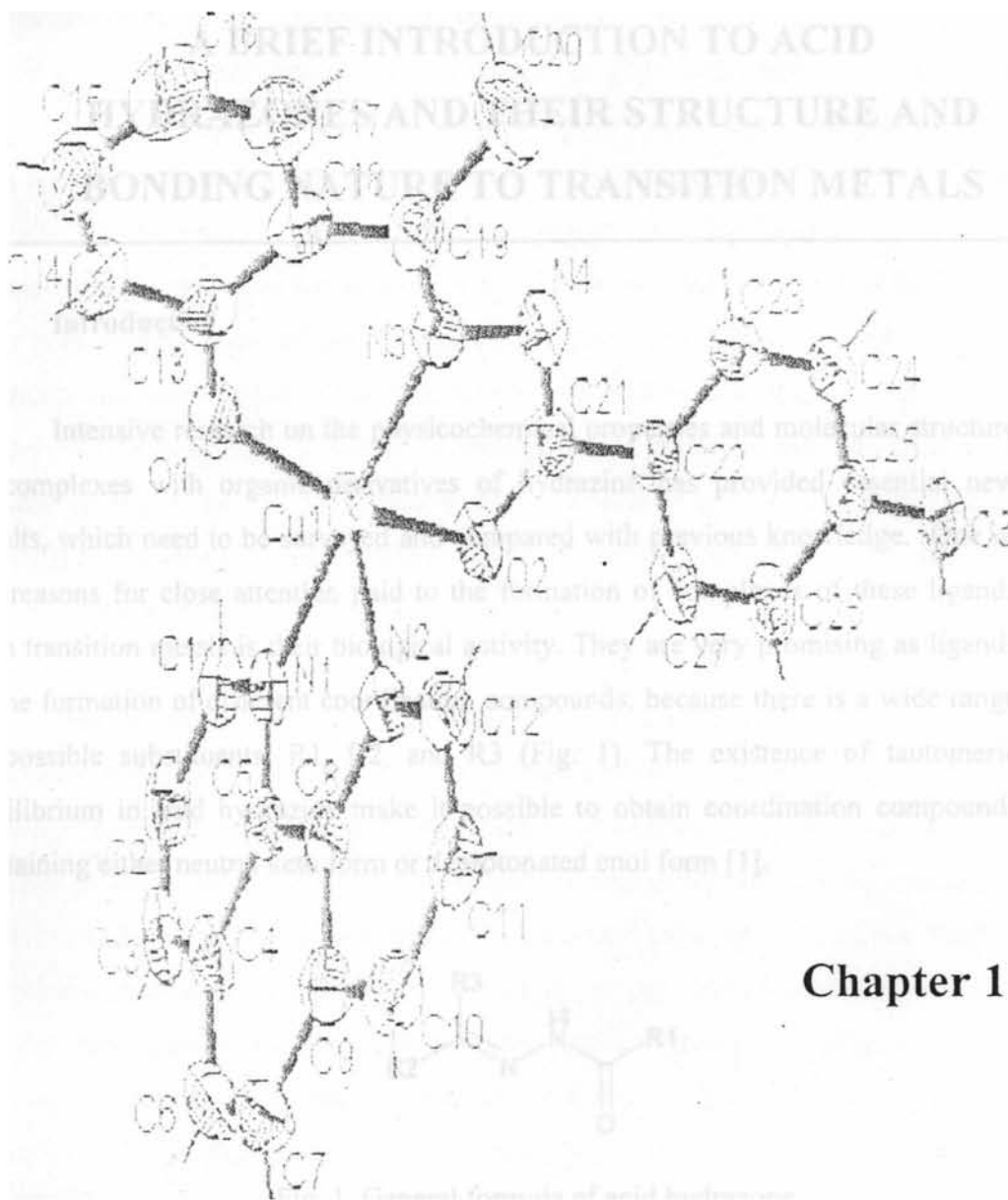
SYNTHESIS, SPECTRAL CHARACTERIZATION AND MAGNETIC STUDIES OF STUDIES OF TERNARY NICKEL(II) COMPLEXES WITH SOME ACID HYDRAZONES AND HETEROCYCLIC BASES

| | Page No. |
|--|----------|
| 6.1 Introduction | 104 |
| 6.2 Experimental | 105 |
| 6.2.1. <i>Materials</i> | 105 |
| 6.2.2. <i>Syntheses of the complexes</i> | 105 |
| 6.2.2.1. <i>Syntheses of NiL²bipy, NiL⁵bip and NiL⁵phen</i> | 105 |
| 6.2.2.2. <i>Synthesis of NiL²H₂O</i> | 106 |
| 6.2.2.3. <i>Syntheses of NiL⁴bip, NiL⁶bip, NiL⁴phen and NiL⁶phen</i> | 107 |
| 6.3. Results and discussion | 107 |
| 6.3.1. <i>Synthesis of nickel(II) complexes</i> | 107 |
| 6.3.2. <i>Magnetic measurements</i> | 108 |
| 6.3.3. <i>IR spectral studies</i> | 110 |
| 6.3.4. <i>Electronic spectral analyses</i> | 115 |
| 6.3.5. <i>Biological activity studies</i> | 117 |
| Concluding remarks | 118 |
| References | 119 |

Chapter 7

SYNTHESIS, SPECTRAL CHARACTERIZATION AND BIOLOGICAL INVESTIGATIONS OF ZINC(II) COMPLEXES OF SOME ACID HYDRAZONES

| | Page No. |
|---|----------|
| 7.1 Introduction | 121 |
| 7.2 Experimental | 122 |
| 7.2.1. <i>Materials</i> | 122 |
| 7.2.2. <i>Syntheses of the zinc(II) complexes</i> | 122 |
| 7.3. Results and discussion | 123 |
| 7.3.1. <i>Syntheses of zinc(II) complexes</i> | 123 |
| 7.3.2. <i>Electronic spectral studies</i> | 124 |
| 7.3.3. <i>Infrared spectral studies</i> | 126 |
| 7.3.4. <i>¹H NMR studies</i> | 127 |
| 7.3.5. <i>Biological activity studies</i> | 130 |
| Concluding remarks | 131 |
| References | 131 |
| SUMMARY AND CONCLUSION OF THE WORK | 132 |
| RÉSUMÉ | 137 |



A BRIEF INTRODUCTION TO ACID HYDRAZONES AND THEIR STRUCTURE AND BONDING NATURE TO TRANSITION METALS

1.1. Introduction

Intensive research on the physicochemical properties and molecular structure of complexes with organic derivatives of hydrazine has provided essential new results, which need to be surveyed and compared with previous knowledge. One of the reasons for close attention paid to the formation of complexes of these ligands with transition metals is their biological activity. They are very promising as ligands in the formation of different coordination compounds, because there is a wide range of possible substituents, R1, R2, and R3 (Fig. 1). The existence of tautomeric equilibrium in acid hydrazide make it possible to obtain coordination compounds containing either neutral keto form or deprotonated enol form [1].

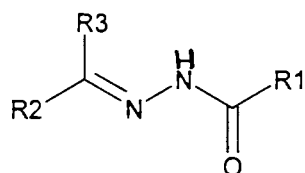


Fig. 1. General formula of acid hydrazone

The chemical properties of hydrazones have been intensively investigated in several research fields because of their chelating capability and their pharmacological applications [2]. The antibacterial and antifungal properties of bis(acylhydrazone) and their complexes with some first transition series metal ions was studied and

reported by *Carcelli et. al.* The evaluation of *in vitro* antimicrobial properties showed some compounds to exhibit good activity against *Gram positive* bacteria [3]. Copper(II) complex of salicylaldehyde benzoylhydrazone was shown to be a potent inhibitor of DNA synthesis and cell growth. This hydrazone also has mild bacteriostatic activity and a range of analogues has been investigated as potential oral iron chelating drugs for genetic disorders such as thalassemia [4-5]. This type of diprotic ligand typically acts as tridentate planar chelating agents coordinating through the phenolic and amide oxygen and imine nitrogen. The actual ionization state is depending upon the condition and metal employed [6]. In base solution both phenolic and amide protons ionized, whereas in neutral and acidic solutions the ligands are monoanionic. However in strongly acidic condition the ligands will be bonded to the metal ion in a neutral state. Synthesis and structural studies of nickel(II) complexes of salicyloylhydrazone of picolinaldehyde and its chelating properties were reported by *Domiano et. al.* [7].

The biological activities and chemical and industrial versatility of metal hydrazone complexes continue to attract considerable attention. For example, Schiff base hydrazones of pyridoxal phosphate and its analogues have been studied in an attempt to better understand the mechanism of action for vitamin B₆ containing enzymes [8-9]. Copper (II) complexes of antitumor ligand, salicyladehyde benzoyl hydrazone have been studied by *Ainscough et al.* [6]. More recently the related systems have been investigated for their ability to act as iron-chelating drugs. The only agent currently in clinical use for the removal of excess iron from humans for disorder such as thalassemia is desferrioxamine. This is a microbial derived hexadentate trihydroxamic acid, which is given by parental injection or trip [10], but the above type ligands had been evaluated as chelating agents for oral administration.

Binary and ternary complexes copper(II) complexes of the ligand salicylaldehyde acetyl hydrazone and its antitumor activities have been reported by *Chan et al.* [11]. The studies showed that the monomeric units being bridged through the phenoxy oxygen. The copper atom has a square pyramidal geometry, with the

basal donor atoms coming from the tridentate ligand (ONO) and symmetry related to phenolate.

Acyl hydrazones of salicylaldehyde subsequently attracted attention. It displays radioprotective properties [12] and a range of acyl hydrazones have been shown to be cytotoxic, the copper(II) complexes again showing enhanced activity.

1.2. Structure, bonding and stereochemistry of the acid hydrazones

Hydrazones have the general formula given below. The functional grouping causes these compound to behave as bidentate ligands for metal ion and owing the availability of $-NH-C=O$ group, acid hydrazones show keto- enol tautomerism (Fig. 2). In solid state they exist in keto form but in solution they exist as an equilibrium mixture keto and enol forms.

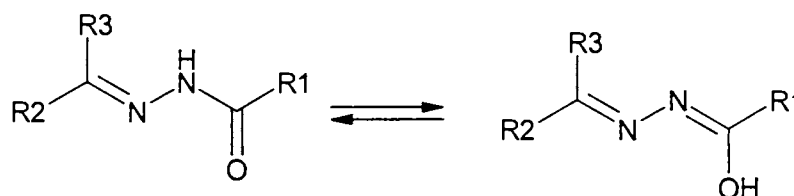


Fig. 2. Tautomerism in acid hydrazone

These types of compounds expected to exist in a *trans* form, but such situation the compound may act as a unidentate ligand, by bonding through enolate oxygen. It is well evident that the stereochemistry of the ligand is much decided by the steric effects of the various substituents in the hydrazone moiety. It is found that most of the compound is in *cis* form, while coordinating to the metal ions. This phenomenon is assumed to be due to chelate effect- increased stability due to better electron delocalisation in chelated ring system- resulting from the coordination with the metal atoms.

The composition and structure of the complexes are determined by the electronic structure of complex forming metal as well as preparation condition [13-14]. They form coordination compounds through the oxygen atom of either carbonyl [15-16] or the enol group and through the imine nitrogen atom, a five membered ring being produced. (Fig. 3)

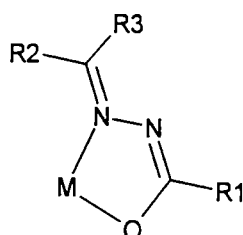


Fig. 3. General mode of coordination of acid hydrazones

Neutral metal complexes can be formed. This type of hydrazones may behave as a terdentate chelating agent, provided R1 residue provides a donor atom in a adequate position, as it occurs in salicyloylhydrazide derivatives, although in these cases, the compounds acts commonly as ON donor ligands if R2 and R3 do not show chelating tendency [17-19] or in the pyridylhydrazide derivatives (NON) ligands. Terdentate ligands may also be obtained if R2 and/or R3 residues are groups such as *o*-hydroxyphenyl (ONO) ligands [19-21]. Chelating ligand with higher number of coordination position may be prepared by convenient selection of the condensation products: aroylhydrazide (R1-CONHNH₂) and di or tri ketones [22 –30]. The oxidation state of the metal ion determines the softness and hardness and hence plays an important role in predicting the stability of the complexes of acid hydrazones. The stability of the complexes also increases with the increase in pi electron delocalisation, size of the molecule and also the nature and size of the rings formed [31].

Hydrazones obtained by condensing substituted acid hydrazide with aromatic 2-hydroxyaldehyde, β-diketones, and keto-acids of the pyruvic type are most effective in complex formation. The systems of this type, which have been studied

most, are benzoyl hydrazone 2-hydroxy aldehyde, which with transition metals ions can give at least four type of coordination (Fig. 4-7).

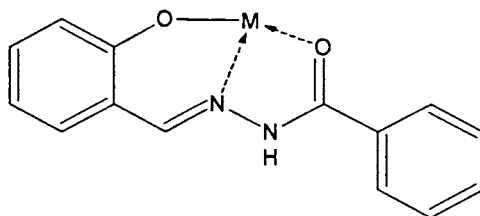


Fig. 4.

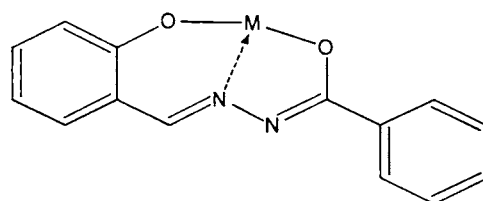


Fig. 5.

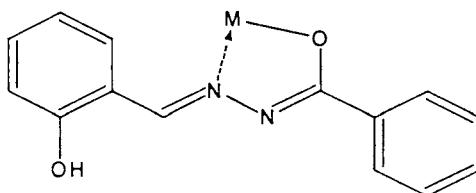


Fig. 6.

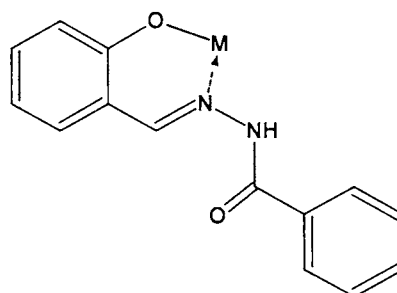


Fig. 7.

Different modes of coordination of substituted acid hydrazones with metal

The reactions of VO(IV), Mn(II), and Cu(II) with these type of ligands in neutral or weakly alkaline solution gives mainly complexes containing enol forms [32-36]. The IR spectra of these complexes contain no bands due to -NH, -OH, or

-C=O groups and bands due to stretches of the -C=N-N=C- hydrazone grouping is shifted to lower wavenumbers compared to the initial aroyl hydrazones, being found in the $\sim 1590\text{ cm}^{-1}$ [1].

1.3. Objectives and scope of the work

- ❖ Preparation of different acid hydrazones and their structural studies and studies on their antimicrobial activity.
- ❖ Synthesis and spectral characterization of the different complexes of copper(II), oxovanadium(IV), manganese(II), nickel(II), zinc(II), etc.
- ❖ Effect of incorporation of heterocyclic bases to the coordination sphere.
- ❖ Change in the biological activity of ligand upon coordination.
- ❖ Development of X-ray quality single crystals and its X-ray diffraction studies
- ❖ Studies on the redox behavior of the coordinated metal ions.
- ❖ Correlation between the stereochemistry and biological activities.

1.4. Structural characterization techniques

Various techniques are used to elucidate the bonding, structure and stereochemistry of the ligands and the complexes prepared. While the ligands are characterized by usual methods such as elemental analysis, IR, UV-visible and NMR spectral techniques, it differs for complexes depending on the nature of the ligands and the metal ions involved. Ligands on complexation with some metal ions to form complexes having paired or unpaired electrons give diamagnetic or paramagnetic respectively. Some of the common physicochemical methods adopted by inorganic chemists are discussed below.

1.4.1. Magnetic measurements

In a magnetic field, the paramagnetic compounds will be attracted while the diamagnetic compounds repelled. In paramagnetic complexes, often the magnetic moment gives the spin only value corresponding to the number of unpaired electron. The variation from the spin only value is attributed to the orbital contribution and it varies with the nature of coordination and consequent delocalisation. In some cases two magnetic centers may be coupled together and may result in extraordinary increase or decrease in the magnetic moment of the complex. For example, a mononuclear complex of copper of the formula $[\text{CuLX}]$ where Cu is in the +2 oxidation state, the complex is expected to have magnetic moment of 1.73 BM - corresponding to d^9 configuration, but in case of $[\text{Cu}(\text{OAc})_2]_2$ the value is lower than 1.73 BM. This is explained on the basis of the assumption that the individual magnetic moments are aligned in opposite directions so that they cancel each other to some extent or can be ascribed as due antiferromagnetic coupling. Thus the value of magnetic moment of a complex would give valuable insights into its constitution and structure. In some cases the variation in the magnetic moment can be explained on the assumption that the compound may be an equilibrium mixture of tetrahedral and square planar geometries- the number of unpaired electrons differ in either geometries and hence the magnetic moment. The magnetic susceptibility measurements thus help to predict the oxidation state of the metal ion to a limited extent and to establish the possible geometry of the compound.

The most widely adopted method for determining the magnetic moment of a complex is by *Gouy's Method* in which the weight difference experienced by a given amount of a substance in the presence and absence is measured. This is compared with that of a standard substance and magnetic moment is determined with the help of suitable equations. Faraday Balance and Vibration Susceptibility Magnetometer are the other instruments used for the magnetic susceptibility measurements [37].

1.4.2. *Electronic spectroscopy*

Electronic spectroscopy is an important and valuable tool for most chemists to draw important information about the structural aspects of the complexes. The ligands, which are mainly organic compounds, have absorption in the ultraviolet region -hence do have bands in the region of the 200 to 350 nm of the electromagnetic spectrum- and in some cases these bands extends over to higher wavelength region due to conjugation. But upon complexation with transition metal ions, due to interaction with the metal ion there will be an interesting change in the electronic properties of the system. New features or bands in the visible region due to d-d absorption and charge transfer spectra from metal to ligand (M→L) or ligand to metal (L→M) can be observed and this data can be processed to obtain information regarding the structure and geometry of the compounds [38].

This technique along with other spectral techniques viz., EPR serves to find out the structural features and to calculate the bonding parameters such (α^2 , β^2 , γ^2 , $K_{||}$, K_{\perp} etc.) [39- 42] and *Racah* Parameters (B and C) [43].

The electronic spectroscopy is also widely used to explore the change in the structural features with change in the pH of the medium. The electronic and structural features of the complexes are widely utilized to investigate the kinetics and mechanisms of the reactions involving transition metal complexes [44-45].

The kinetics of 4-nitrophenylacetate cleavages, by oxime in the presence of Zn^{2+} ions was investigated [46-47].

1.4.3. *Infrared Spectroscopy*

The IR spectroscopy is the widely used as a characterization technique for metal complexes. The basic theory involved is that the stretching modes of the ligands changes upon complexation due to weakening/strengthening of the bonds

involved in the bond formation resulting in subsequent change in the position of the bands appearing in the IR spectrum. The changes in the structural features of the ligands are observed as changes in bands observed, mainly in the fingerprint region i.e., in the $1500 - 750 \text{ cm}^{-1}$. Nakamoto discusses at length the characterization of metal complexes with the help of IR spectroscopy [48]. The bands due to the metal ligand bonds are mainly observed in the far IR region i.e., $50 - 500 \text{ cm}^{-1}$.

1.4.4. EPR spectroscopy

Electronic structure is important concept in many area of chemistry such as inorganic, physical, material and biological. Among the main techniques for describing electronic structure, electron paramagnetic resonance spectroscopy is unique in its ability to selectively probe paramagnetic molecules. In fact EPR spectroscopy can provide a wealth of information about the electronic structure of paramagnetic molecules including those involving metal ions. For complexes those are paramagnetic, in addition to the elemental analysis, IR, and electronic spectroscopic techniques, Electron Paramagnetic Resonance (EPR) spectroscopy acts as an effective and valuable tool to explore the structural features and bonding characteristics of metal complexes. The advances in the ESR spectroscopy have benefited the inorganic chemists with the help of high field and high-resolution spectrometers that helps to resolve the g_{\parallel} and g_{\perp} features of the paramagnetic species. The information obtainable from a low temperature spectrum of diamagnetically diluted paramagnetic species provides important clues to structural traits and bonding properties of the complexes [49].

The single crystal EPR spectrum measurements are also widely employed to derive more information about the geometry of the paramagnetic species formed [50]. Hathaway had extensively surveyed the studies on complexes by using EPR spectroscopy [51]. Various simulation packages are extensively used to simulate the experimental spectrum and hence help to establish the absolute geometry and accurate bonding and structural characteristics of the complexes [52-55]. However,

for diamagnetic complexes, NMR spectroscopy still remains as a valuable tool for establishing the structural characterizations.

1.4.5. X-Ray crystallography

The diffraction/scattering of X-ray radiations by array of atoms in a single crystal of a compound is exploited to establish the structure and geometry of the complexes. At present this versatile techniques is valued as the final word by many chemists for establishing the accurate structure of the complex compounds.

1.4.6. NMR techniques

It is a technique used to characterize ligands and diamagnetic complexes. It consists of four techniques, ^1H NMR ^{13}C NMR, COSY (^1H - ^1H correlation) and HMQC (^1H - ^{13}C correlation).

The proton NMR (^1H NMR) spectrum was recorded at 500 MHz. The assignment is done on the basis of chemical shifts, multiplicities and coupling constants.

^{13}C NMR technique is a relatively new one. There are considerable differences between ^1H NMR and ^{13}C NMR spectra, both in modes of recording as well as appearance. ^{13}C has a spin quantum number equal to $\frac{1}{2}$ and its nuclear magnetic resonance can be observed in the magnetic field of 23,000 gauss at 25.2 MHz. Whereas with the same magnetic field ^1H NMR at 100 MHz. The insufficiency of this method is clear from the fact that only one line can be observed at a given point in time and hence to excite the whole band of frequency simultaneously. It is done by using strong pulse of radio frequency covering a large band of frequencies, which is capable to excite the whole, all resonance of interest at once. Each ^{13}C in organic molecule is spin coupled not only to the directly attached proton, but also to the protons, which are two to four bonds away. Because of this long range coupling

^{13}C spectra appear as broad peaks. By using *proton noise decoupling* technique simplified ^{13}C NMR spectra can be obtained.

Assignments of protonated carbons were made by two dimensional heteronuclear-correlated experiment using delay values, which corresponds to $^1J(\text{C,H})$. The HMQC experiment provides correlation between protons and their attached heteronuclei through the heteronuclear scalar coupling. Thus we can determine the connectivity of each proton to the carbon. This sequence is very sensitive, compare to the older HETCOR, as it is based on proton detection, instead of the detection of the least sensitive low gamma heteronuclei.

1.4.7. Cyclic Voltammetry

Cyclic voltammetry is widely used to study the redox behavior of the coordinated complexes. It gives an insight into the stability of the compound under investigation against electrolytic oxidation and reduction in the solution. In this technique, the potential of a small stationary working electrode is changed linearly with the time starting from a potential where no electrode reaction occurs and moving to potentials where reduction or oxidation of a solute (material being studied) occurs. After traversing the potential region in which one or more electrode reaction takes place, the direction of the linear sweep is reversed and the electrode reactions of the intermediates and products formed during the forward scan, often can be detected. The technique can be carried out using a suitable reference, working and counter electrodes, the selection of which can be made depending on the nature of the compound and the solvent used, in the presence of a supporting electrolyte [56]. The supporting electrolyte is usually added to repress the migration of charged reactants and products. For our systems measurements were made on degassed (N_2 bubbling for 10 minutes) solution in DMF (10^{-3}M) containing 0.1 M tetrabutyl ammonium tetrafluoroborates as supporting electrolyte. The three electrode system consists of a glassy carbon (working) platinum wire (counter or auxillary) and Ag/AgCl (reference) electrodes. Having knowledge of the species involved and an idea about

the redox properties, one can select the range of voltages, and the variation in voltammogram can be recorded at different sweep rates. The peaks in the forward and reverse sweeps can be interpreted to assess the stability of the species. Depending on the nature of the voltammogram obtained they may be termed as reversible ($i_{pa}=i_{pc}$), quasi-reversible ($i_{pa}>i_{pc}$) and irreversible process. If some chemical reaction occurs the return peak of the cyclic voltammogram will be reduced in magnitude, and it will be completely absent if the reaction half-life is much less than the scan duration [57]. The cyclic voltammetric techniques can also be utilized, coupled with electronic spectroscopy, to obtain information about the presence of a new species formed during the oxidation-reduction process and the related stereo chemical and structural changes [58].

1.4.8. *Biological studies*

The biological activities or the therapeutical ability of any compound depends on the minimum amount by which the chemical or substance is required to inhibit the growth or to kill the micro organism that causes the disease, along with a minimum cytotoxicity – a potential to act as a toxin that may generate undesirable symptoms that are harmful to health of living organism and hence decides a drug value of the same

The synthesized chemical ligands and complexes were tested for their antimicrobial activity. Antimicrobial activity is the ability of a compound to inhibit the growth of a given microorganism. The antimicrobial agent may be either bacteriostatic or bactericidal.

The effectiveness of an antimicrobial agent in sensitivity testing is based on the size of the zones of inhibition. When the test substances are introduced on to a lawn of bacterial culture by disc diffusion method, if the bacteria are sensitive, there develops a zone of no growth around the disc, which is referred to as the **zone of inhibition**. The diameter of the zone is measured to the nearest millimeter. Test

substances which produce zone of inhibition of diameters, 9 mm or more are regarded as positive, i.e. having antimicrobial activity; while those cases where the diameter is below 9 mm, the bacteria are resistant to the sample tested and the sample is said to have no antimicrobial activity.

Test organisms

The microorganisms used as test organisms were bacteria isolated from clinical samples.

Two Gram positive bacteria and three Gram negative bacteria were used as test organisms.

A) Gram Positive

1. *Staphylococcus aureus*
2. *Bacillus* sp

B) Gram Negative

3. *Escherichia coli*
4. *Salmonella paratyphi*
5. *Vibrio cholerae* O1

The disc diffusion method was used for screening for the antimicrobial property of the test samples. The MIC (minimum inhibitory concentration) of the complexes showing a positive antimicrobial property was done using the same method.

1. Preparation of discs

Discs of 4 mm diameter were cut out of Whatman No.1 filter paper and autoclaved at 15 psi for 15 minutes. 5 μ L of each of the test chemical samples were dispensed on to the discs under aseptic conditions. The discs were dried at 30⁰ C and stored in sterile vials until further use.

2. Media

Unless otherwise specified, the medium used for growing the cultures was nutrient agar.

Disc diffusion method

A loopful of an overnight slant culture of the test organism was inoculated to 5 ml of sterile physiological saline to make a uniform suspension. This suspension culture was surface spread on nutrient agar plate by swabbing with a sterile cotton swab so as to get a uniform lawn culture.

The discs with the test complexes prepared as mentioned above, were placed on the swabbed surfaces of the plates (4 discs per plate) using sterile forceps.

The plates were incubated at 37°C for 24 hours and then checked for zones of inhibition around the discs.

References

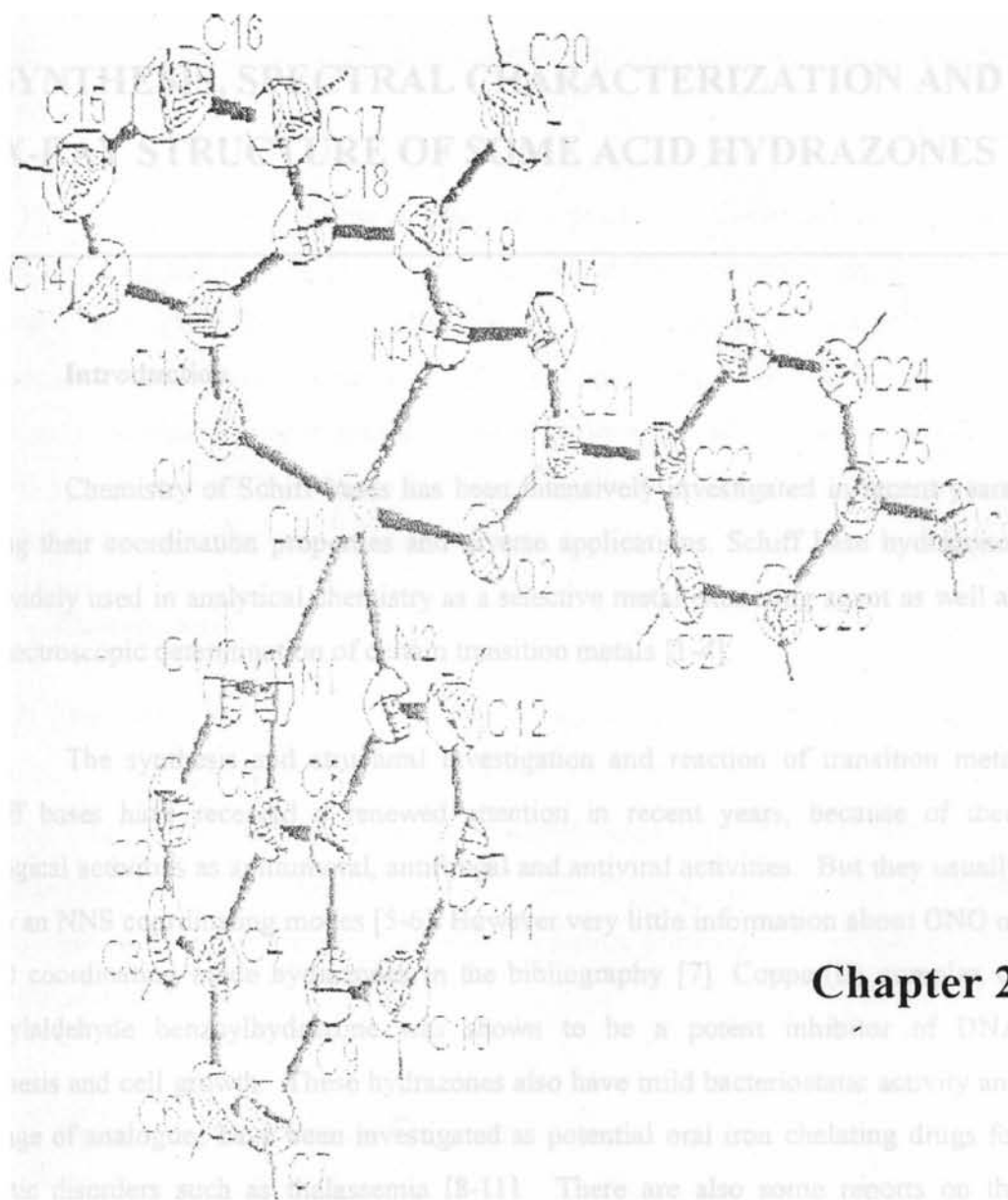
- [1] V. A. Kogan, V. V. Zelentsov, N. V. Gerbeleu, V. V. Lukov, Russian J. Inorg. Chem. 31 (11) (1986) 1628.
- [2] L. F. Lindoy and S. E. Livingstone. Coord. Chem. Rev. 2 (1967) 173.
- [3] M. Carcelli, P. Mazza, C. Pelizzi, G. Pelizzi, Zani, J. Inorg. Biochem. 57 (1995) 43.
- [4] D. K Johnson, T. B Murphy, N. J Rose, W. H. Goodwin, L. Pickart, Inorg. Chim. Acta 67 (1982) 159.
- [5] L. Pickart, W. H Goodwin, W. Burgua; T. B. Murphy; D. K.Johnson; Biochem Pharmacol. 32 (1983) 3868.
- [6] E. W. Ainscough, A. M. Brodie. A. J. Dobbs, J. D. Ranford, Inorg. Chim. Acta 267 (1998) 27.
- [7] P. Domiano, A. Musatti, M. Nardelli C. Pelizzi, Dalton Trans. (1975) 295.

- [8] H. R. Maghler, E. H. Cordes, *Bio. Chem.* Harper & Row, New York, (1971) 393.
- [9] H. M. Dawes, J. M. Waters, T. N. Waters. *Inorg. Chim. Acta* 66 (1982) 29.
- [10] S. Fucharoen, P. T. Rowley, N. W. Paul, *Thalassemia Pathophysiology & Management Part B*, Alan R. Liss, New York (1988).
- [11] S. C. Chan L. L. Koh, P-H. Leung, J. D. Ranford, K.Y. Sim, *Inorg.Chim. Acta* 236 (1995) 101.
- [12] O. V. Arapov; O. F. Alferva; E. I. Levocheskaya; I. Krasil'nikov *Radiobiologiya*, 27 (1987) 843.
- [13] P. N. Shman'ko, S. S. Butsko, Gerbeleu, Zhur. *Neorg. Khim.* 21 {1976} 10 (Russian. *J. Inorg. Chem.* (1976) 9).
- [14] P. N. Buev, S. S. Butsko, A. V. Nikitin, N.I. Pechurova, P. I. Shman'ko, *Koord. Chim.* 6 (1980) 1.
- [15] T. J. Giordano, G. J. Palenik, R. C. Palenik, D. A. Sullivan, *Inorg. Chem.* 18 (1976) 2445.
- [16] J. E. Thomas, R. C. Palenik, G. J. Palenik, *Inorg. Chim, Acta* 37 (1979) 459.
- [17] H. Ohta, *Bull. Chem. Soc. Japan* 31 (1958) 1056.
- [18] P. Domiano, C. Pelizzi, G. Predieri, *Polyhedron* 3 (1984) 281.
- [19] P. Domiano, A. Musatti, M. Nardelli, C. Pelizzi, *J. Chem. Soc., Dalton Trans.* (1975) 295.
- [20] P. Domiano, C. Pelizzi, G. Predieri, *Polyhedron* 3 (1984) 281.
- [21] P. Domiano, A. Musatti, M. Nardelli, C. Pelizzi, G. Predieri, *J. Chem. Soc. Dalton Trans.* (1975) 235.

- [22] Giordano, G. J. Palenik, R. C. Palenik, D. A. Sullivan, *Inorg. Chem.* 18 (1976) 2445.
- [23] J. E. Thomas, R. C. Palenik, G. J. Palenik, *Inorg. Chim. Acta* 37 (1979) 459.
- [24] C. Pelizzi, G. Pelizzi, G. Predieri, *Congr. Naz. Chim. Inorg. (Atti)* 12th (1979) 370.
- [25] S. W. Gaines, G. J. Palenik, R. C. Palenik, *Cryst. Struct. Comm.* 10 (1981) 673.
- [26] C. Lorenzini, C. Pelizzi, G. Pelizzi, G. Predieri, *J. Chem. Soc. Dalton Trans.* (1983) 721.
- [27] C. Pelizzi, G. Pelizzi, *J. Chem. Soc. Dalton Trans.* (1980) 1970.
- [28] G. Paolucci, G. Marangoni, G. Bandoli, *J. Chem. Soc. Dalton Trans.* (1980) 1304.
- [29] C. Pelizzi, G. Pelizzi, G. Predieri, S. Resola, *J. Chem. Soc. Dalton Trans.* (1982) 1349.
- [30] D. B. Pendergrass, Jr. I. C. Paul, *J. Am. Chem. Soc.* 94 (1972) 8730.
- [31] R. S. Bottel, D. Quane. *J. Inorg. Nucl. Chem.* 26 (1964) 1919.
- [32] N. S. Biradar, B. R. Havinale, *Inorg. Chim. Acta* 17 1 (1976) 157.
- [33] D. K. Rastogi, P. C. Pachauri, V. B. Rana, S. K. Dua, *Acta Chim. Acad. Sci. Hung.* 2-3 (1977) 223.
- [34] A. Syamal, K. S. Kale, *Ind. J. Chem.* 16 (1978) 46.
- [35] D. K. Rastogi, S. K. Sahui, V. B. Rana, K. Dua, S. K. Dua, *J. Inorg. Nucl. Chem.* 41 (1979) 21.

- [36] D. K. Rastogi, S. K. Sahu, V. B. Rana, S. K. Dua, *Trans. Met. Chem.* 3 (1978) 56.
- [37] Stephan J. Lippard, *Progress in Inorganic Chemistry*, John Wiley and Sons 29. (1982).
- [38] A. B. P. Lever, *Inorganic Electronic Spectroscopy*, 2nd Edn., Elsevier, NY (1984).
- [39] A. H. Maki, B. R. McGarvey, *J. Chem. Phys.* 29 (1958) 31.
- [40] B. N. Figgis, *Introduction to Ligand Fields*, Interscience, New York, (1966) 295.
- [41] B. J. Hathaway, *Structure and Bonding*, Springer Verlag, 14 (1973) 60.
- [42] B.N. Figgis, *Introduction to ligand fields*, Wiley Eastern Ltd., India (1976) 163.
- [43] B. N. Figgis, *Introduction to ligand fields*, Wiley Eastern Ltd, India (1976) 167.
- [44] A. K. Yatsimirsky, G-T. Paola, E-T. Sigfrido, R-R. Lena, *Inorg. Chim. Acta.* 273 (1998) 167.
- [45] M. J. Sisley, R. B. Jordan, *J. Chem. Soc., Dalton Trans.* (1997) 3883.
- [46] J. Suh and H. Han, *Bioorg. Chem.* 12 (1984) 177.
- [47] J. Suh, M. Cheong and H. Han, *Bioorg. Chem.* 12 (1984) 188.
- [48] K. Nakamoto, *Infrared and Raman Spectra of Coordination Compounds*, 3rd edn, John Wiley and Sons, New York (1978).
- [49] J. E. Wertz and J. R. Boltzon, *Electron Spin Resonance: Elementary Theory and Practical Applications*, McGraw-Hill (1979).

- [50] P. S. Subramanian, E. Suresh and D. Srinivas, *Inorg. Chem.* 39 (2000) 2053.
- [51] B. J. Hathaway, *Structure and Bonding*, Springer Verlag. 14 (1973) 60.
- [52] M. Pasenkiewics-Gierula, J. S. Hyde, J. R. Pilbrow, *J. Mag. Resonance* 55 (1983) 255.
- [53] D. L. Liczwek, R. L. Belford, J. S. Hyde, J. R. Pilbrow, *J. Chem. Phys.* 87 (1983) 2509.
- [54] A. Diaz, R. Pogni, R. Cao, R. Basosi, *Inorg. Chim. Acta* 275 (1998) 552.
- [55] R. Pogni, M. C. Baratto, A. Diaz, R. Basosi, *J. Inorg. Biochem.* 79 (2000) 333.
- [56] M. Noel K. I. Vasu, *Cyclic Voltametry and the frontiers of electrochemistry*, Oxford & IBH Co., New Delhi (1990).
- [57] R. S. Nicolson, I. Shain, *Anal. Chem.* 36 (1964) 706.
- [58] A. Saha, P. Majumdar, S. Goswami, *J. Chem. Soc., Dalton Trans.* (2000) 1703.



SYNTHESIS, SPECTRAL CHARACTERIZATION AND X-RAY STRUCTURE OF SOME ACID HYDRAZONES

2.1. Introduction

Chemistry of Schiff bases has been intensively investigated in recent years, owing their coordination properties and diverse applications. Schiff base hydrazones are widely used in analytical chemistry as a selective metal extracting agent as well as in spectroscopic determination of certain transition metals [1-4].

The synthesis and structural investigation and reaction of transition metal Schiff bases have received a renewed attention in recent years, because of their biological activities as antitumoral, antifungal and antiviral activities. But they usually show an NNS coordinating modes [5-6]. However very little information about ONO or NNO coordinating mode hydrazones in the bibliography [7]. Copper(II) complex of salicylaldehyde benzoylhydrazone was shown to be a potent inhibitor of DNA synthesis and cell growth. These hydrazones also have mild bacteriostatic activity and a range of analogues have been investigated as potential oral iron chelating drugs for genetic disorders such as thalassemia [8-11]. There are also some reports on the catalytic activities their nickel complexes [12-15].

This type of diprotic ligand typically acts as tridentate planar chelating agents coordinating through the phenolic and amide oxygen and imine nitrogen. The actual ionization state is depend upon the condition and metal employed [10]. With copper(II) in basic medum, both the phenolic and amide protons are ionized; in neutral and acidic solutions the ligands are monomeric, whereas strongly acidic conditions are necessary to form compounds formulated with neutral ligands. In moderately acidic media or

alkaline solution, the hydrogen atom of the –CONH– group can split off and neutral metal complex can be formed [2]. Aroyl hydrazones behave as bidentate [16], tridentate [17] and tetradentate [18] ligand forming colored complexes with transition metal ions.

Hydrazones have been the subject of extensive investigation due to their versatile chelating behavior in particular those derived from pyridoxal phosphate and isonicotinic acid [19-20], but those having the side chain at 2- position of the heteroaromatic ring have received much less attention. Acyl hydrazones of salicylaldehyde subsequently attracted attention. It displays radioprotective properties [21] and a range of acyl hydrazones have been shown to be cytotoxic, the transition metal complexes again showing enhanced activity.

2.2. Experimental

2.2.1. Materials

Salicylaldehyde (BDH), 2-hydroxyacetophenone (BDH), benzoic acid hydrazide(Fluka), 4-hydroxybenzoic acid hydrazide (Fluka), nicotinic acid hydrazide (Fluka) were of Analar grade and used with out further purification. All the solvents were used after purification.

2.2.2. Physical measurements and Instrumentation

Elemental analyses were carried out using a Heraeus Elemental Analyzer at RSIC, CDRI, Lucknow, India. IR spectra, in the range of 4000-400 cm^{-1} were recorded on a Shimadzu DR 8001 series FTIR instrument as KBr pellets. The ^1H NMR, ^{13}C NMR, COSY and HMQC spectra were recorded by using Bruker DRX500, using $\text{DMSO}-d_6$ as solvent and TMS as standard. Solid state reflectance was recorded on Ocean Optics, Inc. SD2000 Fiber Optic Spectrometer.

2.2.3. Syntheses of acid hydrazones

Acid hydrazide (1 mmol) dissolved in methanol and refluxed with methanolic solutions of salicylaldehyde or 2-hydroxyacetophenone (1 mmol), in presence of a few drops of glacial acetic acid for 6 h. On cooling the reactant media, crystals of hydrazones were separated out. All the compounds were recrystallised from methanol and characterized by analytical and different spectral methods. Schemes used for the synthesis of the ligands have been shown below.

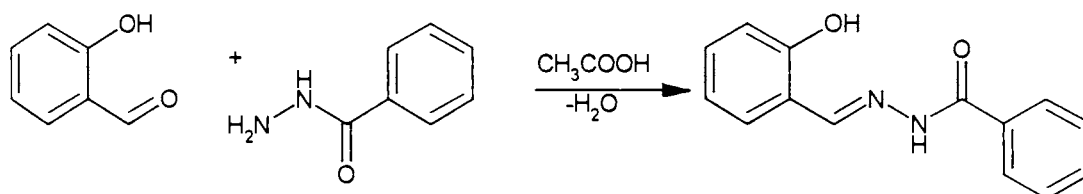


Fig. 1. Scheme of synthesis of H₂L¹

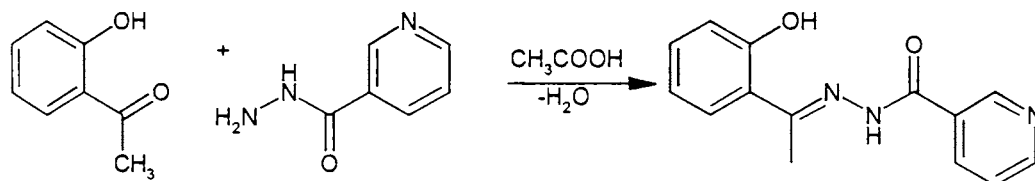


Fig. 2. Scheme of the synthesis of H₂L²

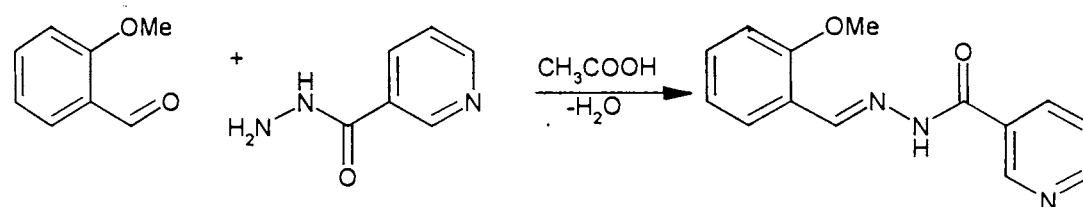
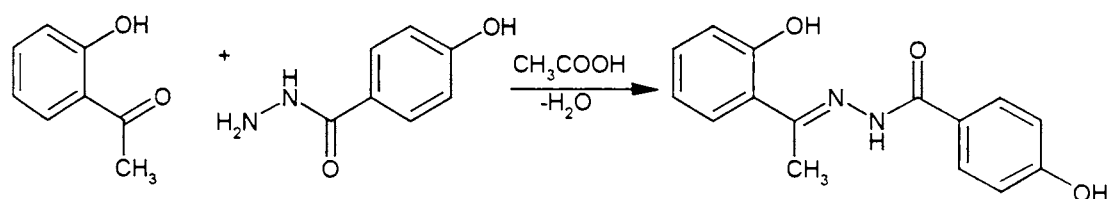
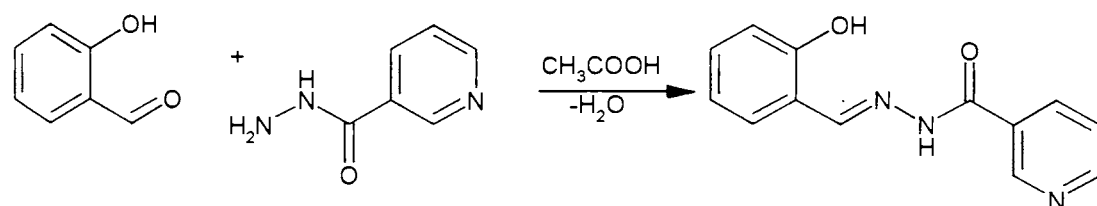
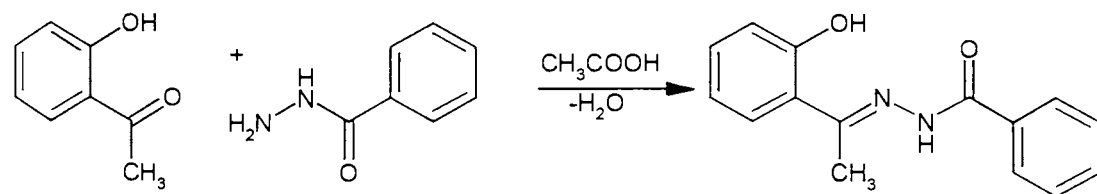


Fig. 3. Scheme of synthesis of HL³

Fig. 4. Scheme of synthesis of H₂L⁴Fig. 5. Scheme of synthesis of H₂L⁵Fig. 6. Scheme of synthesis of H₂L⁶

2.3. Result and discussion

2.3.1. Syntheses of the hydrazones

The hydrazones were synthesized by the direct condensation of the acid hydrazide with aldehydes/ketones in the presence of glacial acetic acid. The elemental analyses were in good agreement with the proposed empirical formulae.

These hydrazones can exist in either keto or enol form or an equilibrium mixture of the two since it has an amide $-\text{NH}-\text{C}=\text{O}$ group. However IR and NMR spectra of these compounds indicate that, in solid state they are in the keto forms. The physical constants, color partial elemental analyses data are given in Table 1.

Table 1. Physical constants, color and appearance and analytical data of ligands

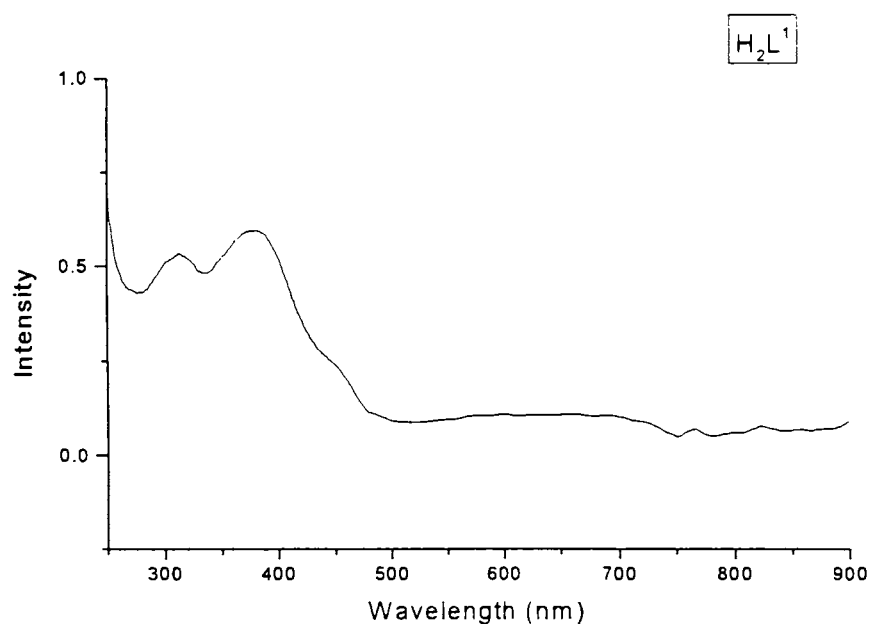
| Compound | Melting point °C | Colour and appearance | Analytical Data found (calculated) | | |
|---|------------------|--------------------------|------------------------------------|------------------|------------------|
| | | | C% | H% | N% |
| H ₂ L ¹ (C ₁₄ H ₁₂ N ₂ O ₂) | 160-162 | Pale yellow Prismatic | 69.74 (70.00) | 5.19 (5.00) | 11.51 (11.66) |
| H ₂ L ² (C ₁₄ H ₁₃ N ₃ O ₂) | 180-182 | Pale yellow Needles | 66.12 (65.85) | 66.12 (65.85) | 16.95 (16.46) |
| HL ³ (C ₁₄ H ₁₃ N ₃ O ₂) | 174-176 | Colourless needles | 65.43 (65.87) | 5.32 (5.13) | 15.98 (16.46) |
| H ₂ L ⁴ (C ₁₅ H ₁₄ N ₂ O ₃) | 182-184 | Yellow | 66.66 (66.70) | 5.22 (5.26) | 10.36 (10.43) |
| H ₂ L ⁵ (C ₁₃ H ₁₁ N ₃ O ₂) | 171-173 | Pale yellow | 60.70 (60.23) | 4.83 (4.60) | 16.55 (16.21) |
| H ₂ L ⁶ (C ₁₃ H ₁₄ N ₂ O ₂) | 172-174 | Colourless needles | 71.20 (70.85) | 5.22 (5.55) | 12.36 (12.58) |

2.3.2. Electronic spectral studies

Solid state reflectance data shows the $\pi \rightarrow \pi^*$ transition is at 34274-31950 cm^{-1} , $n \rightarrow \pi^*$ of the azomethine is found at 29590-28571 cm^{-1} and $n \rightarrow \pi^*$ of carbonyl is at 27778-26110 cm^{-1} [22]. Electronic spectral data are presented in Table 2.

Table 2. Electronic spectral assignment of ligands (cm^{-1})

| Compound | $n-\pi^*$ | $\pi-\pi^*$ |
|------------------------|--------------|-------------|
| H_2L^1 | 26315, 22222 | 32259 |
| H_2L^2 | 29590, 26110 | 31950 |
| HL^3 | | 31237 |
| H_2L^4 | 31746 | 31746 |
| H_2L^5 | | 33333 |
| H_2L^6 | 28571 | 34247 |

Fig. 7. Electronic spectrum of H_2L^1

2.3.3. IR spectral studies

Significant IR bands of the compound and their tentative assignments are discussed here. A broad band obtained at $\sim 3400 \text{ cm}^{-1}$ is assigned to be due to the

phenolic -OH stretching. Other major bands are at ~ 3200 , ~ 1670 and ~ 1610 cm^{-1} which are attributed to $\nu(\text{NH})$, $\nu(\text{C}=\text{O})$ and $\nu(\text{C}=\text{N})$ respectively [10-11]. The IR spectra assignments are presented in Table 3.

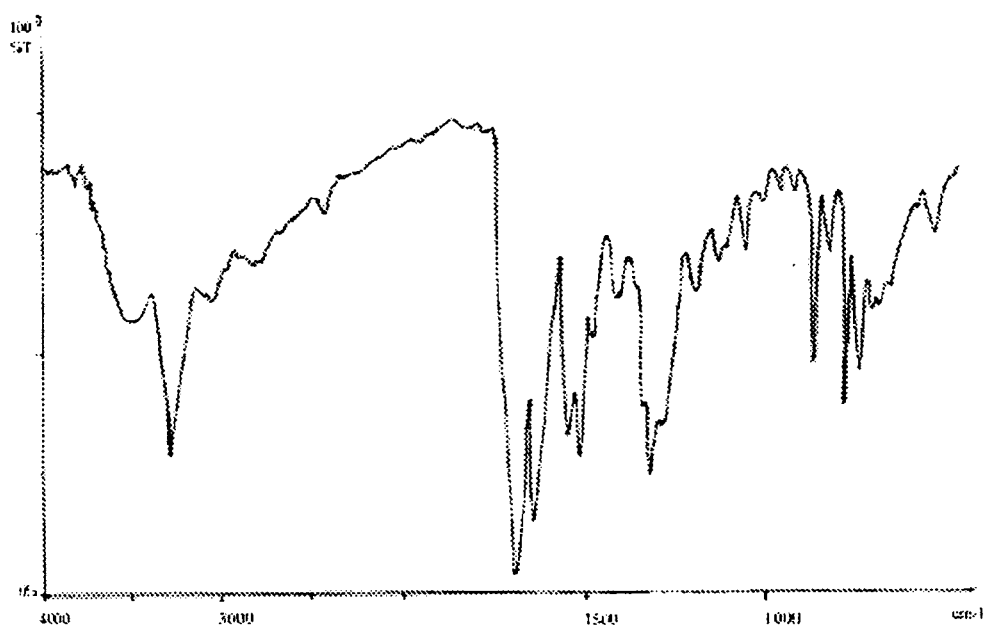


Fig. 8. IR spectrum of H_2L^4

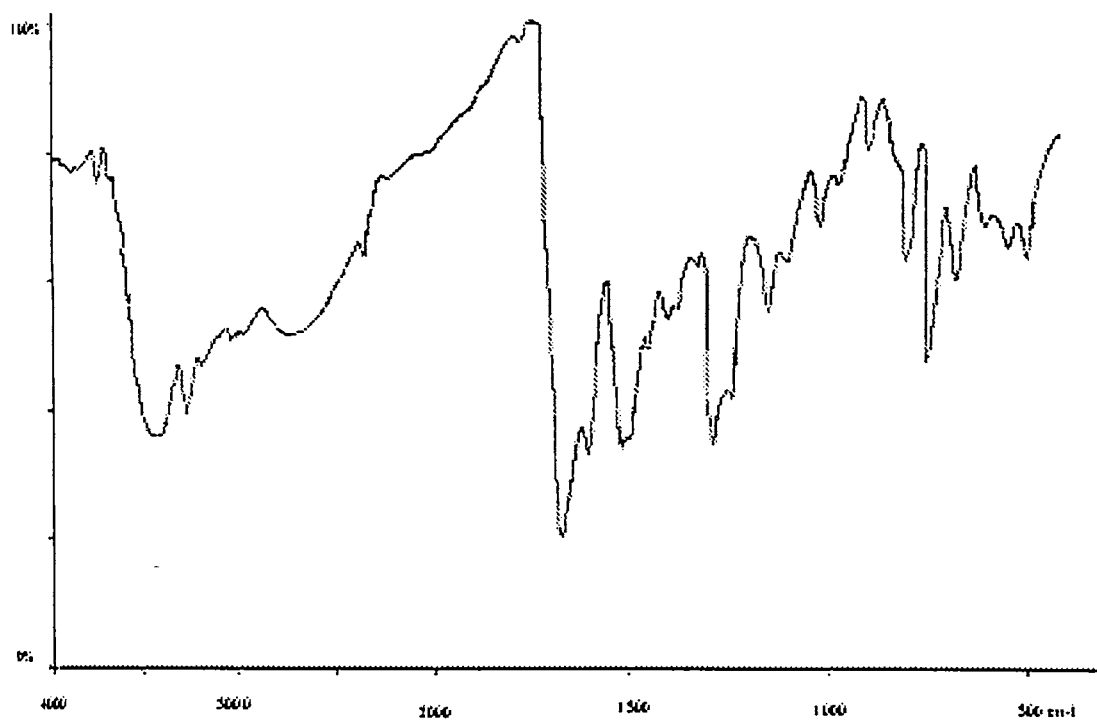
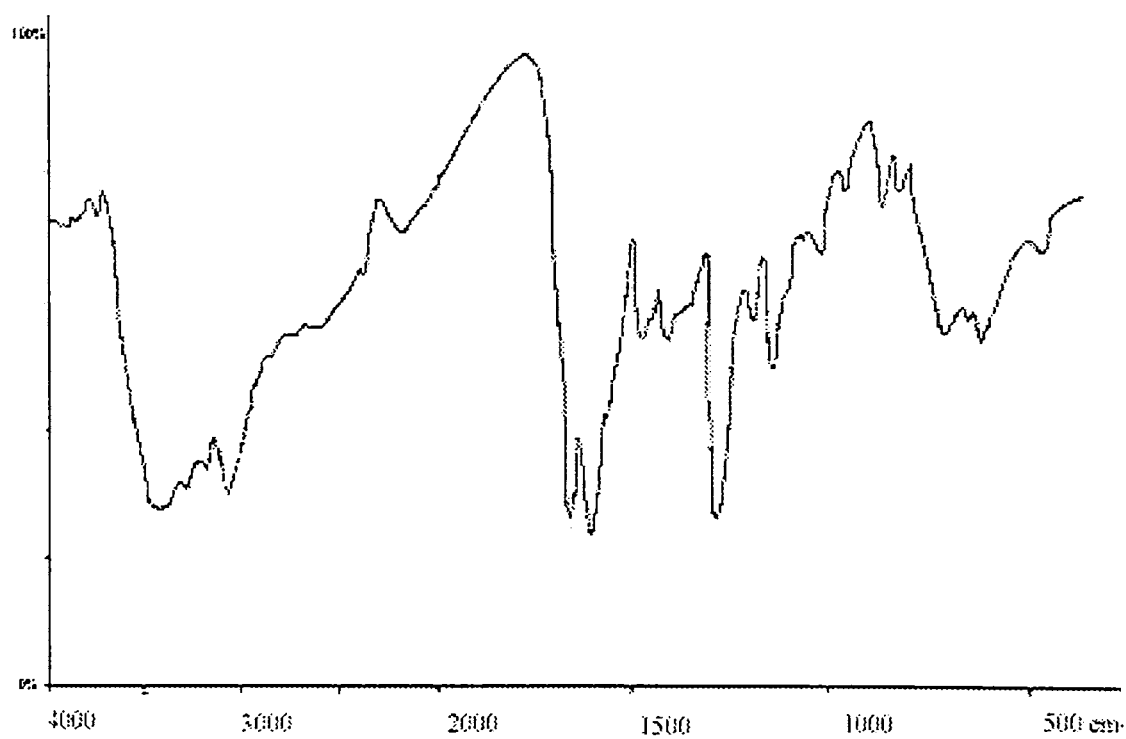
Fig. 9. IR spectrum of H_2L^2 Fig. 10. IR spectrum of H_2L^5

Table 3. IR spectral assignments of the hydrazones (cm^{-1})

| Compound | $\nu(\text{OH})$ | $\nu(\text{NH})$ | $\nu(\text{C}=\text{N})$ |
|------------------------|------------------|------------------|--------------------------|
| H_2L^1 | 3424 | 3160 | 1620 |
| H_2L^2 | 3432 | 3208 | 1603 |
| HL^3 | - | 3214 | 1608 |
| H_2L^4 | 3410 | 3124 | 1610 |
| H_2L^5 | 3451 | 3052 | 1609 |
| H_2L^6 | 3429 | 3217 | 1615 |

2.3.4. ^1H NMR spectral studies

The complete assignment of the ^1H NMR spectra is given here. The spectrum was recorded at 500 MHz. The assignment is done on the basis of chemical shifts, multiplicities and coupling constants. The ligands do not show any peak attributed to enolic $-\text{OH}$ proton indicating that they exist in keto forms.

H_2L^2 (2-hydroxyacetophenone nicotinic acid hydrazone)

The signals at $\delta=13.28$ ppm and $\delta=11.56$ ppm represent OH and NH respectively. Upon addition of D_2O the intensities of both OH and NH protons significantly decrease, confirming the assignment. We got one more singlet at $\delta=9.1$, which is found to be coupled with a proton of H(12) ($\delta=8.3$) from the ^1H - ^1H correlation spectra. Hence it is assigned to be of H(13), for which a doublet is expected. A singlet of three protons at $\delta=2.5$ was attributed to the methyl group protons which are chemically and magnetically equivalent. At $\delta=6.9$ we got a quartet which is assigned to be a merged form of one triplet and a doublet corresponding to H(4) and H(2). OH $\delta=13.28(\text{s})$, NH $\delta=11.56(\text{s})$, H(13) $\delta=9.1(\text{s})$, H(11) $\delta=8.8(\text{d})$ $J=3.5$ Hz, H (12) $\delta=8.3(\text{d})$ $J=8$ Hz, H(10) $\delta=7.6(\text{dd})$ $J=5$ Hz, $J=7.5$ Hz, H(1)

$\delta=7.7(d) J=8$ Hz, H(3) $\delta=7.3(t) J=8$ Hz, $J=7.5$ Hz, H(2) $\delta=6.95(d) J=8.5$ Hz, H(4) $\delta=6.90(d) J=7.5$ Hz, H(14) $\delta=2.5(s)$.

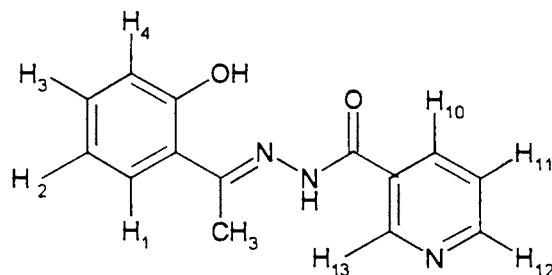


Fig. 11. Formula of H_2L^2

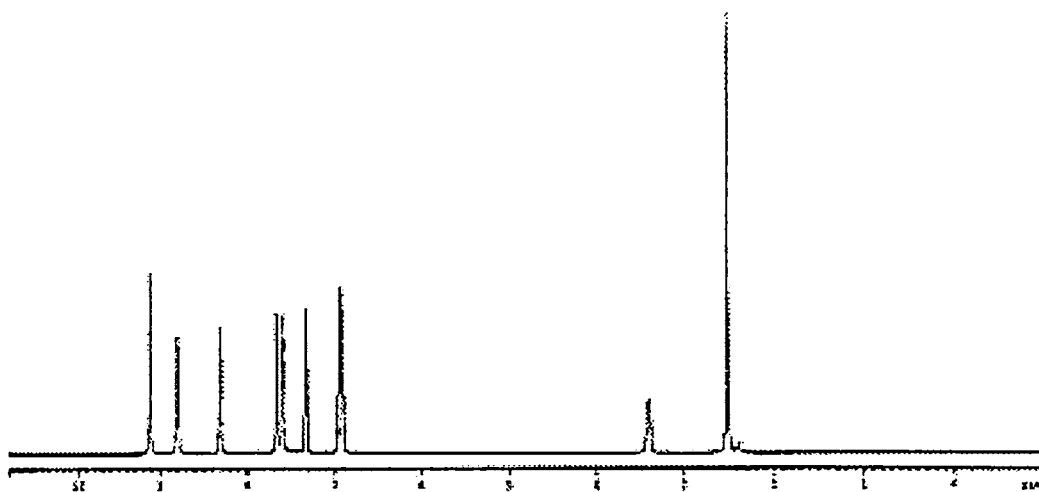


Fig. 12. 1H NMR Spectrum of H_2L^2

HL³ (2-methoxybenzaldehyde nicotinic acid hydrazone)

The 1H NMR spectrum of the compound gives four singlets. One is an exchangeable proton at $\delta=12.0$ ppm, whose intensity decreases significantly upon adding D_2O , which represents NH proton. The singlet at $\delta=3.8$ ppm is assigned to

the OMe. The other singlet at $\delta=9.1$ and $\delta=8.8$ ppm are assigned to be of H(13) and H(7) respectively. OCH₃ $\delta=3.8$ (s), NH $\delta=12.0$ (s), H(13) $\delta=9.1$ (s), H(11) $\delta=8.75$ (d) $J=7.5$ Hz, H (12) $\delta=8.3$ (d) $J=7$ Hz, H(10) $\delta=7.5$ (dd) $J=7.9$ Hz $J=3.7$ Hz, H(1) $\delta=7.9$ (d) $J=7.8$ Hz, H(3) $\delta=7.45$ (d) $J=8$ Hz, $J=7.8$ Hz, H(2) $\delta=7.0$ (t) $J=7$ Hz $J=7.4$ Hz, H(4) $\delta=7.0$ (t) $J=7$ Hz $J=7.4$ Hz, H(7) $\delta=8.8$ (s).

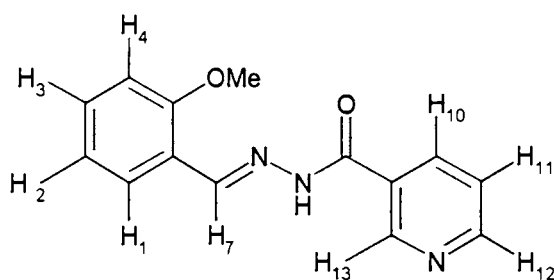


Fig. 13. Formula of HL³

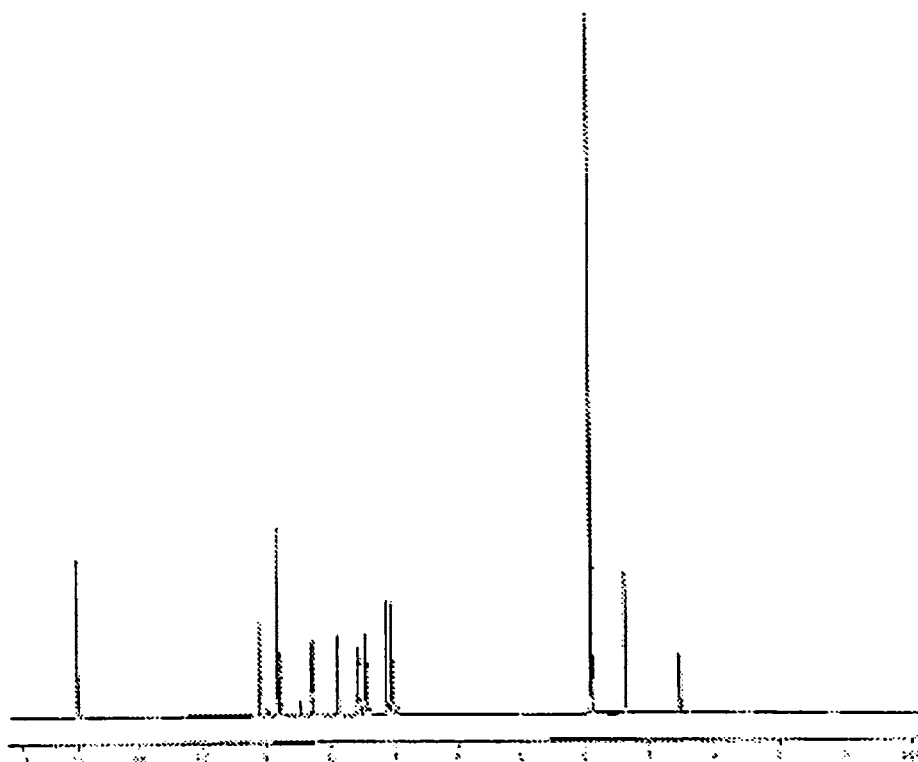
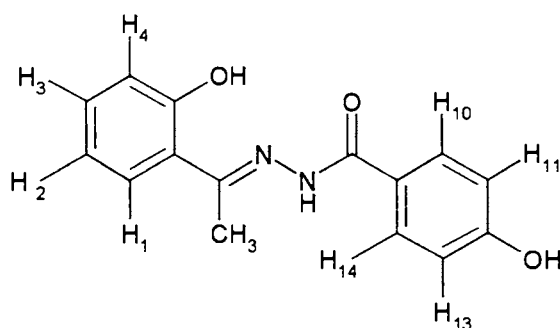


Fig. 14. ¹H NMR spectrum of HL³

H₂L⁴ (2-hydroxyacetophenone 4-hydroxybenzoic acid hydrazone)

For this compound four singlet are observed. The singlet at $\delta=13.3$ ppm and $\delta=11.1$ ppm represent OH and NH respectively. The -OH is obtained at a down field due to possibility of the formation of intramolecular hydrogen bonding with azomethine nitrogen. Upon addition of D₂O the intensities of both OH and NH protons significantly decrease. This supports the assignment. The peak at $\delta =10.2$ ppm is assigned to the OH attached to C(12), which also an exchangeable proton. Another singlet is there at $\delta=2.5$ ppm which represent the aliphatic CH₃. OH $\delta=13.3$ (s), NH $\delta=11.1$ (s), H(13) $\delta=6.9$ (d) $J=8$ Hz,, H(11) $\delta=6.9$ (d) $J=8$ Hz, H (14) $\delta=7.9$ (d) $J=7.8$ Hz, H(10) $\delta=7.9$ (d) $J=7.8$ Hz, H(1) $\delta=7.6$ (d) $J=7.5$ Hz, H(3) $\delta=7.3$ (t) $J=8$ Hz, $J=7.8$ Hz, H(2) $\delta=6.9$ (t) $J=7.4$ Hz, $J=7.8$ Hz H(4) $\delta=6.9$ (d) $J=8$ Hz, H(14) $\delta=7.9$ (d) $J=7.9$ Hz, H(15) $\delta=2.5$ (s) OH $\delta=10.2$ (s).

Fig. 15. Formula of H₂L⁴

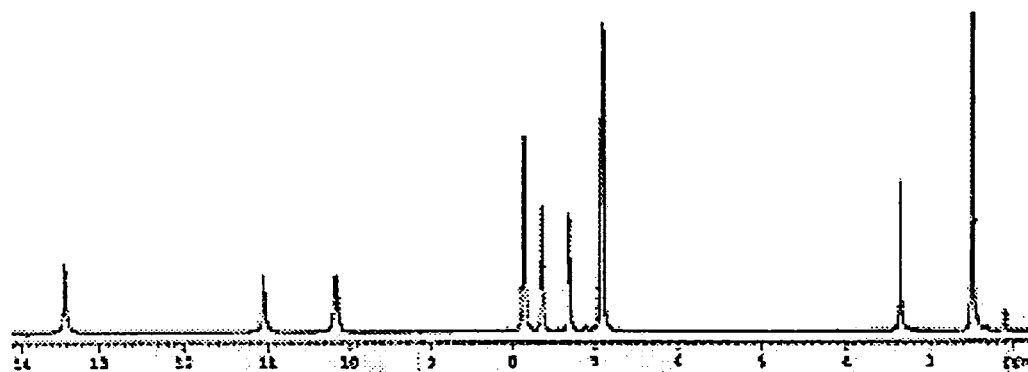
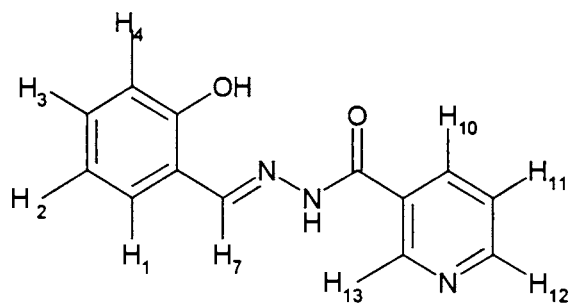


Fig. 16. ^1H NMR spectrum of H_2L^4

H_2L^5 (salicylaldehyde nicotinic acid hydrazone)

The singlet at $\delta=12.3$ ppm and $\delta=11.2$ ppm represent OH and NH respectively. Upon addition of D_2O the intensities of both OH and NH protons significantly decrease, confirming the assignment. We got two more singlet at $\delta=9.1$ ppm and $\delta=8.6$ ppm, are assigned to be of H(13), for which a doublet is expected as in the previous case and H(7) respectively. OH $\delta=12.3$ (s), NH $\delta=11.2$ (s), H(13) $\delta=9.1$ (s), H(11) $\delta=8.8$ (d) $J=3.8$ Hz, H (12) $\delta=8.3$ (d) $J=7.9$ Hz, H(10) $\delta=7.6$ (dd) $J=5.4$ Hz, $J=7.7$ Hz, H(1) $\delta=7.6$ (d) $J=7.9$ Hz, H(3) $\delta=7.3$ (t) $J=8$ Hz, $J=7.5$ Hz, H(2) $\delta=6.9$ (d) $J=8$ Hz, H(4) $\delta=6.9$ (d) $J=7.5$ Hz, H(7) $\delta=8.6$ (s).

Fig. 17. Formula of H₂L⁵

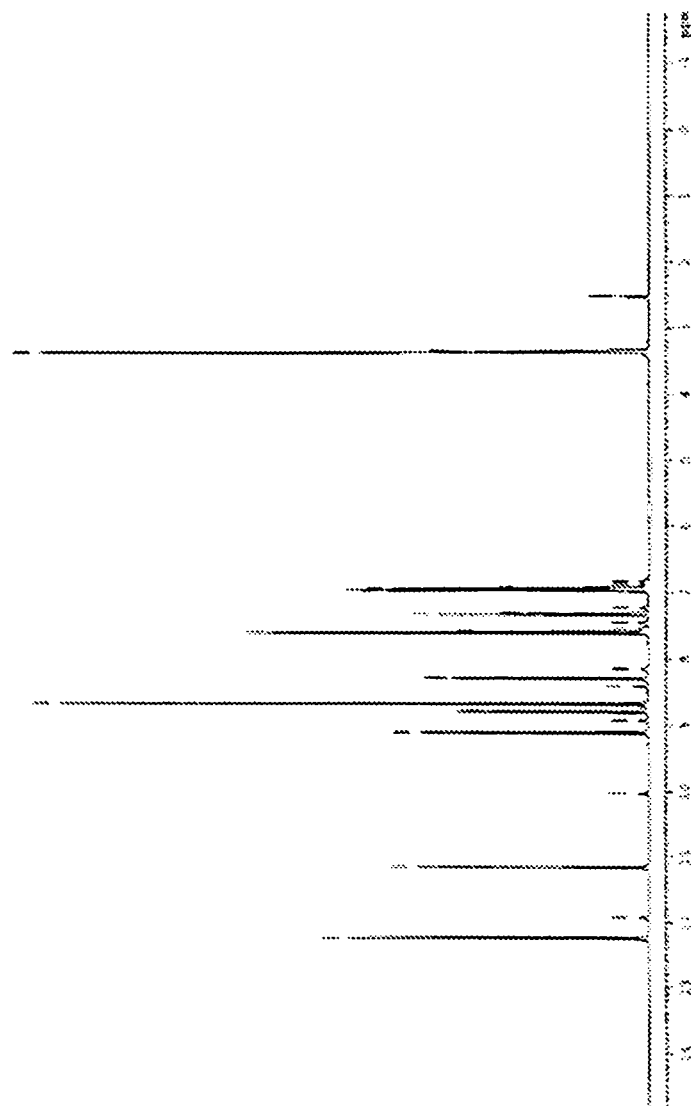


Fig. 18. ^1H NMR of H_2L^5

H₂L⁶ (2-hydroxyacetophenone benzoic acid hydrazone)

The singlet at $\delta=13.3$ ppm and $\delta=11.3$ ppm represent OH and NH respectively. Upon addition of D₂O the intensities of both OH and NH protons significantly decrease, confirming the assignment. One more singlet is there at $\delta=2.5$ ppm which represent the aliphatic CH₃. OH $\delta=13.3$ (s), NH $\delta=11.3$ (s), H(14) $\delta=7.6$ (d), $J=7.5$ Hz H(13) $\delta=8.1$ (d) $J=7$ Hz, H(11) $\delta=8.1$ (d) $J=7$ Hz, H (12) $\delta=7.59$ (d) $J=7.5$ Hz, H(10) $\delta=7.65$ (d) $J=7$ Hz, H(1) $\delta=7.56$ (d) $J=7.5$ Hz, H(3) $\delta=7.35$ (t) $J=7$ Hz, $J=7.5$ Hz, H(2) $\delta=6.95$ (t) $J=7.5$ Hz, $J=7.5$ Hz H(4) $\delta=6.95$ (t) $J=7.5$ Hz $J=8$ Hz, H(15) $\delta=2.5$ (s).

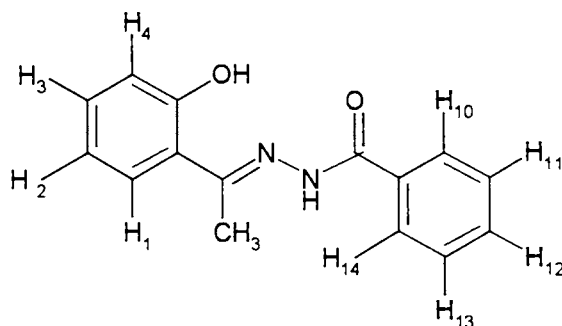


Fig.19. Formula of H₂L⁶

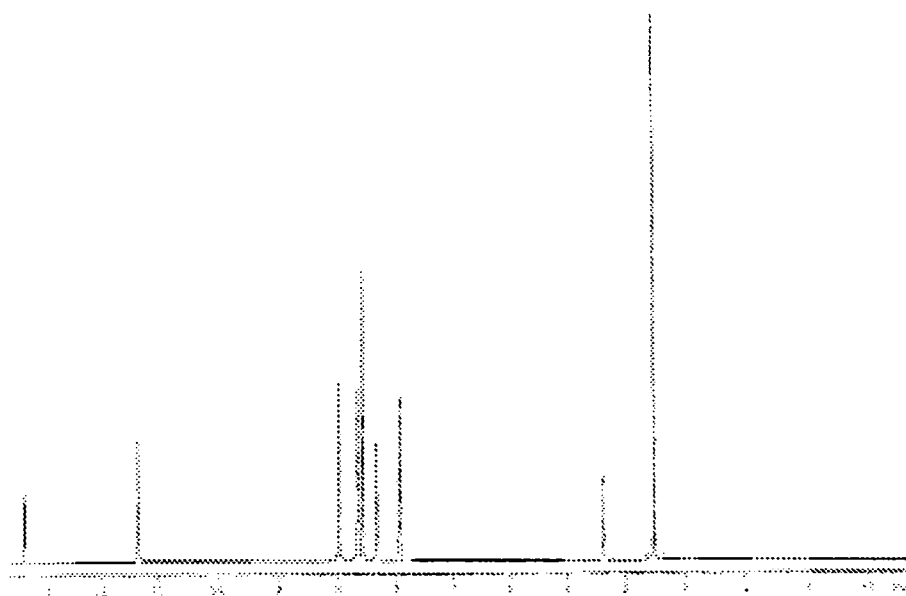


Fig. 20. ^1H NMR of H_2L^6

2.3.5. ^{13}C NMR and $^1\text{H}/^{13}\text{C}$ correlation spectral studies of H_2L^2

Complete assignment of $^{13}\text{C}\{-^1\text{H}\}$ NMR spectra, recorded at 125.76 MHz is given below. Assignment of protonated carbons were made by two dimensional heteronuclear-correlated experiment using delay values which corresponds to $^1J(\text{C,H})$. The HMQC experiment provides correlation between protons and their attached heteronuclei through the heteronuclear scalar coupling. This sequence is very sensitive (compare to the older HETCOR) as it is based on proton detection, instead of the detection of the least sensitive low gamma heteronuclei). From HMQC it is evident that C(5), C(6), C(7), C(8) and C(9) are nonprotonated carbons. C(5) $\delta=159.6$, C(4) $\delta=119$, C(3) $\delta=133$, C(2) $\delta=119$, C(1) $\delta=129$, C(6) $\delta=118$, C(7) $\delta=159.4$, C(14) $\delta=15$, C(8) $\delta=164$, C(9) $\delta=120$, C(10) $\delta=129$, C(11) $\delta=153$, C(12) $\delta=137$, C(13) $\delta=150$. ^{13}C NMR of compound H_2L^2 .

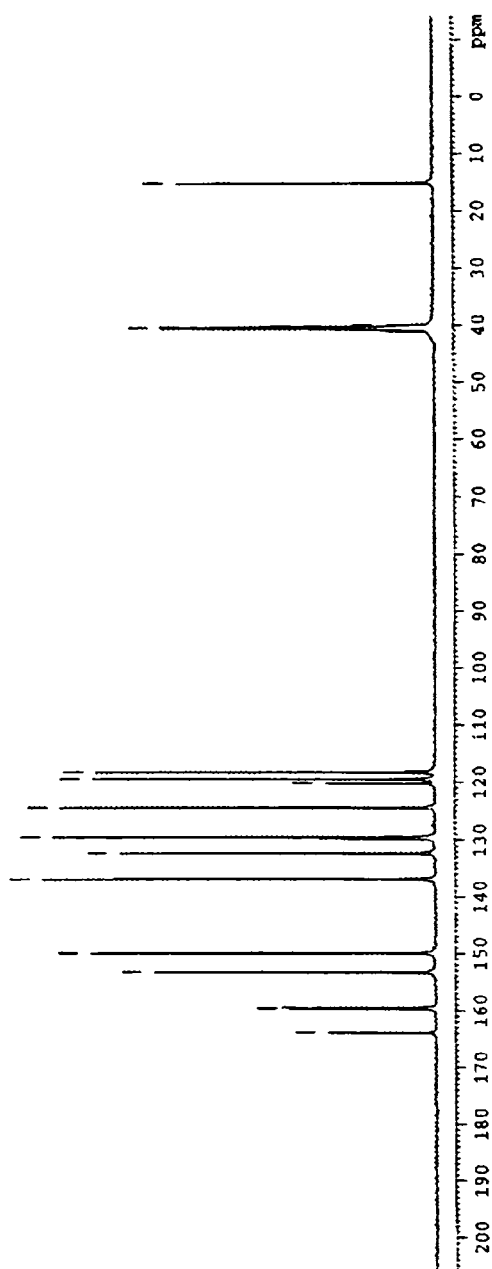


Fig. 21. ^{13}C NMR spectrum of H_2L^2

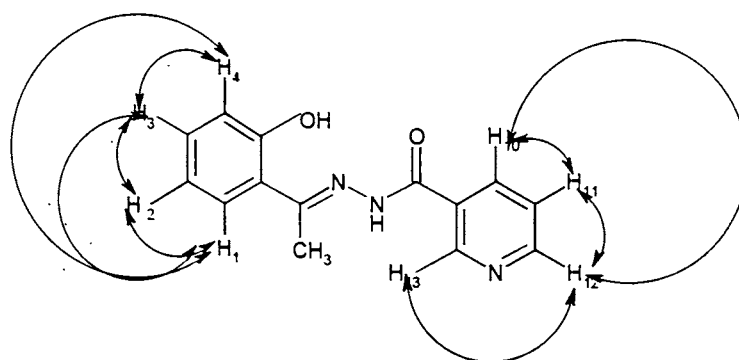
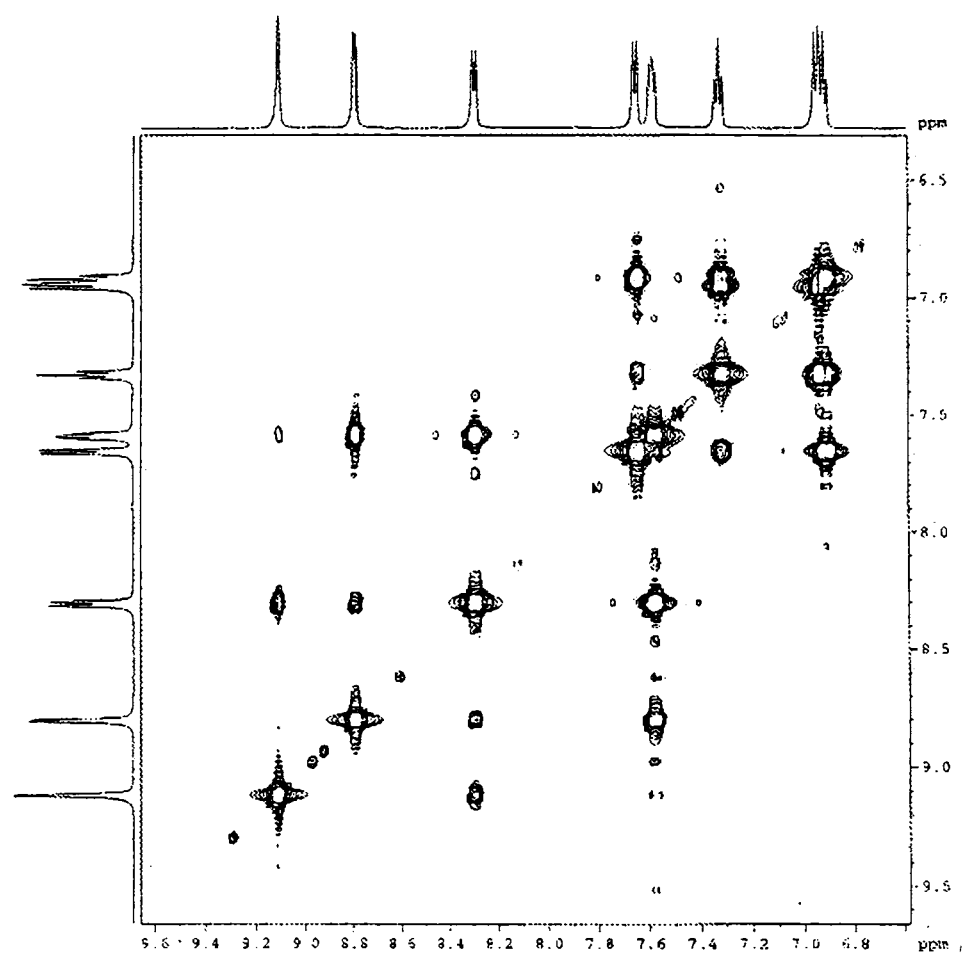


Fig.22. $^1\text{H}/^1\text{H}$ coupling observed in COSY of H_2L^2

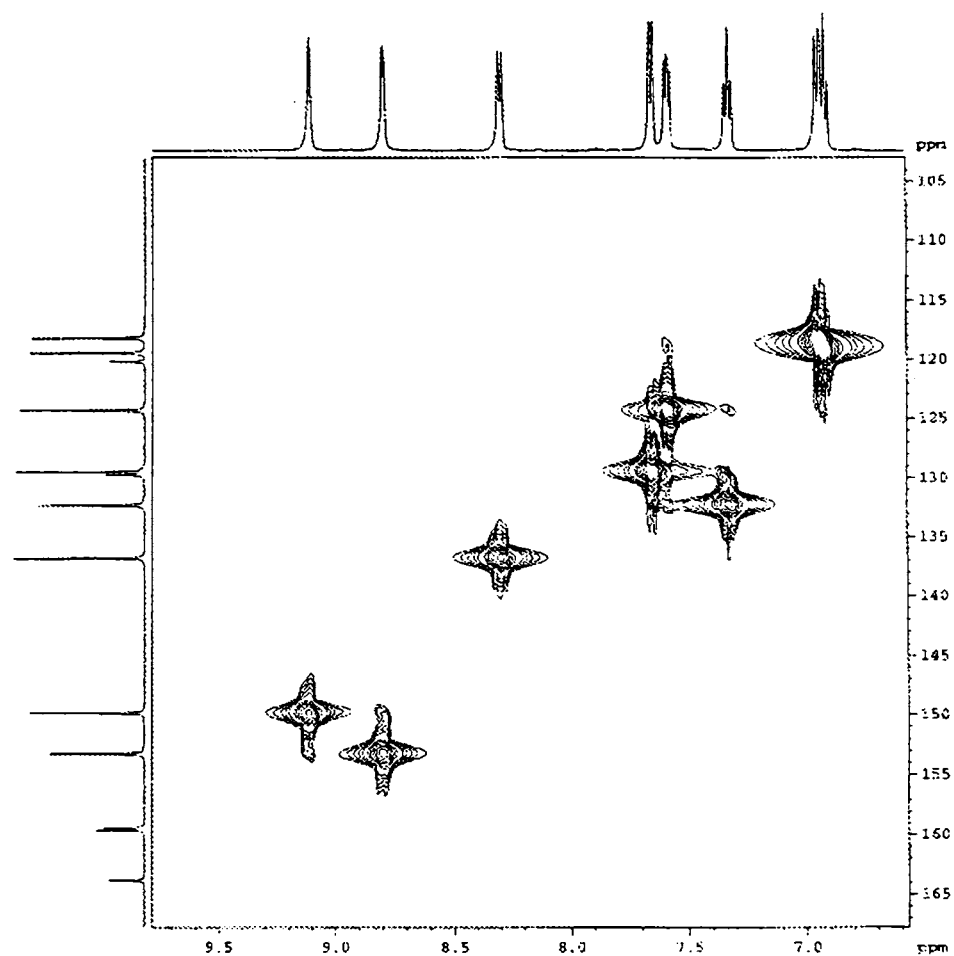


Fig. 22. ^{13}C - ^1H HMQC spectrum of H_2L^2

2.3.6. X-Ray data collection, structure solution and refinement

Single crystals of the H_2ApNH were obtained by slow evaporation of a methanol solution of the compound. A crystal, of size $0.18 \times 0.42 \times 0.52 \text{ mm}^3$, was mounted on glass fiber with epoxy cement for the X-ray crystallographic study. A summary of the crystallographic data for the title complex at 213 K is gathered in

Table 4. The data was collected with a 1-K SMART CCD diffractometer using graphite-monochromated MoK_{α} radiation with a detector distance of 4 cm and swing angle of -35° . A hemisphere of the reciprocal space was covered by combination of three sets of exposures; each set had a different of angle (0, 88, 180°) and each exposure of 30 sec covered 0.3° in ω . The structures were solved by direct methods and refined by least-square on F_o^2 using the SHELXTL [23] software package. The selected bond lengths and bond angles of H_2L^2 are listed in Table 5.

The molecule of H_2L^2 crystallizes into an orthorhombic lattice with a non-centrosymmetric space group $Pca2_1$. There are two crystallographically unique molecules of H_2L^2 in the asymmetric unit. The molecular structure showing 30% displacement ellipsoids with atomic-numbering scheme is shown in Fig. 24. The molecular packing of the molecule in a unit cell is shown in Figure 25.

The C8-O1 bond, which averages 1.242(6) Å in H_2L^2 is shorter than the C=O bond 1.236(4) in 3-formylpyridine semicarbazone [24] indicating considerable amount of the bond delocalisation with the pyridyl ring. As expected the C7-N1 bond length is 1.284(6) Å is comparable to the corresponding bond length of 1.291 Å reported for 2-hydroxyacetophenone thiosemicarbazone [25]. The O atom and the hydrazinic N1 atom are *trans* with respect to C8-N2 bond. Structure of the compound reveals quasi coplanarity of the whole molecular skeleton with localization of the double bonds in the central $-C=N-N-C=O$ which has an *E*- configuration with respect to the double bond of the hydrazone bridge. A *trans* - *cis* configuration is fixed around the N2-N1 (1.382 Å) single bond [26]. The phenolic ring maintains coplanarity with the central chain. The angle N2-C8-O1 (123.9°) is significantly greater than C9-C8-O1 (121.4°) possibly in order to relive repulsion between lone pairs of electrons on atoms N1 and O1. The central part of the molecule C7-N1-N2-C8-C9, adopts a completely extended conformation. The bond lengths C7-N1 (1.284 Å) and C8-O1 (1.242 Å) are typical of double bonds. So that the chain is likely correspond to C7=N1-N2-C8=O1. A similar observation was reported for a related molecule pyridoxal isonicotinoyl hydrazone [27].

Table 4. Summary of crystal data and structure refinement for H₂ApNH

| | |
|--|---|
| Empirical Formula | C ₁₄ H ₁₄ N ₃ O ₂ |
| Formula weight | 256.28 |
| Color; Shape | Greenish Brown; Block |
| Measured temperature | 213(2) K |
| Crystal system | Orthorhombic |
| Space group | <i>Pca</i> 2 ₁ |
| Unit cell dimensions | a= 8.2221(1)(5)Å, α=90° b=11.3743(1)Å, β=90° c=26.3962(4)Å, γ=90° |
| Volume V [Å ³] | 2468.59(5) |
| Z | 8 |
| D _x [g . cm ⁻³] | 1.379 |
| μ [mm ⁻¹] | 0.095 |
| Absorption Correction | Empirical |
| F(000) | 1080 |
| θ range [°] | 3.06 to 28.27 ° |
| Completeness to θ | 92.2% |
| <i>h, k, l</i> | -10/10,-15/12,-31/34 |
| Reflections collected | 14083 |
| Reflections unique | 5588 |
| <i>T</i> _{max} / <i>T</i> _{min} | 0.9831 and 0.9540 |
| Number of parameters | 345 |
| <i>GoF</i> | 1.004 |
| Final <i>R</i> indices [<i>I</i> ≥2σ(<i>I</i>)] | R1 = 0.0995, wR2 = 0.2415 |
| Residual highest peak and deepest hole | 1.142 and -0.746 e. Å ⁻³ |

Table 5. Selected bond lengths (Å) and bond angles (deg) of H₂ApNH

| | | | |
|------------|----------|------------------|----------|
| O(1)-C(8) | 1.242(6) | C(7)-N(1)-N(2) | 117.7(4) |
| O(2)-C(5) | 1.355(6) | C(8)-N(2)-N(1) | 120.8(4) |
| N(1)-C(7) | 1.284(6) | C(13)-N(3)-C(12) | 122.7(5) |
| N(1)-N(2) | 1.382(5) | O(2)-C(5)-C(6) | 124.1(4) |
| N(2)-C(8) | 1.339(6) | O(2)-C(5)-C(4) | 115.8(4) |
| N(3)-C(13) | 1.362(7) | N(1)-C(7)-C(6) | 116.3(4) |
| N(3)-C(12) | 1.374(7) | N(1)-C(7)-C(14) | 123.6(5) |
| C(1)-C(6) | 1.387(6) | O(1)-C(8)-N(2) | 123.9(5) |
| | | N(2)-C(8)-C(9) | 114.7(5) |
| | | C(10)-C(9)-N(3) | 119.8(6) |
| | | N(3)-C(9)-C(8) | 120.5(5) |
| | | C(9)-C(8)-O(1) | 121.4(6) |

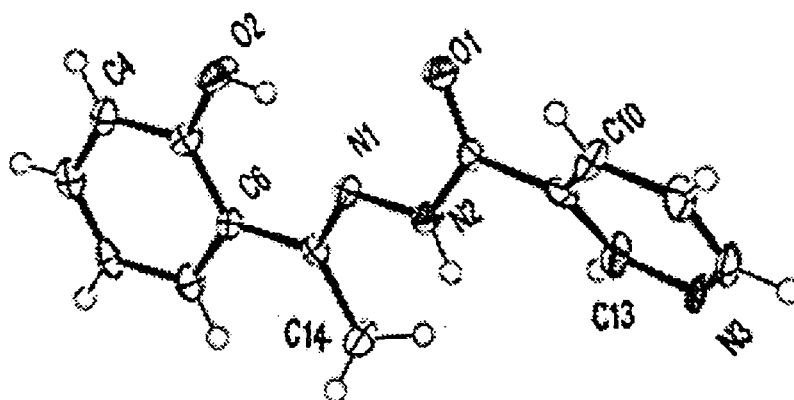


Fig. 24. Perspective view of one crystallographically unique molecule H₂L² with atom numbering scheme with atom numbering schemes and displacement ellipsoids at 50% probability level. Hydrogen atoms are shown as small spheres of arbitrary radii.

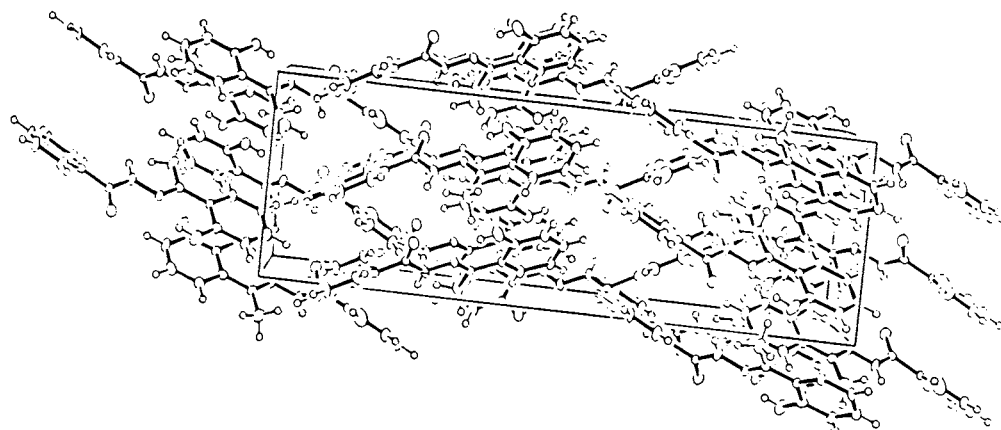


Fig. 25. Packing diagram of the compound H_2L^2

Concluding remark

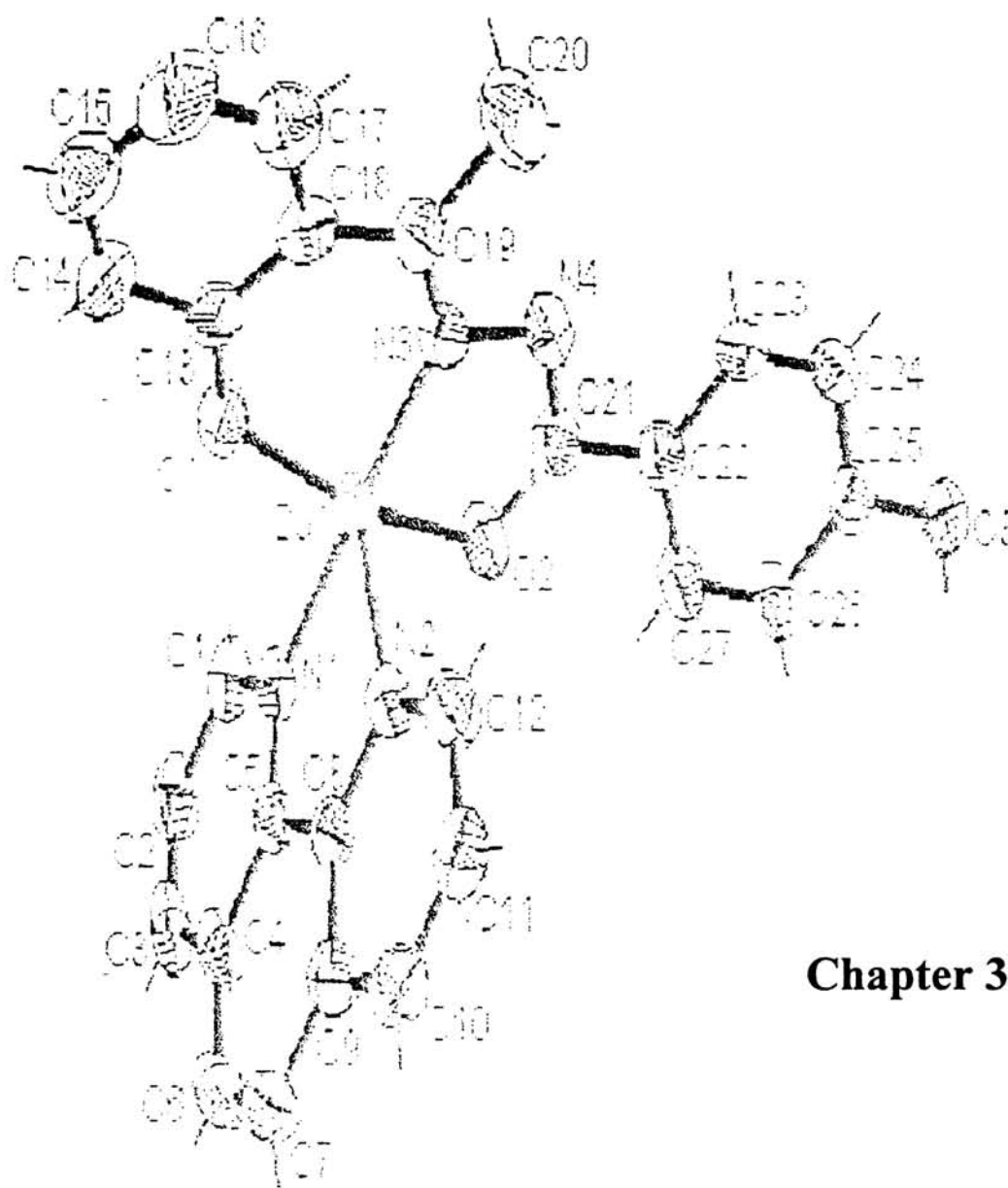
We had prepared five acid hydrazones, in which four are new compounds and studied and characterized by different physicochemical methods. Complete NMR assignments for one hydrazone was made using COSY homonuclear and HMQC heteronuclear correlation techniques. Solid state reflectance were also studied in order to understand the electronic structure of the all compounds. The crystal and molecular structures of one ligand was determined. The compound crystallizes into an orthorhombic lattice with a non-centrosymmetric space group $Pca2_1$ with two crystallographically unique molecules in an asymmetric unit. The geometry reveals quasi co-planarity in the whole molecular skeleton with localization of the double bonds in the $C=N-N-C=O$ with an *E*- configuration.

Reference:

- [1] M. Gallego, M. García-Vargas, M. Valcárcel, *Analyst* 104 (1979) 613.
- [2] M. Gallego, M. García-Vargas, F. Pino, M. Valcárcel, *Microchem. J* 23 (1978) 353.
- [3] S. S. Patel, A. D. Sawant, *Indian J. Chem. Tech* 8 (2001) 88.
- [4] K. H. Reddy, K. B. Chandrasekhar, *Indian J. Chem* 40A (2001) 727.
- [5] D. X. West, A. E. Liberta, S. B. Pandhey, R. C. Chikate, P. B. Sonawane, A. S. Kumbhar, R. G. Yerande, *Coord. Chem. Rev.* 123 (1993) 49.
- [6] D. Kovala-Demertzi, A. Domopoulou, M. Demertzis, C. Raptopoulou, A. Terzis, *Polyhedron* 13 (1994) 1917.
- [7] F. H-Ureña, N. A. I-Cabeza, M. N. M-Carretero, A. L. P-Chamorro, *Acta Chim. Slov.* 47 (2000) 481.
- [8] D.K.Johnson, T. B. Murphy, N.J.Rose, W.H.Goodwin, L.Picakrt *Inorg. Chim. Acta* 67 (1982) 159.
- [9] J. D. Ranford, J. J. Vittal, Yu. M. Wang, *Inorg. Chem* 37 (1998) 1226.
- [10] E. W. Ainscough, A. M. Brodie, A. J. Dobbs, J. D. Ranford, *Inorg. Chim. Acta* 267 (1998) 27.
- [11] S. C. Chan, L. L. Koh, P-H Leung, J. D. Ranford, K. Y. Sim, *Inorg. Chim. Acta* 236 (1995) 101.
- [12] C. Gosden, K. P. Healy, D. Pletcher, *J. Chem. Soc. Dalton Trans* (1978) 972.
- [13] C. Gosden, J. B. Kerr, D. Pletcher, R. Rosas, *J. Electroanal. Chem. Interfacial Electrochem.* 117 (1981) 101.

- [14] S. Bance, R. J. Cross, L. J. Farrugia, S. Kunjady, L. L. Meason, K. W. Muir, Maureen O'Donnel, R. D. Peacock, D. Stirling, S. J. Teat, *Polyhedron* 17 (1998) 4179.
- [15] K. P. Healy, D. Pletcher, *J. Organomet. Chem* 186 (1980) 401.
- [16] R. C. Aggarwal, T. R. Rao, *Tans. Met.Chem.* 2 (1977), 21 , R. C. Aggarwal, T. R. Rao, *Trans. Met.Chem.* 2 (1977) 57.
- [17] P. Domiano, A. Musatti, M Nardelli, C Pelizzi, *J. Chem. Soc., Dalton Trans.* (1975) 295.
- [18] Rastogi, DK, S.K Sahni, V. B. Rana, S.K Dua *Trans. Met Chem.* 3 (1978) 56.
- [19] T B. Murphy, N. J. Rose, V. Schomaker A. Aruffo, *Inorg. Chim Acta* 108 (1985) 183.
- [20] Z. Huszti., G. Szilagyi E. Kasztreiner, *Biochem. Pharmacol.* 32 (1983) 627.
- [21] O. V Arapov, O. F Alferva E. I. Levocheskaya, I. Krasil'nikov, *Radiobiologiya*, 27 (1987) 843.
- [22] H. Beraldo, W. F. Nacif, D. X. West, *Spectrochim. Acta* 57A (2001) 1847.
- [23] G. M. Sheldrick, *SHELXTL Version 5.1*, Bruker AXS Inc., Madison, USA. (1997).
- [24] H. Beraldo, W. F. Nacif, D. X. West, *Spectrochim. Acta* 57A (2001) 1847.
- [25] M. S. García, J. V. Martínez, R. A. Toscano, *Acta Crystallogr. C Cryst. Struc. Commun.* 44 (1988) 1247.
- [26] A. Lyubchova, A. C. Barbi, J. P. Doucet, *Acta Crystallogr. C Cryst. Struc. Commun.* 51 (1995) 1893.

- [27] J. P. Souron, M. Quarton, F. Robert, A. Lyubchova., A. C. Barbi., J. P. Doucet, *Acta Cryst.: C Cryst. Struc. Commun.* 51 (1995) 2179.



Chapter 3

**SYNTHESES, SPECTRAL CHARACTERIZATION, X-
RAY STRUCTURE, ELECTROCHEMICAL STUDIES
AND BIOLOGICAL INVESTIGATIONS OF COPPER(II)
TERNARY COMPLEXES 2-
HYDROXYACETOPHENONE 4-HYDROXYBENZOIC
ACID HYDRAZONE AND HETEROCYCLIC BASES**

3.1. Introduction

Copper is the third most abundant transition metal element in the biological systems, with an occurrence of 80-120 mg in the human body. The function of copper in the biological systems is primarily in redox reactions associated with the reduction of oxygen to water with transfer of oxygen to substrate. In attempt to model the physical and chemical behavior of the biological copper system an extensive effort was made to synthesis and characterize a plethora of coordination compounds [1-5].

Copper(II) complexes are outstanding as reagents or catalysts in the reaction of organic compounds. The importance of copper(II) species in oxygenation reactions has been reviewed [6-7]. The question of copper promoted reactions in *aromatic chemistry and the role of organometallic compounds in organic reactions has been widely investigated. In general the role of copper is intimately involved and related to the presence of copper(I) and copper(II) oxidation states, although there is little or no information on the stereochemistry of the various copper(I) and copper(II) or of their mechanism of involvement.*

The chemical properties of hydrazones have been intensively investigated in several research fields because of their chelating capability and their pharmacological applications. The antibacterial and antifungal properties of bis(acylhydrazone) and their complexes with some first transition series metal ions was studied and reported by *Carcelli et.al.* The evaluation of vitro antimicrobial properties showed some compounds to exhibit good activity against Gram positive bacteria [8]. Copper(II) complex of salicylaldehyde benzoylhydrazone was shown to be a potent inhibitor of DNA synthesis and cell growth. This hydrazone also has mild bacteriostatic activity and a range of analogues has been investigated as potential oral iron chelating drugs for genetic disorders such as thalassemia [9-11]. Intriguingly, the copper(II) complexes was shown to be significantly more potent than metal free chelate, leading to the suggestion that the metal complex was biologically active species. Prior to this the ligand found to possess mild bacteriostatic activity [12]. Because of the biological interest in this type of chelate system, several structural studies have been carried out in copper(II) [13-14]. With salicylaldehyde and its analogue. This type of diprotic ligand typically acts as tridentate planar chelating agents coordinating through the phenolic and amide oxygen and imine nitrogen. The actual ionization state is depend upon the condition and metal employed [13] with copper(II) with base, both the phenolic and amide protons are ionized; in neutral and acidic solutions the ligands are monoanionic, whereas strongly acidic conditions are necessary to form compounds formulated with neutral ligands.

In this chapter we report syntheses, analytical and spectral characterization electrochemical and structural studies and biological investigation of two ternary copper(II) complexes of aroyl hydrazones, derived from 4-hydroxybenzoic acid hydrazide and 2-hydroxyacetophenone (H_2L^4), and bidentate heterocyclic bases, 2,2'-bipyridine and 1,10-phenanthroline.

3.2. Experimental

3.2.1. Materials

Copper(II) chloride dihydrate (BDH) was of Analar grade and used without further purification. All the solvents were dried using standard methods before use.

3.2.2. Syntheses of complexes

Mixed ligand complexes CuLB , where L is the dianion of 2-hydroxyacetophenone 4-hydroxybenzoic acid hydrazone, B is the heterocyclic base, 2, 2' bipyridine or 1,10 phenanthroline were prepared as follows. To a hot ethanolic solution of 1 mmol of appropriate heterocyclic base, H_2L^4 (0.25 g, 1 mmol) in hot ethanol and filtered solution of copper(II) chloride dihydrate (0.2 g, 1 mmol) in ethanol was added. Resultant homogeneous green solution was stirred for 2 h. The green product formed was filtered and washed with hot ethanol, followed by ether, and dried in *vacuo* over P_4O_{10} . The X-ray quality single crystal of CuL^4phen was obtained from DMF solution by slow evaporation over a period of 2 weeks.

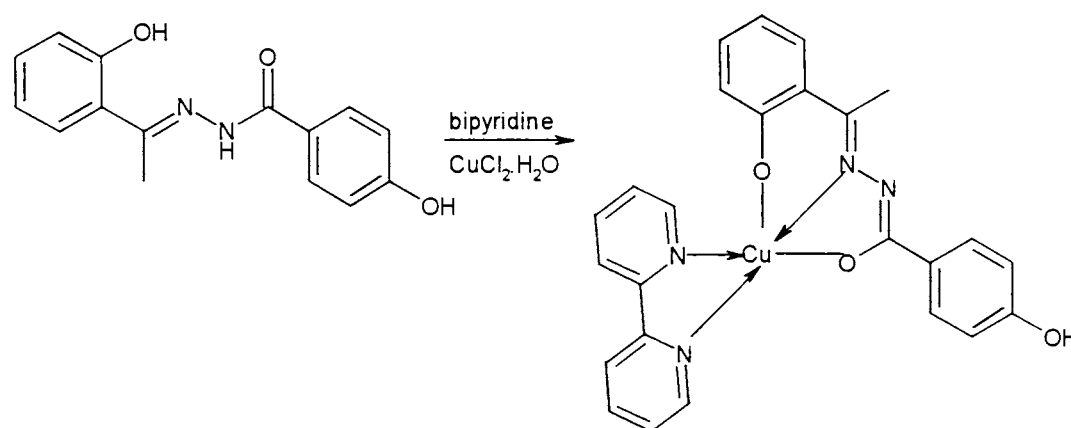


Fig. 1. Scheme of the synthesis of CuL^4bipy

3.2.3. *Physical measurements and instrumentation*

Cyclic voltametric studies were carried out on a Cypress system model CS-1090/model CS-1087 Computer controlled electroanalytical system. Measurements were made on degassed (N₂ bubbling for 10 minutes) solution in DMF (10⁻³ M) containing 0.1 M tetrabutyl ammonium tetrafluoro borate supporting electrolyte. The three electrode system consists of a glassy carbon (working) platinum wire (counter or auxiliary) and Ag/AgCl (reference) electrodes.

3.2.4. *X-Ray data collection, structure solution and refinement*

A dark green monoclinic crystal of CuL⁴phen having approximate dimensions 0.275 x 0.225 x 0.175 mm was sealed in glass capillary, and intensity data were measured at 212 K, on an Enraf-Nonius CAD-4 diffractometer equipped with graphite-monochromated Mo K α ($\lambda = 0.70930 \text{ \AA}$) radiation. Unit cell dimensions were obtained using 25 centered reflections in the θ range 5.54° - 12.20°. The intensity data were collected by ω -scan mode within $1.75 < \theta < 24.92^\circ$ for hkl ($0 \leq h \leq 10$, $0 \leq k \leq 18$, $-21 \leq l \leq 21$) in monoclinic system. The trial structure was obtained by direct methods using SHELXS-97 [15]. And refinement by full matrix least square on F² (SHELXL-97) [16]. The non hydrogen atoms were refined with anisotropic thermal parameters. All hydrogen atoms were geometrically fixed and allowed to refine a riding model. Absorption corrections were employed using ψ -scan ($T_{\text{max}} = 1.000$ and $T_{\text{min}} = 0.982$).

3.3. Results and discussion

3.3.1. *Syntheses of copper(II) complexes*

The colors, elemental analyses, stoichiometries of H₂L⁴ and its complexes are presented in the Table 1. The elemental analyses data are consistent with 1:1:1 ratio

of the metal ion : hydrazone : heterocyclic base for the complexes prepared. The complexes are insoluble in most of the common polar and non polar solvents. They are soluble in DMF and DMSO. The conductivity measurements in DMF showed that the complexes are non electrolytes

The magnetic moment in the polycrystalline state at 300 K of the complexes were found to be 1.85-1.93 BM, which are consistent with the spin only values for mononuclear d^9 copper(II) systems [17].

Table 1. Colours, elemental analyses and magnetic susceptibilities of copper(II) complexes

| Compound | Formula | Colour | Found (calculated) % | | | μ_{eff} BM |
|---------------------------|--|--------|----------------------|-------------|---------------|--------------------------|
| | | | C | H | N | |
| H_2L^4 | $\text{C}_{15}\text{H}_{14}\text{N}_2\text{O}_3$ | yellow | 66.70 (66.66) | 5.26 (5.22) | 10.43 (10.36) | - |
| CuL^4bipy | $\text{CuC}_{25}\text{H}_{20}\text{N}_4\text{O}_3$ | green | 61.92 (61.53) | 3.98 (4.13) | 11.59 (11.48) | 1.85 |
| CuL^4phen | $\text{CuC}_{27}\text{H}_{20}\text{N}_4\text{O}_3$ | green | 62.87 (63.34) | 4.04 (3.94) | 10.86 (10.94) | 1.93 |

3.3.2. EPR spectral studies

The EPR parameters obtained for the complexes in frozen DMF solution are presented in Table 2. The copper(II) ion, with d^9 configuration, has an effective spin of $S=3/2$ and associated with a spin angular momentum $m_s = \pm 1/2$ leading to a doubly degenerate spin state in absence of magnetic field. In magnetic field this degeneracy is lifted and the energy difference between these states is given by $\Delta E = h\nu = g\beta H$, where h is the Planck's constant, ν is the frequency g is the Lande splitting factor (equal to 2.0023 for free electron), β is the electronic Bohr magneton and H is the magnetic field. For the case of $3d^9$ copper(II) ion the appropriate spin Hamiltonian assuming a B_{1g} ground state is given by

$$H = \beta [g_{\parallel} H_z S_z + g_{\perp} (H_x S_x + H_y S_y)] + A I_z S_z + B (I_x S_x + I_y S_y)$$

The EPR spectra of the Cu(II) complexes in frozen DMF solution (77 K) gave axial spectra. The spectra of the complexes consist of four well defined hyperfine lines due to copper nuclei in the parallel region. However, for CuL⁴phen four hyperfine splitting due to copper nucleus is observed in the perpendicular region also. But the superhyperfine splitting due to coordinated nitrogen is not visible for both the complexes.

The $g_{\parallel} > g_{\perp}$ value suggest a distorted square pyramidal structure and rules out the possibility of trigonal bipyramidal structure which would be expected to have $g_{\perp} > g_{\parallel}$. Thus the polyhedron consists of one phenanthroline / bipyridine nitrogen, azomethine nitrogen, phenolate oxygen and enolate oxygen of hydrazone form base of the pyramid and the remaining nitrogen of the heterocyclic base occupies the apical position of the square pyramid [18-19].

EPR spectra are simulated to get accurate values of various magnetic parameters. The energies of d-d transitions were used to evaluated the bonding parameters α^2 , β^2 and γ^2 which may be regarded as measures of covalency of in plane σ bonds, in plane π bonds and out plane π bonds respectively.

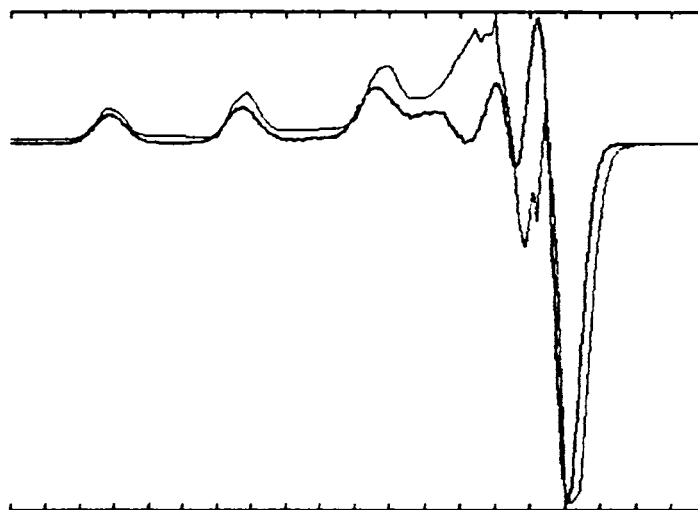


Fig. 2. Simulated best fits of CuL_4phen (green-exp.)

The geometric parameter,

$$G = (g_{\parallel} - 2) / (g_{\perp} - 2),$$

For axial spectra measures the exchange interaction between copper(II) centers in polycrystalline state. If $G > 4.0$ exchange interaction is negligible and if it is less than 4.0 considerable exchange interaction is indicated. In this complex $G = 4.09 - 4.56$ indicates exchange interaction is negligible. The observed g values in the complex lie above 2.040 with $G > 4.0$ are consistent with a $d_{x^2-y^2}$ ground state and with square base pyramidal stereochemistry [20-21]. The relatively high values of A_{\parallel} ($>150 \times 10^{-4} \text{ cm}^{-1}$), suggests small axial interaction [22].

The value of in plane π bonding parameter α^2 can be estimated from the expression and found to be ~ 0.78 .

$$\alpha^2 = -A_{\parallel} / 0.036 + (g_{\parallel} - 2.0023) + 3/7 (g_{\perp} - 2.0023) + 0.04$$

The orbital reduction factor $K_{\parallel} = \alpha^2 \beta^2$ and $K_{\perp} = \alpha^2 \gamma^2$ were calculated using the following expressions

$$K_{\parallel}^2 = (g_{\parallel} - 2.0023) \Delta E(d_{xy} \rightarrow d_{x^2-y^2}) / 8\lambda_0$$

$$K_{\perp}^2 = (g_{\perp} - 2.0023) \Delta E(d_{xz, yz} \rightarrow d_{x^2-y^2}) / 2\lambda_0$$

Where λ_0 is the spin orbit coupling constant and is of the value of -828 cm^{-1} for copper(II) d^9 system.

According to Hathaway for pure σ bonding $K_{\parallel} \approx K_{\perp} \approx 0.77$ for in plane π bonding $K_{\parallel} < K_{\perp}$ while for out plane π bonding $K_{\parallel} > K_{\perp}$. In this complex $K_{\parallel} > K_{\perp}$ stronger out of plane π bonding. The metal-ligand in plane σ bond is purely ionic if α^2 is unity. The trend of β^2 value is opposite to that observed for α^2 , indicating the competitive mechanism of in plane σ and π bonding. The value of γ^2 shows there is appreciable out of plane π bonding, which is further supported by $K_{\parallel} > K_{\perp}$.

The Fermi contact hyperfine interaction term, which is the measure of contribution of the s electron to the hyperfine interaction, can be estimated from the expression:

$$K_0 = A_{iso}/P\beta^2 + (g_{av} - 2.0023)/\beta^2$$

Where P is the free ion dipolar term and its value is 0.036. K_0 is a dimensionless quantity and is generally found to have a value of 0.30. The K_0 value obtained is in good agreement with the theoretical one, indicating the mixing of the 4s orbital with d orbital possessing an unpaired electron.

The empirical factor $f = g_{\parallel} / A_{\parallel}$, is an index of tetragonal distortion is calculated as 120.24 and 126.70 cm. The value may vary from 105-135 for small to

extreme distortion. The value here indicates medium distortion from the geometry the greater tetrahedral distortion may be due to flexible structure or the in vivo environment in which complex located in solvent system. Recent studies have shown that the biological activity is related to geometry at the metal site in terms of SOD like activity. The compounds with more tetrahedral distortion are reported to display higher activity [23-25].

Table 2. EPR and bonding parameters of copper(II) complexes

| | CuL ⁴ phen | CuL ⁴ bipy |
|------------------------|------------------------|------------------------|
| $g_{ }$ | 2.2402 | 2.2194 |
| g_{\perp} | 2.0586 | 2.0481 |
| $g_{av/iso}$ | 2.1193 | 2.1052 |
| $A_{ } (cm^{-1})$ | 186.0×10^{-4} | 175.1×10^{-4} |
| $A_{\perp} (cm^{-1})$ | 13.6×10^{-4} | 13.510^{-4} |
| $A_{av/iso} (cm^{-1})$ | 68.1×10^{-4} | 64.9×10^{-4} |
| G | 4.09 | 4.562 |
| α^2 | 0.818 | 0.764 |
| β^2 | 0.936 | 0.955 |
| γ^2 | 0.911 | 0.882 |
| K_o | 0.313 | 0.297 |
| $K_{ }$ | 0.767 | 0.731 |
| K_{\perp} | 0.74 | 0.674 |
| $f (cm)$ | 120.24 | 126.70 |

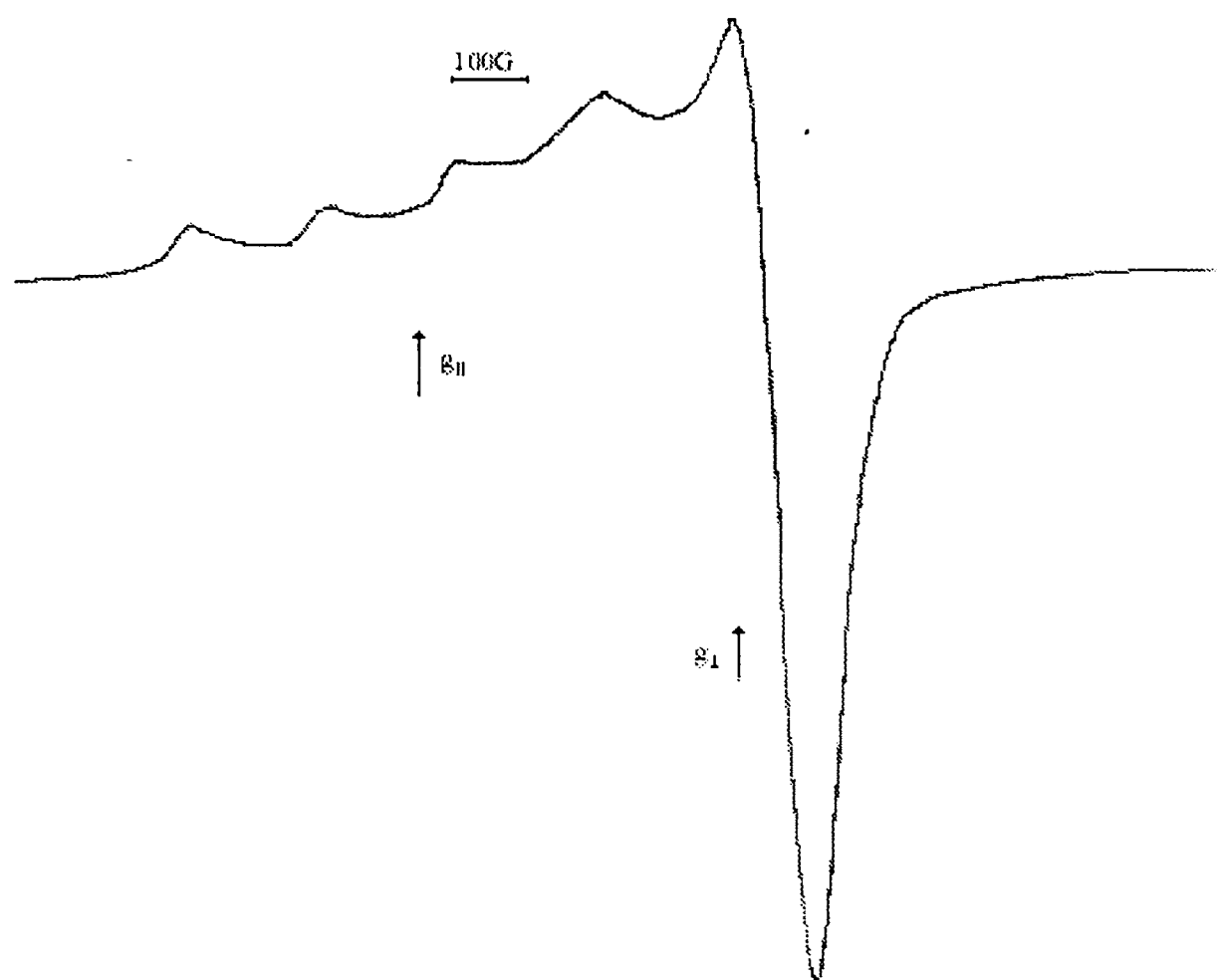


Fig. 3. Solution EPR spectra of CuL^4bipy at 77 K

3.3.3. Electronic spectral studies

The significant electronic absorption bands in the spectra of the complexes recorded in solid state, and are presented in the Table 3. The hydrazone ligands have $\pi \rightarrow \pi^*$ at 42553 and $n \rightarrow \pi^*$ at 31746 cm^{-1} . A second $n \rightarrow \pi^*$ band is found at 27778 cm^{-1} . There is a slight shift in these bands during complexation. The charge transfer maxima range from 21978 to 28736 cm^{-1} for complexes and may be assigned to an

O→Cu charge transfer transition, LMCT [26]. The d-d absorption maxima range from 16394 to 11560 cm^{-1} and tend to be indicative of tetragonal geometries [13, 27].

Table 3. Electronic spectral assignments (cm^{-1})

| Compound | d→d | LMCT | n→π* | π→π* |
|-----------------------|---------------------|-------|--------------|-------|
| H ₂ L | - | - | 31746, 27778 | 42553 |
| CuL ⁴ phen | 18149, 16393, 14066 | 21978 | 30675, 28248 | 42545 |
| CuL ⁴ bipy | 16394, 15385, 13889 | 22875 | 31746, 28736 | 36364 |

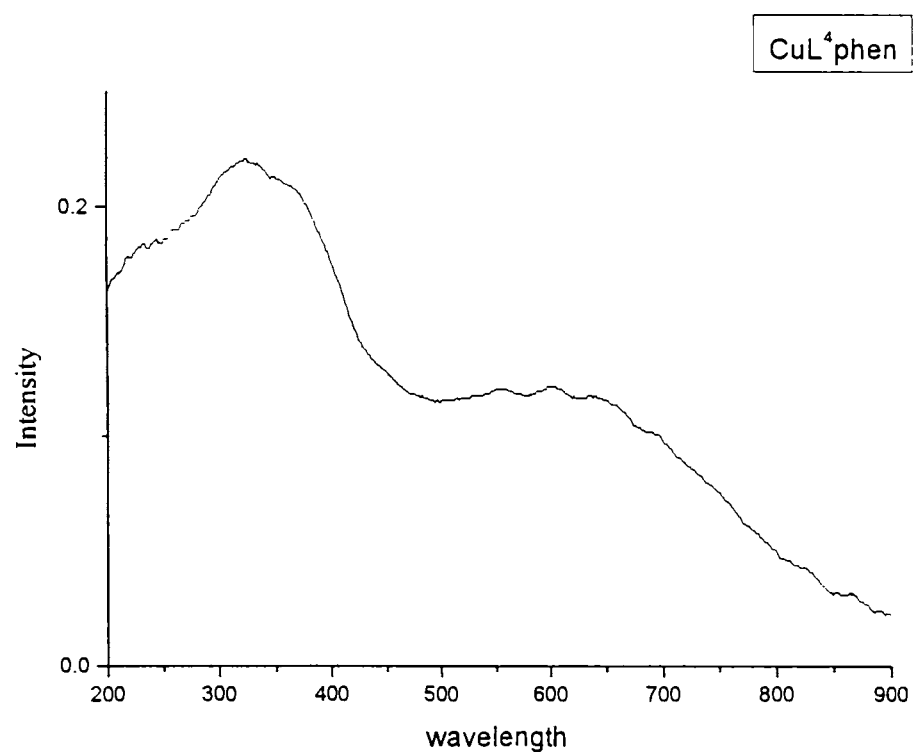


Fig. 4. electronic spectra of CuL⁴phen

3.3.4 IR spectral studies

The tentative infrared spectral assignments of H_2L^4 and CuL^4phen and CuL^4bipy are presented in the Table 4. The peak at 1610 cm^{-1} corresponding to $\nu(C=N)$ in the IR spectrum of uncomplexed hydrazone shifts to $\sim 1592\text{ cm}^{-1}$ upon complexation indicating azomethine nitrogen coordination [18-19, 28].

Further proof for the complexation for azomethine nitrogen is obtained from the appearance of a new band $\sim 423\text{ cm}^{-1}$ which is assignable for the $\nu(Cu-N)$ for the complexes. The increase in $\nu(N-N)$ in the spectra of complexes from 1001 to $\sim 1020\text{ cm}^{-1}$, is due to the increase in the double bond character offsetting the loss of electron density via donation to metal and is a further confirmation of coordination of the ligand through the azomethine atom. The spectral band of $\nu(N-H)$ of hydrazone disappears in the complexes indicating the deprotonation of N-H proton and coordination via enol oxygen. The IR spectra show a sharp band at $\sim 1500\text{ cm}^{-1}$ indicates the newly formed $N=C$, confirming the coordination of hydrazone takes place in the form of enol rather than as keto form. The loss of OH proton indicated by the absence of the band at $\sim 3400\text{ cm}^{-1}$ in the complexes. The $\nu(C-O)$ also decreased from 1279 to $\sim 1240\text{ cm}^{-1}$ when compared to the uncomplexed ligand. The fourth and fifth position are occupied by the nitrogen atoms of the heterocyclic bases, these $\nu(Cu-N)$ bands are assigned in $400-291\text{ cm}^{-1}$ indicated by the heterocyclic ring breathing in the finger print region of $1400-600\text{ cm}^{-1}$. The second OH group in the aromatic ring remains uncomplexed indicated by a band at $\sim 3057\text{ cm}^{-1}$ in the complexes.

Table 4. Selected IR frequencies of H₂L and copper(II) complexes (cm⁻¹)

| Compound | C=N | N=C | Cu-N | Cu-N (Heterocyclic base) | N-N | Heterocyclic breathing | Cu-O | C-O |
|-------------------------------|------|------|------|--------------------------------|------|---------------------------|------|------|
| H ₂ L ⁴ | 1610 | - | - | - | 1001 | - | - | 1279 |
| CuL ⁴ phen | 1593 | 1499 | 423 | 419, 304 | 1018 | 1430, 727 | 400 | 1243 |
| CuL ⁴ bipy | 1598 | 1503 | 420 | 422, 310 | 1022 | 1432, 861 | 391 | 1237 |

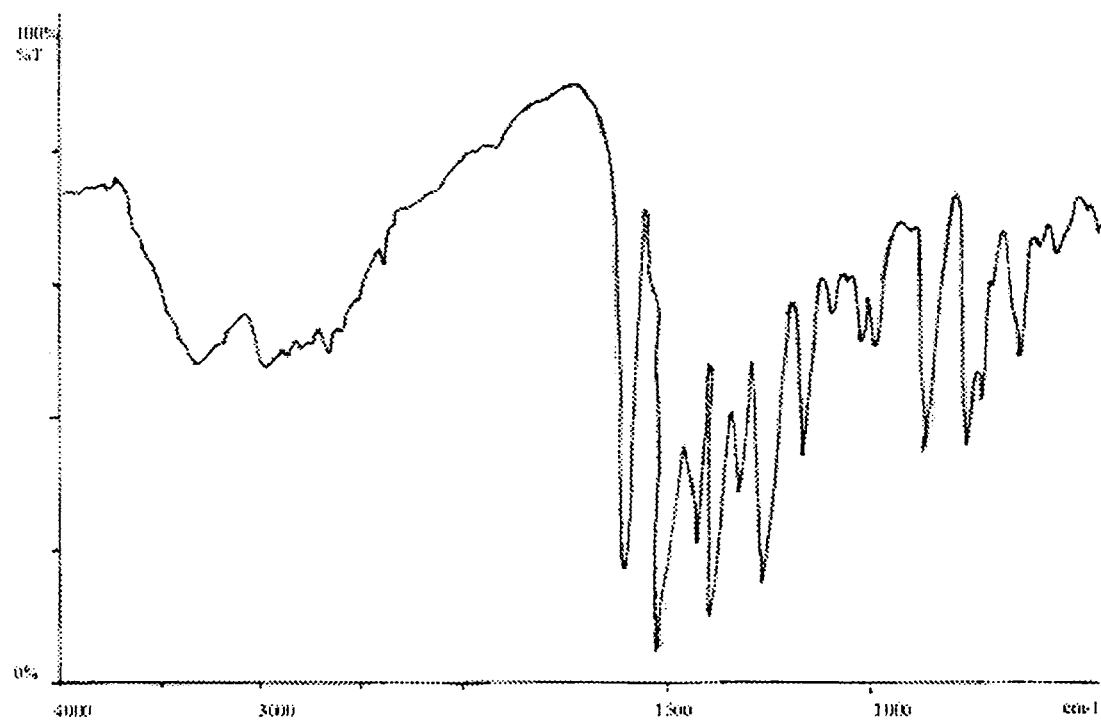
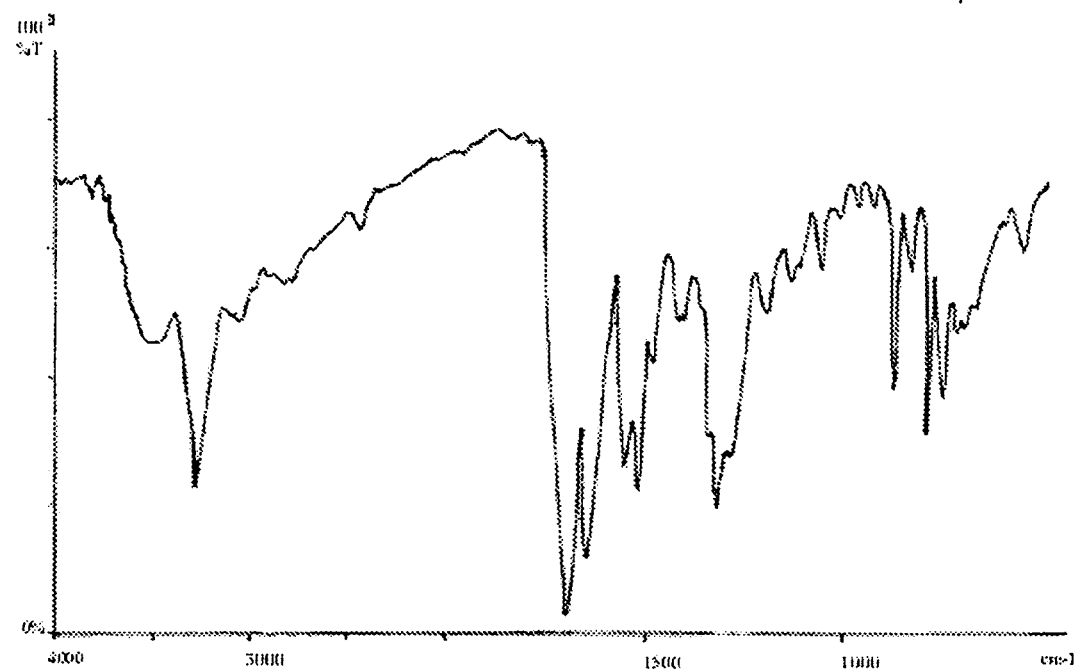
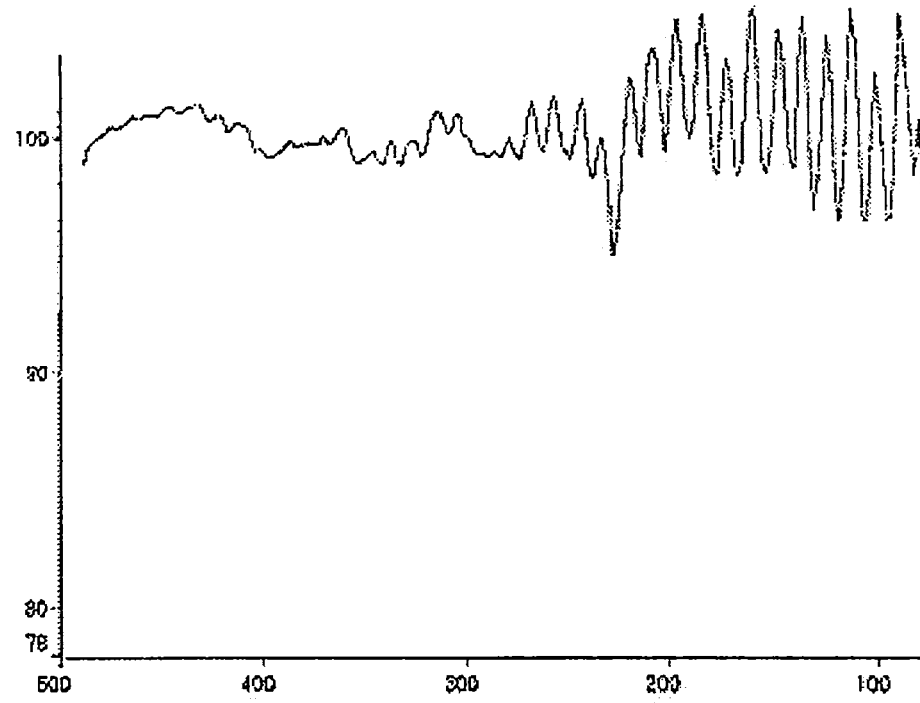


Fig. 5. IR spectra of H_2L^4 and CuL^4phen (cm^{-1})



Far IR spectrum of the H₂L⁴

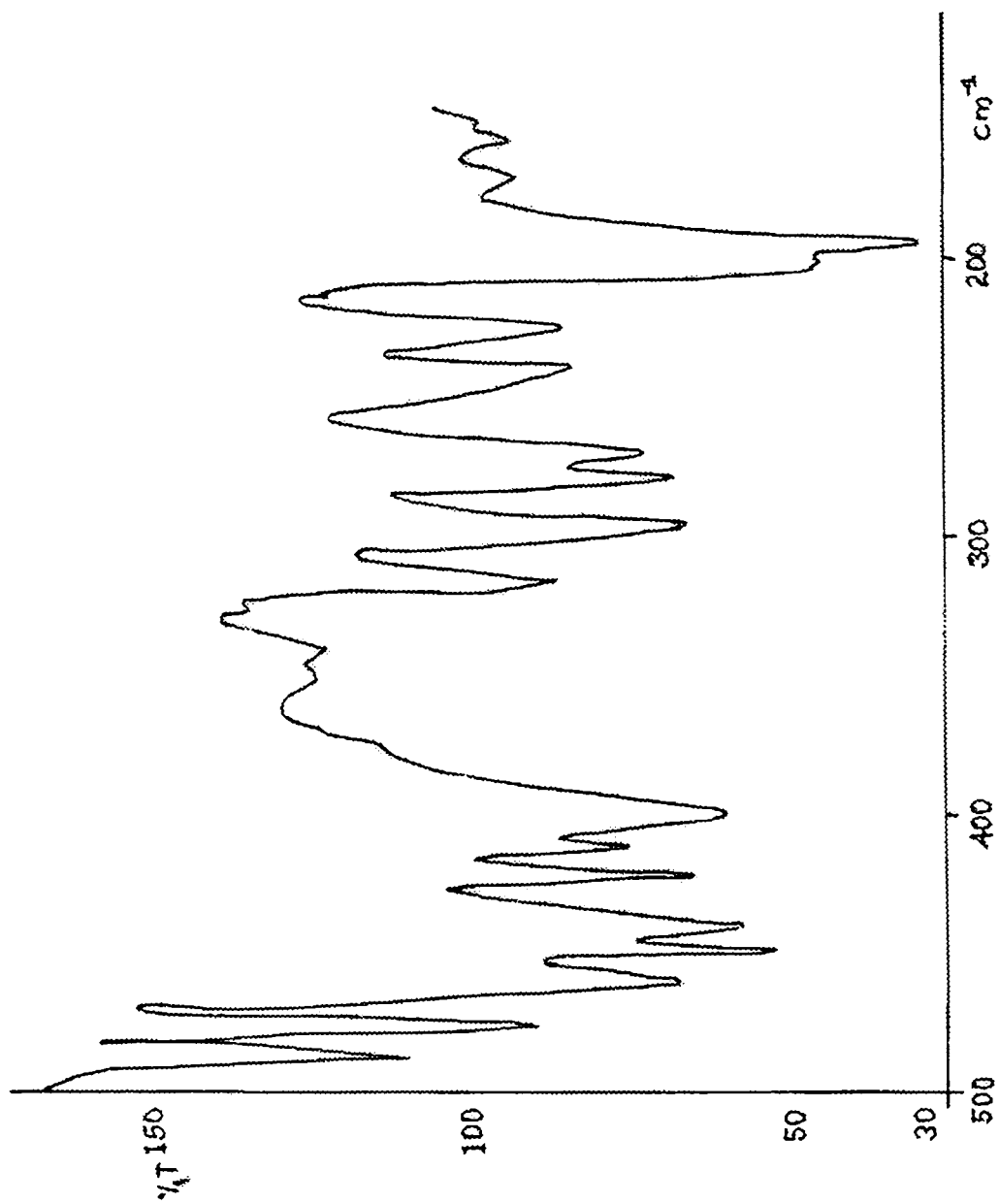


Fig. 6. Far IR Spectra of CuL⁴phen (cm⁻¹)

3.3.5. Crystal structure of CuL^4phen

The molecular structure of the complex along with the selected bond angles and bond lengths are summarized in the Table 6. The compound crystallized in a monoclinic lattice with a space group $P 2_1/c$. The unit cell volume contains 4 molecules. The copper in the mononuclear complex is a five coordinate and is having approximate square pyramidal geometry. The basal coordination positions are occupied by the phenolato oxygen O(1), azomethine nitrogen N(3), enolate oxygen O(2) of the hydrazone, and phen nitrogen N(1). The apical position occupied by second nitrogen of phen N(2) is at a larger distance (2.241) than compared to N(1) (2.047). The four base atoms are coplanar showing a significant distortion from square geometry indicated by O(1)-Cu(1)-O(2) bond angle (162.76). The central copper atom is displaced from basal plane in the direction of axial nitrogen, which is evident from the bond angles of N(1)-Cu(1)-N(3) (176.31), O(1)-Cu(1)-N(3) (91.90). The bond angles O(1)-Cu(1)-N(2) (101.34), N(1)-Cu(1)-N(2) (77.81), N(3)-Cu(1)-N(2) (102.55) indicate the distortion from the perfect square pyramidal geometry. One of the reasons for the deviation from an ideal stereochemistry is the restricted bite angle imposed by both the L and phen ligands. O(1)-Cu(1)-N(2) bond angle is 101.34 and O(2)-Cu(1)-N(2) bond angle 95.79 indicating that slight tilting of the axial Cu(1)-N(2) bond in the direction of O(2)-Cu(1). Bond away from the O(1)-Cu(1) bond. The variation in Cu(1)-N(1) (2.047), Cu(1)-N(2) (2.241), and Cu(1)-N(3) (1.938) indicate the different strength of the bond formed by each of the coordination nitrogen atoms. The difference in bond lengths can be attributed the difference in extent of π back donating between the phen and hydrazone moieties [19]. The packing of the complex is stabilized by intermolecular hydrogen bonding interactions and C-H π interaction between the atoms. The H-bonding parameters are listed in the Table 7 and 8.

Table 5. Crystal data and structure refinement for CuL⁴phen

| | |
|---------------------------------|---|
| Empirical formula | C ₂₇ H ₂₀ Cu N ₄ O ₃ |
| Formula weight | 512.01 |
| Temperature | 212(2) K |
| Wavelength | 0.70930 Å |
| Crystal system | monoclinic |
| Space group | P 2 ₁ /c |
| Unit cell dimensions | a = 8.4240(9) Å b = 15.4330(14) Å c = 17.8140(11) Å α = 90.000(7)° β = 95.190(7)° γ = 90.000(8)° |
| Volume | 2306.5(4) Å ³ |
| Z, Calculated density | 4, 1.474 Mg/m ³ |
| Absorption coefficient | 0.985 mm ⁻¹ |
| F(000) | 1052 |
| Crystal size | 0.275 x 0.225 x 0.175 mm |
| Theta range for data collection | 1.75 to 24.92° |
| Index range | 0 ≤ h ≤ 10, 0 ≤ k ≤ 18, -21 ≤ l ≤ 21 |
| Reflections collected / unique | 3139 / 3139 [R(int) = 0.0000] |
| Completeness to 2θ | 24.92 (74.8%) |
| Absorption correction | ψ-scan |
| Max. and min. transmission | 1.000 and 0.982 |
| Refinement method | Full-matrix least-squares on F ² |
| Data / restraints / parameters | 3139 / 0 / 396 |
| Goodness-of-fit on F | 1.050 |

| | |
|--------------------------------------|--|
| Final R indices [$I > 2\sigma(I)$] | $R_1 = 0.0410$, $wR_2 = 0.0882$ |
| R indices (all data) | $R_1 = 0.0628$, $wR_2 = 0.0985$ |
| Largest diff. peak and hole | 0.383 and -0.276 ($e \cdot \text{\AA}^{-3}$) |

Table 6. Selected bond lengths(\AA) and bond angles($^\circ$) for the compound CuL^4phen

| | | | |
|-------------|----------|------------------|------------|
| Cu(1)-O(1) | 1.926(3) | O(1)-Cu(1)-N(3) | 91.90(13) |
| Cu(1)-N(3) | 1.938(3) | O(1)-Cu(1)-O(2) | 162.76(12) |
| Cu(1)-O(2) | 1.954(3) | N(3)-Cu(1)-O(2) | 82.39(13) |
| Cu(1)-N(1) | 2.047(3) | O(1)-Cu(1)-N(1) | 91.63(12) |
| Cu(1)-N(2) | 2.241(3) | N(3)-Cu(1)-N(1) | 176.31(14) |
| N(1)-C(1) | 1.321(5) | O(2)-Cu(1)-N(1) | 93.92(11) |
| N(1)-C(5) | 1.360(5) | O(1)-Cu(1)-N(2) | 101.34(12) |
| N(2)-C(12) | 1.323(5) | N(3)-Cu(1)-N(2) | 102.55(12) |
| N(2)-C(8) | 1.348(5) | O(2)-Cu(1)-N(2) | 95.79(12) |
| N(3)-C(19) | 1.297(5) | N(1)-Cu(1)-N(2) | 77.81(12) |
| N(3)-N(4) | 1.406(4) | C(1)-N(1)-C(5) | 118.0(4) |
| N(4)-C(21) | 1.310(5) | C(1)-N(1)-Cu(1) | 126.0(3) |
| O(1)-C(13) | 1.336(5) | C(5)-N(1)-Cu(1) | 116.0(3) |
| O(2)-C(21) | 1.300(4) | C(12)-N(2)-C(8) | 117.7(4) |
| O(3)-C(25) | 1.370(5) | C(12)-N(2)-Cu(1) | 131.7(3) |
| O(3)-H(103) | 0.91(6) | C(8)-N(2)-Cu(1) | 110.7(2) |
| C(1)-C(2) | 1.401(6) | C(19)-N(3)-N(4) | 117.7(3) |
| C(1)-H(1) | 0.98(4) | C(19)-N(3)-Cu(1) | 128.6(3) |
| C(2)-C(3) | 1.346(7) | N(4)-N(3)-Cu(1) | 113.3(2) |
| | | C(21)-N(4)-N(3) | 109.6(3) |
| | | C(13)-O(1)-Cu(1) | 124.3(3) |
| | | C(21)-O(2)-Cu(1) | 108.5(3) |

Table 7. π - π interaction

| D-A | Cg-Cg Å | α ° | β ° |
|--------------------------|---------|------------|-----------|
| Cg(6)-Cg(6) ¹ | 3.6243 | 0 | 25.48 |
| Cg(6)-Cg(8) ¹ | 3.5232 | 1.6 | 23.02 |
| Cg(7)-Cg(8) ² | 3.5479 | 2.12 | 19.89 |
| Cg(8)-Cg(8) ² | 3.7596 | 0 | 28.18 |

Table 8. C-H π interactions

| X-H.....Cg | H-Cg Å | \angle X-H-Cg ° | X-Cg Å |
|--|-----------|-------------------|------------------|
| C(3)-H(3)-Cg(4) ² | 3.257 | 101.54 | 3.5370 |
| C(15)-H(15)-Cg(10) ³ | 3.120 | 177.88 | 4.0012 |
| C(20)-H(20)-Cg(10) ⁴ | 3.245 | 160.89 | 4.1621 |
| Cg (6) N(1) C(1) C(2) C(3)C(4)C(5) | | | 1: 1-x, -y, 1-z |
| Cg (7) N(2)C(8) C(9) C(10)C(11)C(12) | | | 2: 2-x, -y, 1-z |
| Cg (8) C(4)C(5)C(8)C(9)C(7)C(6) | | | 3: 1-x, ½+y, ½-z |
| Cg (10) C(22)C(23)C(24)C(25)C(26)C(27) | | | 4: -1+x, y, z |

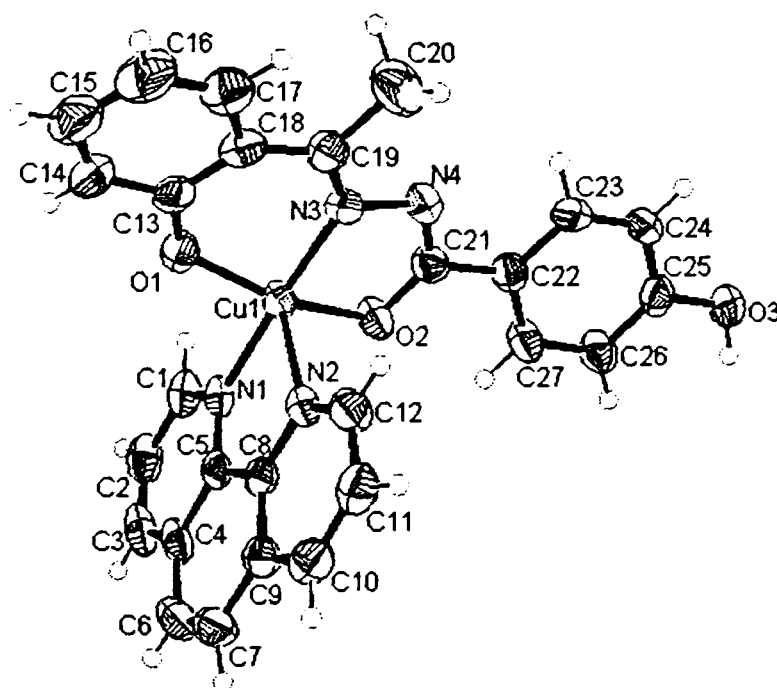


Fig. 7. A view of the compound CuL⁴phen with the atom numbering scheme. Displacement ellipsoids are drawn at 50% probability level and hydrogen atoms are shown as small spheres of arbitrary radii.

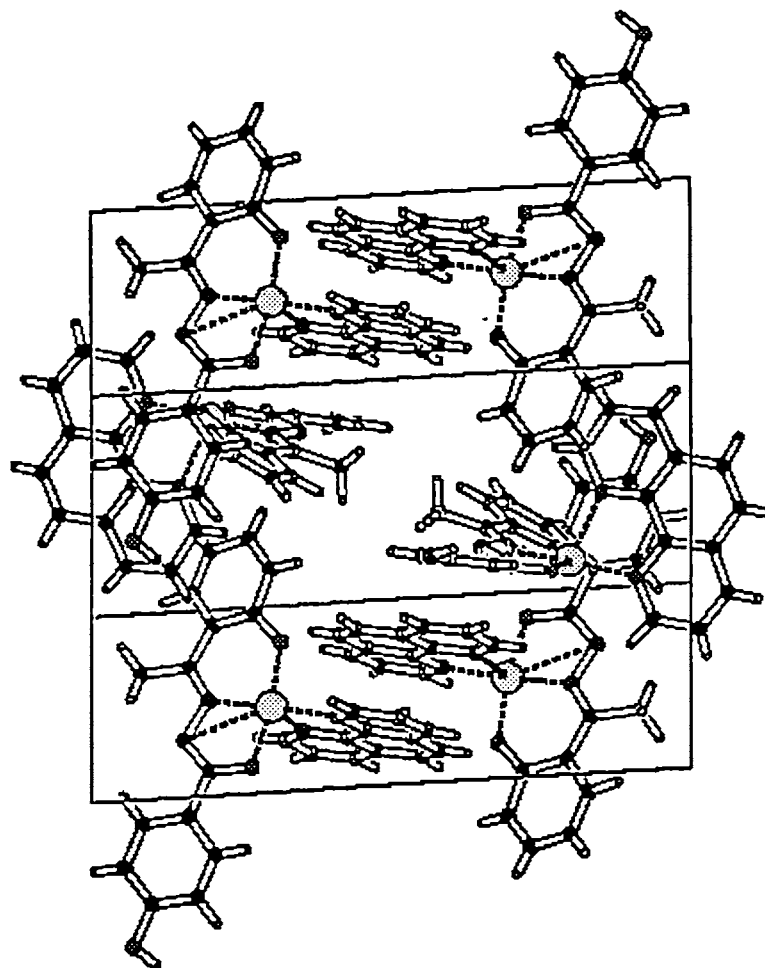


Fig. 8. Packing diagram for the compound CuL^4Phen

3.3.6. *Biological activity studies*

The synthesized chemical ligands and complexes were tested for their antimicrobial activity. The antimicrobial agent may be either bacteriostatic or bactericidal.

The effectiveness of an antimicrobial agent in sensitivity testing is based on the size of the zones of inhibition. When the test substances are introduced on to a lawn of bacterial culture by disc diffusion method.

Test organisms

The microorganisms used as test organisms were bacteria isolated from clinical samples. Two Gram positive bacteria and three Gram negative bacteria were used as test organisms.

A) Gram Positive

1. *Staphylococcus aureus*

2. *Bacillus sp*

B) Gram Negative

3. *Escherichia coli*

4. *Salmonella paratyphi*

5. *Vibrio cholerae 01*

The disc diffusion method was used for screening for the antimicrobial property of the test samples.

The free ligand showed no or little activity against both the *Gram positive* and *Gram negative* bacteria. CuL^4bipy found to be active against *Gram positive Bacillus sp.* but both are active against *Gram negative Vibrio cholerae 01*. CuL^4phen is found to be active against *Staphylococcus aureus*. The results of the antimicrobial studies were given in the Table 9.

Table 9. The antimicrobial activities of H_2L^4 and the complexes

| Compound | Microbial activity inhibition zone | | | | |
|---------------------------|------------------------------------|---------------------------|-------------------------|------------------------------|-----------------------------|
| | <i>Bacillus sp.</i> | <i>Vibrio cholerae 01</i> | <i>Escherichia coli</i> | <i>Staphylococcus aureus</i> | <i>Salmonella paratyphi</i> |
| H_2L^4 | - | - | - | - | - |
| CuL^4bipy | +9mm | +11mm | - | -8mm | -8mm |
| CuL^4phen | -8mm | +10mm | - | +9mm | - |

3.3.7. Electrochemical studies

The electrochemical properties of the metal complexes have been studied in order to monitor spectral and structural changes accompanying electron transfer [29].

Examination of the experimental data shows that the reduction of copper(II) is reversible. In this type of electron transfer process, the current is controlled by a mixture of diffusion and charge transfer kinetics and can be defined by the following criteria [30], $(E_{pa} - E_{pc})$ is greater than 59 mV and increases with increase in V . I_{pc}/I_{pa} is equal to unity indicates the chemical reversibility of the redox change and the value of $E_p - E_{p1/2}$ is $56.5/n$ mV, is also an indication of the reversibility of the reaction. The reversibility, associated with the reduction based on the E_p value, probably arises from the relaxation process involved in the stereochemical change from copper(II) to copper(I) [31]. The copper(II) to copper(I) redox processes are influenced by the coordination number, stereochemistry and the hard / soft character of the ligand's donor atoms. However due to inherent difficulties in relating coordination number and stereochemistry of the species present in solution, redox processes are generally described in terms of nature of the ligand present [32-33].

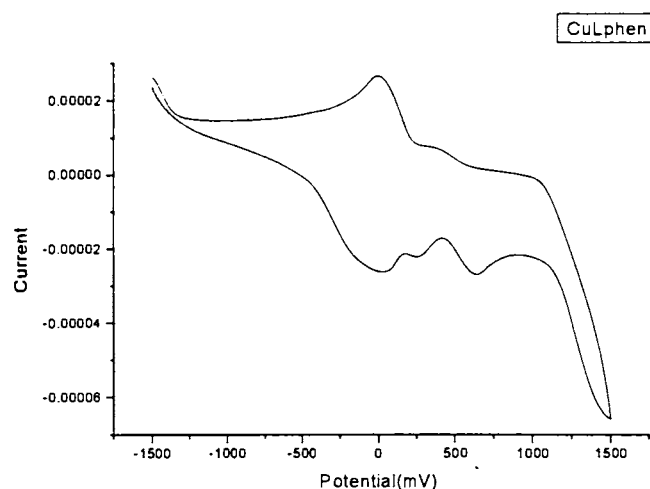


Fig. 8. Cyclic voltammogram for 10^{-3} M CuL^4phen in DMF at 300 K

Concluding remarks

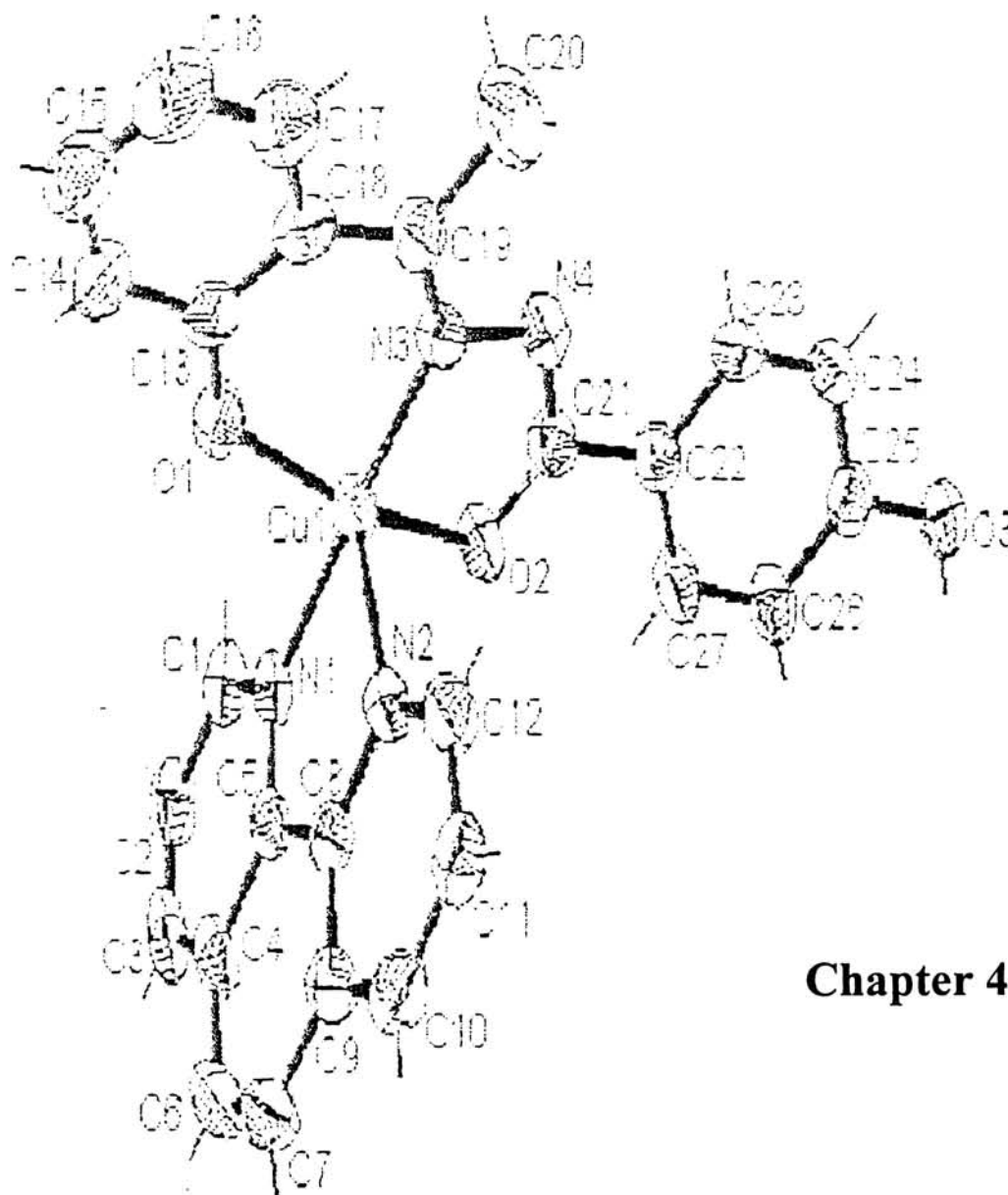
This chapter deals with the detailed preparative and physicochemical studies of two new heterocyclic base adducts of copper(II) complexes of general formula CuLB , where L is the dianion of 2-hydroxyacetophenone 4-hydroxybenzoic acid hydrazone and B is the heterocyclic base, 2, 2'-bipyridine (bipy) or 1, 10-phenanthroline (phen), have been synthesized and characterized by different physicochemical methods. The molar conductivity measurements in DMF solution indicate the non-electrolyte nature of both complexes. The electronic and IR spectroscopic data indicate that the complexes have square pyramidal geometry with one dibasic tridentate ligand L^{2-} , and one bidentate heterocyclic base. The coordination takes place through the deprotonated hydroxyl group, azomethine nitrogen and oxygen from the hydrazide moiety. The magnetic susceptibility values at room temperature are consistent with the spin only value for monomeric copper(II) species. EPR studies of all compounds gave axial spectra. Simulation EPR spectra gave the correct values for g and A for each compound. The g values indicate that the unpaired electron resides in the $d_{x^2-y^2}$ orbital. The crystal and molecular structure of CuL^4phen was determined by single crystal X-ray diffraction method. The compound crystallizes into monoclinic lattice with space group $P2_1/c$. Investigations on antimicrobial activities showed that they are moderately active against *Gram negative* bacteria. The electrochemical analysis showed that the Cu(II)/Cu(I) system is reversible.

References

- [1] K. Seff, *Acc. Chem. Res.* 9 (1976) 121.
- [2] H. S. Lee, W. V. Cruz, K. Seff, *J. Chem. Phys.* 86 (1982) 3562.
- [3] R. Osterberg, *Coord. Chem. Rev.* 12 (1974) 309.
- [4] I. Solomon, W. Penfield, D. E. Wilcox, *Struct. Bonding (Berlin)* 53 (1983).
- [5] H. S. Lee, K. Seff, *J. Phys. Chem.* 85 (1981) 397.
- [6] K. D. Karlin, J. Zubieta, *Copper Coord. Chem. Biological and Inorganic Perspectives*, Adenine Press, NY, (1983).
- [7] K. D. Karlin J. Zubieta, *Biological and Inorganic Copper Chemistry*, Adenine Press, NY, (1986).
- [8] M. Carcelli, P. Mazza, C. Pelizzi, G. Pelizzi, Zani, *J. of Inorg. Biochem.* 57 (1995) 43.
- [9] D. K. Johnson, T. B. Murphy, N. J. Rose, W. H. Goodwin, L. Pickart, *Inorg. Chim. Acta* 67 (1982) 159.
- [10] L. Pickart, W. H. Goodwin, W. Burgua, T. B. Murphy, D. K. Johnson, *Biochem. Pharmacol.* 32 (1983) 3868.
- [11] J. D Ranford, J. J. Vittal, Yu. M. Wang, *Inorg. Chem.* 37 (1998) 1226.
- [12] H. A. Offe, W. Siefken, *Domagk Gz, Naturforsch.* 7B (1952) 462.
- [13] E. W. Ainscough, A. M. Brodie, A. J. Dobbs, J. D. Ranford, *Inorg. Chim. Acta* 267 (1998) 27.

- [14] S. C. Chan, L. L. Koh, P-H Leung, J. D. Ranford, K. Y. Sim, *Inorg. Chim. Acta* 236 (1995) 101.
- [15] G. M. Sheldrick, SHELXS-97, Program for solution of Crystal Structures, University of Göttingen, Germany (1997).
- [16] G. M. Sheldrick, SHELXL-97, Program for solution of Crystal Structures, University of Göttingen, Germany (1997).
- [17] F. A. Cotton, G. Wilkinson, C. A. Murillo, M. Bochmann, *Advanced Inorganic Chemistry*, New York (1999) 867.
- [18] P. Bindu, M. R. P. Kurup, T. R. Satyakeerthy, *Polyhedron* 18 (1999) 321.
- [19] R. P. John, A. Sreekanth, M. R. P. Kurup, Anwar Usman, Abdul Razak Ibrahim H. K. Fun, *Spectrochim. Acta Part A*. 59 (2003) 1349.
- [20] B. J. Hathaway, A. A. G. Tomlison, *Coord. Chem. Rev.* 5 (1970) 1.
- [21] C. R. K. Rao, P. S. Zacharias, *Polyhedron*, 16(1997) 1201.
- [22] B. S. Garg, M. R. P. Kurup, S. K. Jain, Y. K. Bhoon, *Trans. Met. Chem.* 13 (1988) 309.
- [23] A. Diaz, R. Pogni, R. Cao, R. Basosi, *Inorg. Chim. Acta* 552 (1998) 275.
- [24] W. A. Alves, I. A. Bagatin, Ana Maria Da Costa Ferreira, *Inorg. Chim. Acta* 321 (2001) 11.
- [25] U. Sakaguchi, A. W. Addison, *J. Chem. Soc. Dalton Trans.* (1979) 600.
- [26] Mikuriya, H. Okawa and S. Kida, *Bull. Chem. Soc. Japan* 53 (1980) 3717.
- [27] A. B. P. Lever, *Inorg. Electronic Spectroscopy*, Elsevier, Amsterdam (1968).
- [28] M. R. P. Kurup *Trans. Met. Chem.* 22 (1997) 578.

- [29] A. M. Bond, R. L. Martin, *Coord. Chem. Rev.* 54 (1984) 23.
- [30] R. S. Nicholson, *Anal. Chem.* 37 (1965) 1351.
- [31] A. R. Hentrickson, R. L. Martin, N. M. Rhode, *Inorg. Chem.* 15 (1976) 2115.
- [32] B.J. Hathaway, In. *Comprehenssive Coordination chemistry*, vol. 5.
- [33] G. Wilkinson, R. D. Gillard, J. A McCleverty, editors. Pergomon Press, Oxford (1987).



Chapter 4

SYNTHESIS, SPECTRAL CHARACTERIZATION, AND BIOLOGICAL INVESTIGATIONS OF TERNARY OXOVANADIUM(IV) COMPLEXES OF SOME ACID HYDRAZONES AND 2, 2'- BIPYRIDINE

4.1. Introduction

The coordination chemistry of vanadium has received considerable attention since the discovery of vanadium in enzyme like bromoperoxidase and azetobactorvinelandii [1]. Its biological significance is further exemplified by its incorporation in natural products (amavadin in mushroom), in blood of sessile marine organism and enzyme in potent inhibitor of phosphoryl transfer [2]. Several vanadium compounds have recently been investigated in animal model systems as treatment for diabetes [3]. Studies are ongoing in clinical trial in human beings with organic transition metal complexes [4]. In addition human studies with vanadate have recently been reported [5].

The oxovanadium(IV) ion, VO^{2+} is considered to be the most stable oxo-metal species known and probably the most stable diatomic ion [6]. The ion forms wide variety of stable complexes of which, the physico-chemical properties notably electronic spectra, are of great interest. Most of these properties stem from the ground state electronic configuration of vanadium atom, $[\text{Ar}] 3d^1$, which shows similarities to Cu^{2+} , d^9 system. The ion also lends itself to study by EPR because of the isotropic purity of the ^{51}V isotope, its high nuclear spin $I=7/2$, and single unpaired outer electron [7]. It forms stable anionic, cationic and neutral complexes with various types of ligands.

Schiff bases contain reactive N=C sites which can be readily reduced to produce N-H functionalities that have a rather extensive chemistry. This N-H chemistry can be manipulated to produce potentially versatile chelate for vanadyl species [8].

In chapter we report synthesis, analytical and spectral characterizations of some oxovanadium(IV) complexes with four different aroyl hydrazones, derived from acid hydrazides namely, benzoic acid hydrazide, nicotinic acid hydrazide and 4-hydroxybenzoic acid hydrazides and salicylaldehyde and 2-hydroxyacetophenone. A bidentate heterocyclic base 2, 2' bipyridine was used as auxiliary ligands for coordination with oxovanadium(IV).

4.2. Experimental

4.2.1 Materials

Vanadium(IV) oxide acetylacetonate (Merck) was of Analar grade and used without further purification. All the solvents were dried using standard methods before use

4.2.2 Syntheses of complexes

Vanadium(IV) oxide acetylacetonate (1 mmol) was dissolved in dichloromethane. To a stirred ethanolic solution of hydrazones (1 mmol) and 2,2'-bipyridine (1 mmol), under dinitrogen atmosphere vanadyl solution was added. Resultant homogeneous brown solutions were continued to stirring for 3 hrs. Reddish orange products formed were filtered and washed with cold ethanol, followed by ether, and dried *in vacuo*.

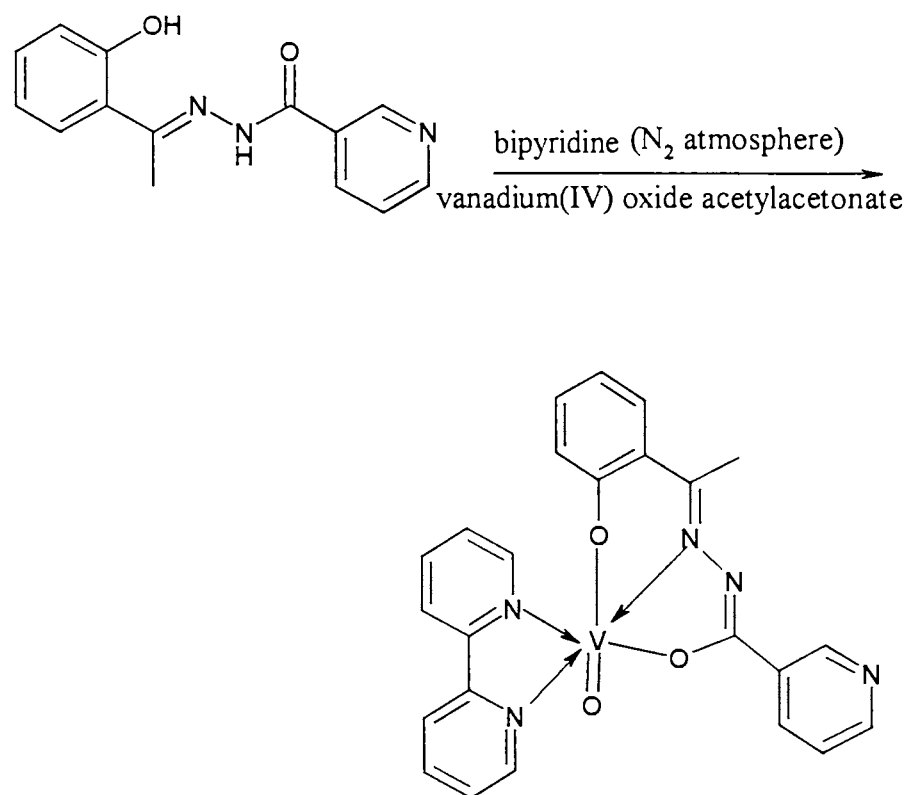


Fig. 1. Scheme of the synthesis of the complexes

4.3. Results and discussion

4.3.1. Synthesis of the oxovanadium(IV) complexes

The ligand were found to coordinate as dianionic L^{2-} on complexation to oxovanadium(IV). The complexes were found to be readily formed from vanadium(IV) oxide acetylacetonate solution in ethanol by H_2L in presence of heterocyclic base, 2, 2'- bipyridine. The elemental analysis of the complexes is in agreement with the formula $VOLbipy$. All the compound are found to be sparingly soluble in water, ethanol and methanol and soluble in DMF and DMSO. Conductivity measurement in DMF shows the complexes to be nonconductors.

4.3.2. Magnetic measurements

The magnetic moment obtained for the complexes are in the range of 1.57-1.91. The values are consistent with the spin only values of systems having one electron. These are magnetically diluted complexes in which metal ion is not involved in magnetic exchange with the neighboring metal ion through exchange force and orbital contribution to the magnetic moment is quenched [9].

Table 1. Colours and elemental analyses the ligands and complexes

| Compound | Colour | Analytical data found (calculated) | | |
|-------------------------------|----------------|------------------------------------|-------------|---------------|
| | | C % | H % | N % |
| H ₂ L ¹ | Pale yellow | 69.74 (70.00) | 5.19 (5.00) | 11.51 (11.66) |
| (VO)L ¹ (bipy) | Reddish orange | 63.17 (62.58) | 4.06 (3.93) | 12.19 (12.14) |
| H ₂ L ² | Pale yellow | 66.12 (65.85) | 5.24 (5.13) | 16.95 (16.46) |
| (VO)L ² (bipy) | Reddish orange | 60.47 (60.51) | 4.13 (4.02) | 14.55 (14.70) |
| H ₂ L ⁴ | Pale yellow | 66.66 (66.70) | 5.22 (5.26) | 10.36 (10.43) |
| (VO)L ⁴ (bipy) | Reddish orange | 61.34 (61.11) | 4.23 (4.10) | 11.24 (11.4) |
| H ₂ L ⁵ | Pale yellow | 60.70 (60.23) | 4.83 (4.60) | 16.55 (16.21) |
| (VO)L ⁵ (bipy) | Reddish orange | 59.19 (59.79) | 3.84 (3.71) | 14.64 (15.15) |

4.3.3. Electronic spectral analysis

The solid state visible spectra show the characteristic series of absorption bands common to vanadyl systems. In terms of Ballhausen and Gray model for the one electron transitions [10], accordingly, the first absorption band ~14300 cm⁻¹ region can be assigned to the electronic transition ²B₂→²E (d_{xy}→d_{xz}, d_{yz}), the second signal ~18200 cm⁻¹ due to ²B₂→²B₁ (d_{xy}→d_{x²-y²) and ²B₂→²A₁ (d_{xy}→d_{z²}).}

Table 2. Electronic spectral assignments (cm^{-1})

| Compound | ${}^2B_2 \rightarrow {}^2B_1$ | LMCT | $n \rightarrow \pi^*$ | ${}^2B_2 \rightarrow {}^2E$ |
|---------------------------|-------------------------------|-------|-----------------------|-----------------------------|
| (VO)L ¹ (bipy) | 18518 20560 | 25125 | 33333 | 14705 |
| (VO)L ² (bipy) | 18450 20408 | 23809 | 34722 31520 | 14306 |
| (VO)L ⁴ (bipy) | 18398 20320 | 25120 | 30769 | 14520 |
| (VO)L ⁵ (bipy) | 18248 19230 | 24390 | 34482 | 14285 |

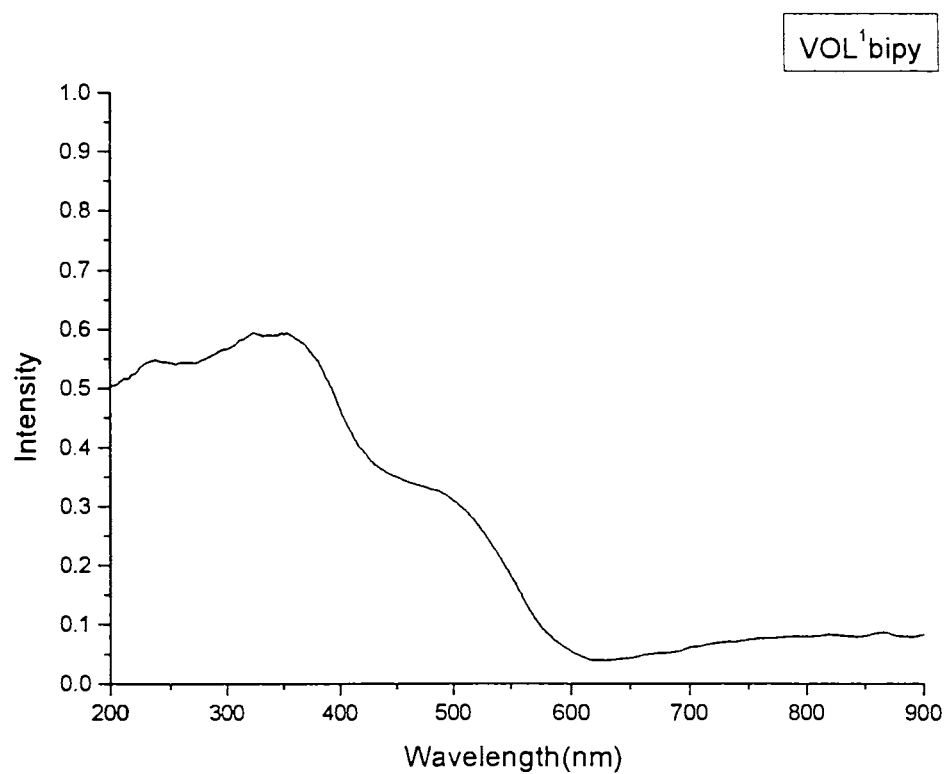


Fig. 2. Electronic spectrum of VOL¹bipy

4.3.4. *Electron paramagnetic resonance spectral studies*

Electron paramagnetic resonance spectroscopy examines the transition between electron spin state separated by the presence of an external magnetic field. These states are separated by an energy dependent g of the observed species and magnetic field applied. The value g of vanadyl epr spectra is typically less than free electron value. These electronic states are then split by spin of nucleus termed hyperfine splitting. The spin value of ^{51}V is $I = 7/2$, so the states are split into $2I + 1 = 8$ different energy levels, each separated by a hyperfine splitting constant, A . further splitting of states by nearby nuclei, such as ^{14}N referred to superhyperfine coupling. For the vanadyl case, due to electron residing in a sigma non-bonding orbital pointing away from the ligands in the equatorial (xy) plane, superfine coupling to nitrogen-containing ligands is not resolved in a typical X-band EPR spectrum. Therefore there is no additional splitting of EPR absorption. For oxovanadium, due to strong vanadium-oxygen interaction in vanadyl unit axial or nearly EPR spectra are usually observed for vanadyl complexes.

In these cases, all spectra were recorded in DMF solution at liquid nitrogen temperature (77 K) and axially anisotropic spectra are obtained with two sets of eight line pattern with $g_{\parallel} < g_{\perp}$ and $A_{\parallel} > A_{\perp}$ relationship is characteristics of an axially compressed d_{xy}^1 configuration [11-12].

The spectra show two type of resonance components, one set is due to parallel features and other set due to perpendicular features, which indicate axially symmetric anisotropy with sixteen line hyperfine splitting, characteristic of interaction between the electron and vanadium nuclear spins, g_o and A_o values are remarkably constant for all complexes. Ligand nitrogen or hydrogen superhyperfine splittings are not observed on vanadium line. This indicates the unpaired electrons to be in b_{2g} orbital (d_{xy} , 2B_2 ground state) localized in metal, thus excluding the possibility of its interaction with ligands [13-18].

The spectra signals are characteristic of mononuclear VO^{2+} species. The isotropic parameter g_o and A_o are ~ 1.98 and ~ 88 G respectively. These values are

in range of typical for VO²⁺ octahedral complexes [19-20]. It is reported the *g* and *A* values are very sensitive to the vanadium coordination environment and may be used to distinguish between the species with different coordination environment. In the present case *A* and *g* values for all the complexes are almost same and therefore no appreciable change in the coordination environment.

The molecular orbital coefficients α^2 and β^2 were also calculated for the complexes by using the following equations.

$$\alpha^2 = [2.0023 - g_{||} E / 8\lambda \beta^2]$$

$$\beta^2 = 7/6 [(-A_{||}/P) + (A_{\perp}/P) + (g_{||} - 5/14 g_{\perp}) - 9/14 g_e]$$

where $P = 128 \times 10^{-4} \text{ cm}^{-1}$, $\lambda = 135 \text{ cm}^{-1}$ and *E* is the electronic transition energy of ²B₂ → ²E. The lower values for α^2 compared to β^2 indicated that in-plane σ bonding is more covalent than in-plane π bonding [21].

The in-plane π bonding parameter β^2 observed are consistent with those observed for McGarvey and Kilvelson for vanadyl complexes of acetyl acetone.

Table 3. EPR and bonding parameters of oxovanadium complexes

| | (VO)L ¹ (bipy) | (VO)L ² (bipy) | (VO)L ⁴ (bipy) | (VO)L ⁵ (bipy) |
|--|---------------------------|---------------------------|---------------------------|---------------------------|
| μ BM | 1.90 | 1.67 | 1.60 | 1.61 |
| <i>g</i> | 1.960 | 1.963 | 1.964 | 1.956 |
| <i>g</i> _⊥ | 1.992 | 1.994 | 1.998 | 1.986 |
| <i>g</i> _{av/iso} | 1.981 | 1.981 | 1.986 | 1.979 |
| <i>A</i> (cm ⁻¹) | 145.99×10 ⁻⁴ | 147.65×10 ⁻⁴ | 146.97×10 ⁻⁴ | 141.54×10 ⁻⁴ |
| <i>A</i> _⊥ (cm ⁻¹) | 46.38×10 ⁻⁴ | 49.13×10 ⁻⁴ | 52.51×10 ⁻⁴ | 50.99×10 ⁻⁴ |
| <i>A</i> _{av/iso} (cm ⁻¹) | 79.96×10 ⁻⁴ | 82.2×10 ⁻⁴ | 84.34×10 ⁻⁴ | 82.00×10 ⁻⁴ |
| α^2 | 0.616 | 0.589 | 0.578 | 0.869 |
| β^2 | 0.947 | 0.939 | 0.903 | 0.704 |

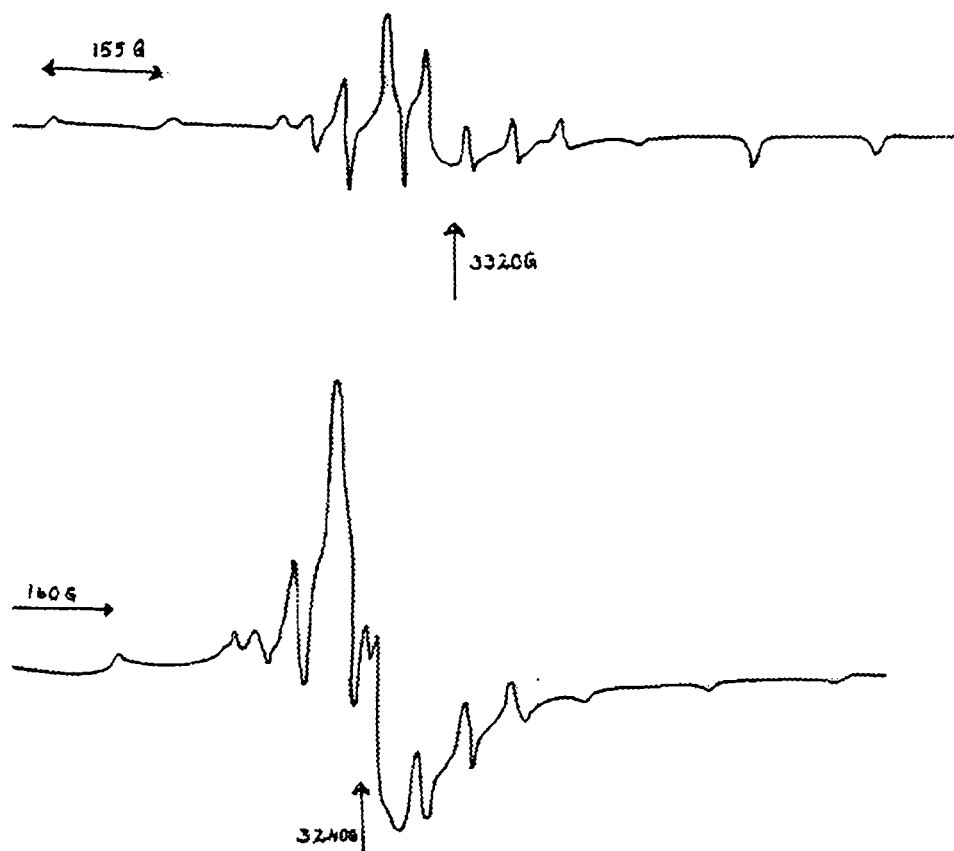


Fig. 3. EPR spectra of VOL²bipy and VOL⁵bipy

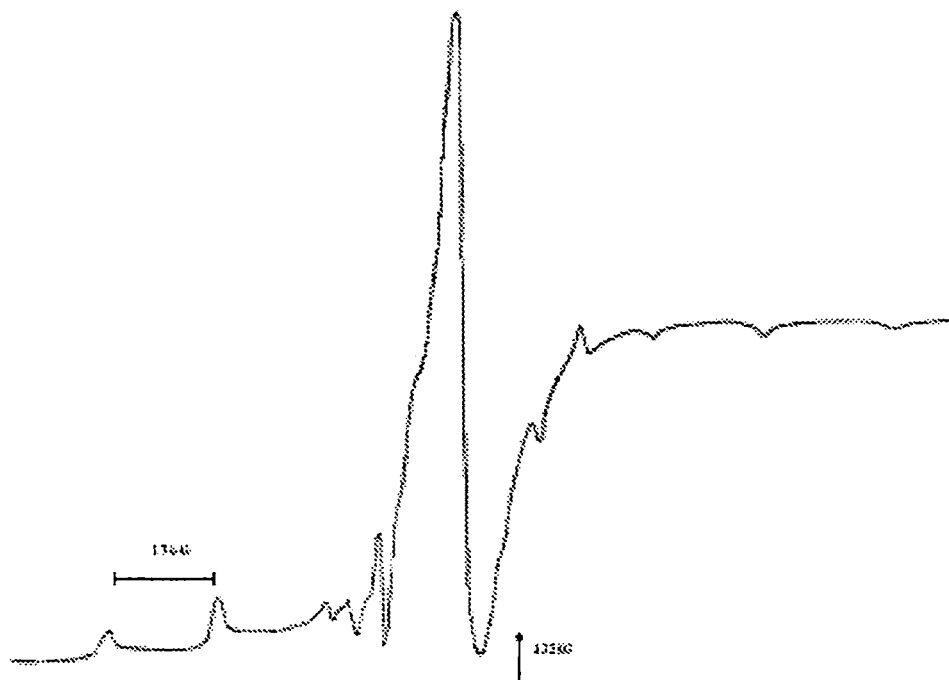


Fig. 4. EPR spectrum of VOL¹bipy

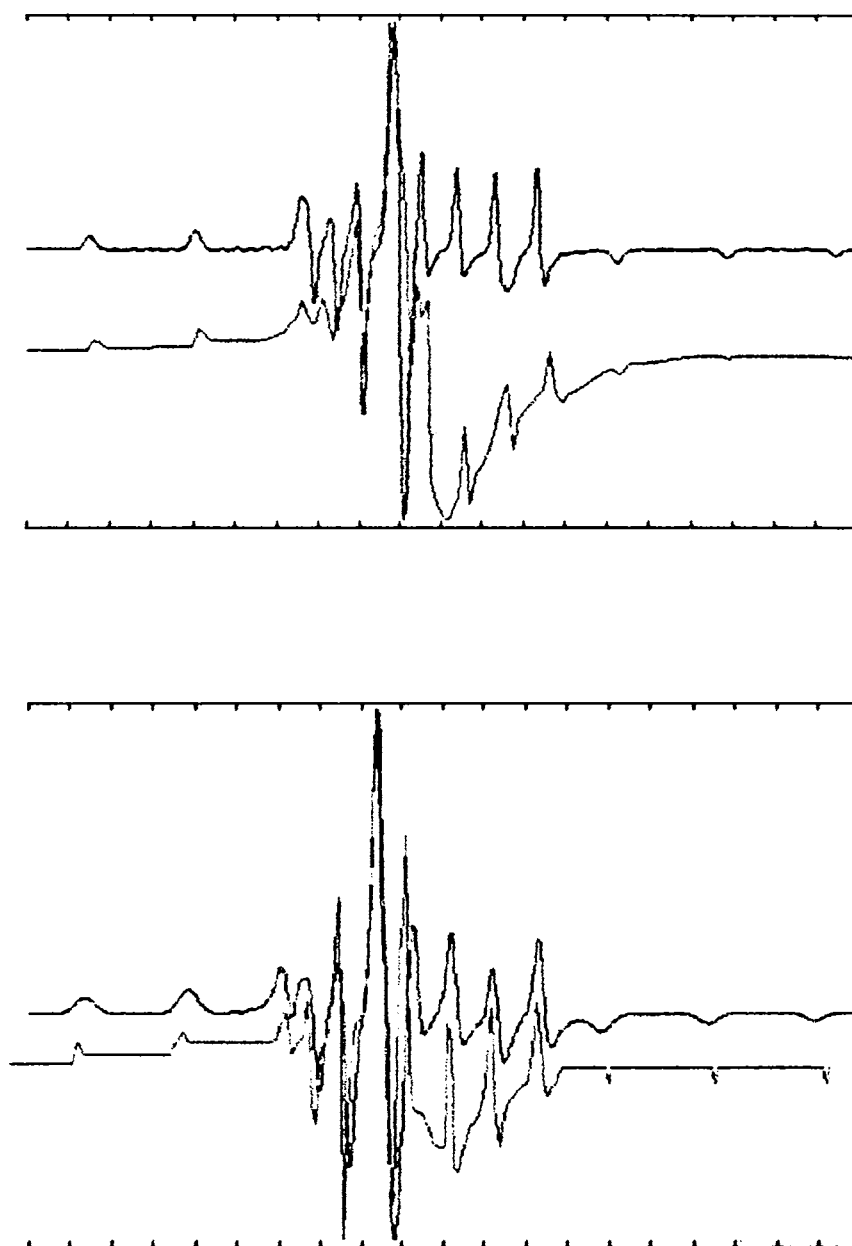


Fig. 5. Simulated best fits of EPR spectra of VOL²bipy and VOL⁵bipy (green-exp.)

4.3.5. Infrared spectral studies

Compound H_2L^1 , H_2L^2 , H_2L^4 and H_2L^5 show a band around 3400 and 3200 cm^{-1} , which are due to OH stretching mode and NH stretching mode of free OH group and NH respectively. These bands are absent in complexes, which suggests deprotonation of the phenolic group indicating the coordination through phenolic oxygen, and enolisation of the carbonyl group, followed by deprotonation. IR spectra of complexes show sharp band at 1536-1510 cm^{-1} due to newly formed N=C bond indicating the coordination of hydrazones take place in the form of enol rather than as keto form. The lowering of the band approximately 1610 cm^{-1} (C=N) by 20-13 cm^{-1} , is explicit evidence for coordination of the hydrazone through the azomethine nitrogen. The spectrum of the complexes exhibit a symmetric shift in the position of the band in the region 1600-1350 cm^{-1} due to C=C and C=N vibrational modes and their mixing patterns are different from those present in ligands spectra. Coordination of heterocyclic base is indicated by weak bands in the region of 455-443 cm^{-1} , are due to (V-N) stretching vibrations. Weak bands in the region 520-510 cm^{-1} indicate V-O (aryl) bond, resulting from the coordination of phenolic oxygen. A very sharp peak at 963-955 cm^{-1} suggests the presence of V=O bond in complexes. The frequency range observed in complexes indicates V=O bond is weakened by strong σ and π electron donation by enolate and phenoxy groups to the antibonding orbital of the V=O group [22-23]. The variations in frequency suggest that the $d\pi - p\pi$ overlap between vanadium and oxygen atom is influenced by substituents and co-ligands [11,24-25].

Table 4. Selected IR frequencies of ligands and oxovanadium(IV) complexes

| Compound | $\nu_{C=N}$ | $\nu_{N=C}$ | ν_{C-O} | $\nu_{V=O}$ | ν_{V-O} | ν_{V-N} | ν_{bipy} |
|-----------------|-------------|-------------|-------------|-------------|-------------|-------------|----------------|
| H_2L^1 | 1620 | | | | | | |
| $(VO)L^1(bipy)$ | 1600 | 1536 | 1344, 1469 | 955 | 518 | 455, 419 | 1438, 712, 616 |
| H_2L^2 | 1603 | | | | | | |
| $(VO)L^2(bipy)$ | 1589 | 1528 | 1366, 1471 | 963 | 510 | 443, 417 | 1436, 722, 628 |
| H_2L^4 | 1610 | | | | | | |
| $(VO)L^4(bipy)$ | | 1535 | 1347, 1458 | 970 | 515 | 448, 415 | 1440, 718, 619 |
| H_2L^5 | 1609 | | | | | | |
| $(VO)L^5(bipy)$ | 1595 | 1522 | 1352, 1469 | 957 | 520 | 458, 418 | 1439, 722, 621 |

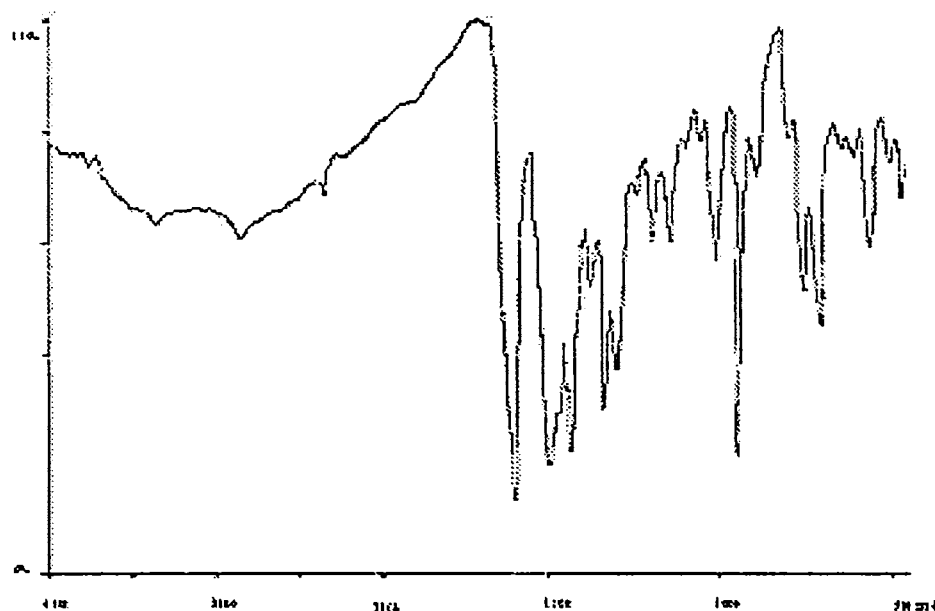


Fig. 6. IR Spectra of $(VO)L^1(bipy)$

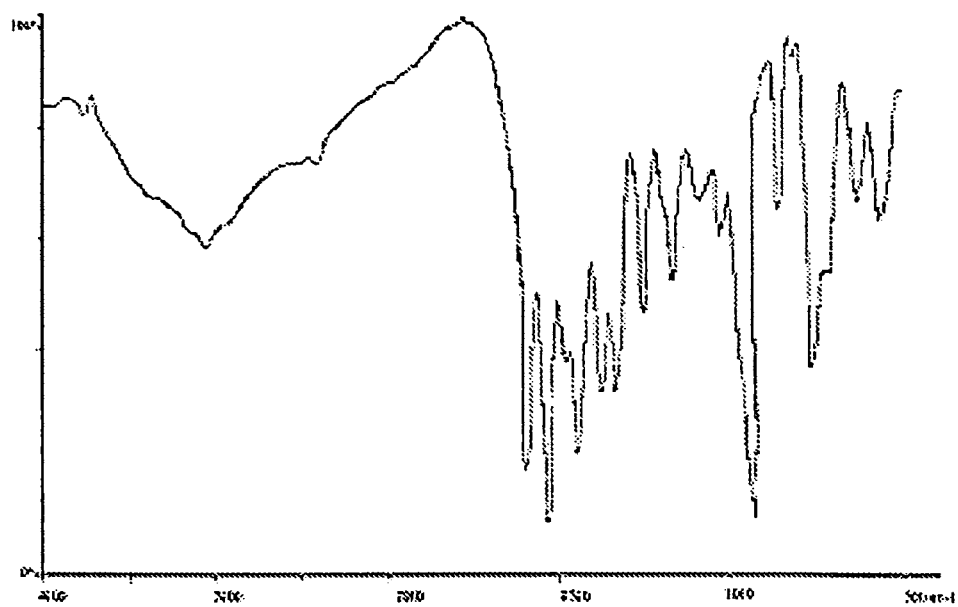


Fig. 7. IR Spectrum of $(VO)L^2(bipy)$

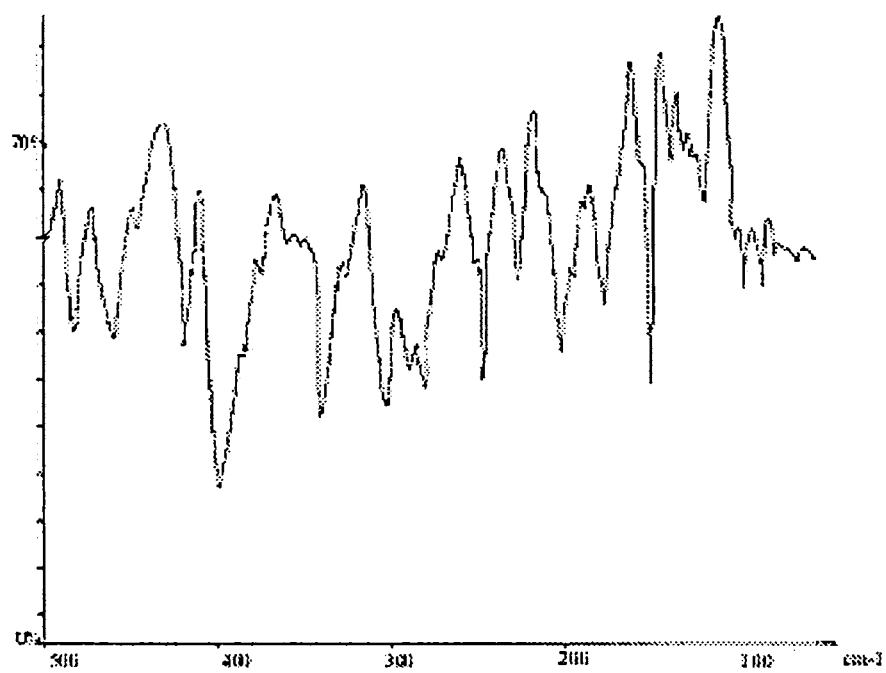


Fig. 8. Far IR spectrum of $(VO)L^5(bipy)$

4.3.6. Biological activity studies

The synthesized chemical ligands and complexes were tested for their antimicrobial activity. The antimicrobial agent may be either bacteriostatic or bactericidal.

The effectiveness of an antimicrobial agent in sensitivity testing is based on the size of the zones of inhibition. When the test substances are introduced on to a lawn of bacterial culture by disc diffusion method.

Test organisms

The microorganisms used as test organisms were bacteria isolated from clinical samples. Two Gram positive bacteria and three Gram negative bacteria were used as test organisms.

A) Gram Positive

1. *Staphylococcus aureus*
2. *Bacillus sp*

B) Gram Negative

3. *Escherichia coli*
4. *Salmonella paratyphi*
5. *Vibrio cholerae O1*

The disc diffusion method was used for screening for the antimicrobial property of the test samples.

The free ligands showed no or little activity against both the Gram positive and gram negative bacteria. The results of the antimicrobial studies were given in the Table 5. from the results the compounds (VO)L¹(bipy) and (VO)L²(bipy) are more active than (VO)L⁴(bipy) and (VO)L⁵(bipy)

Table 5. The antimicrobial activities of H₂L and the complexes

| Compound | Microbial activity inhibition zone | | | | |
|-------------------------------|------------------------------------|---------------------------|-------------------------|------------------------------|-----------------------------|
| | <i>Bacillus sp.</i> | <i>Vibrio cholerae O1</i> | <i>Escherichia coli</i> | <i>Staphylococcus aureus</i> | <i>Salmonella paratyphi</i> |
| H ₂ L ¹ | - | - | - | - | - |
| H ₂ L ² | - | - | - | - | - |
| H ₂ L ⁴ | - | - | - | - | - |
| H ₂ L ⁵ | - | - | - | - | - |
| (VO)L ¹ (bipy) | + | + | - | + | + |
| | 9 mm | 10 mm | | 8 mm | 8 mm |
| (VO)L ² (bipy) | + | + | - | + | - |
| | 8 mm | 9 mm | | 8 mm | |
| (VO)L ⁴ (bipy) | | - | - | - | + |
| | - | | | | 8 mm |
| (VO)L ⁵ (bipy) | + | - | - | - | - |
| | 8 mm | | | | |

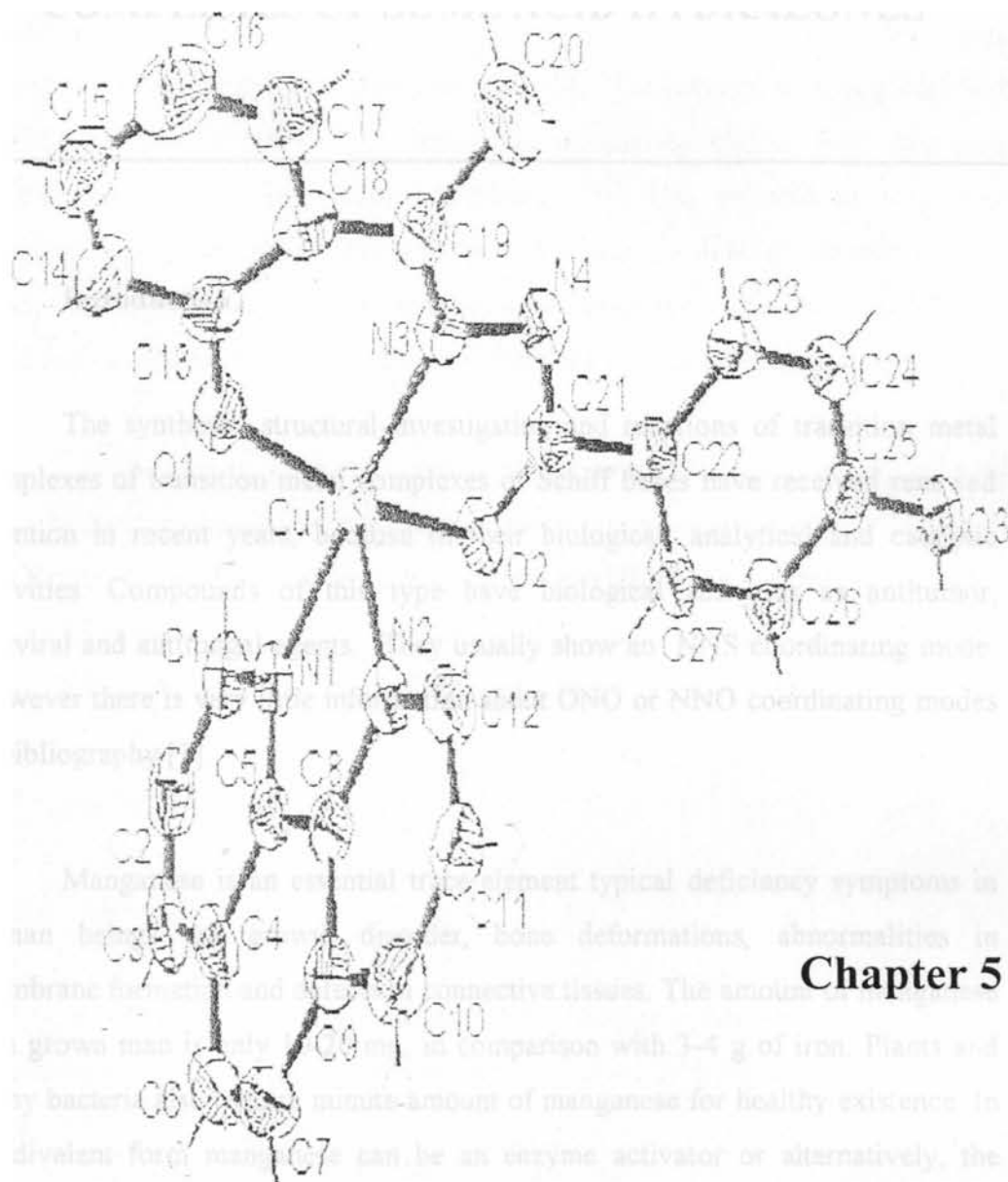
Concluding remark

An interesting series of heterocyclic adduct of oxovanadium(IV) complexes have been synthesized by the reaction of vanadium(IV) oxide acetylacetonate with some hydrazones in presences of heterocyclic base, 2,2'-bipyridine and characterized by analytical and different spectral techniques, like IR, far IR, EPR and UV-Vis spectral studies and magnetic studies. The EPR spectra indicate the free electron resides in the d_{xy} orbital. The coordination geometry around oxovanadium(IV) in all complexes are octahedral with one dibasic tridentate ligand L²⁻, and one bidentate heterocyclic base. The coordination takes place through the deprotonated hydroxyl group azomethine nitrogen and oxygen from the hydrazide moiety. And the oxygen of the oxovanadium species occupies the sixth position of the octahedron. All electronic transitions were assigned. The values are consistent with distorted octahedral structure. All the compounds are paramagnetic. EPR studies of all compounds gave axial spectra and the bonding parameters are calculated for all the compounds.

References

- [1] C. J. Carrano, C. M. Nunn, R. Quan, J. A. Bonadies V. L. Pecoraro, *Inorg. Chem.* 29 (1990) 941.
- [2] X. Li, M. S.Lah, V. L. Pecoraro, *Inorg. Chem.* 27 (1988) 465.
- [3] Debbie c. Crans, *J. Inorg. Biochem.* 80 (2000) 123.
- [4] P. Kinetek, Phase I study of KP-102, Newsedge Corporation, Vancouver, Canada, (1998).
- [5] M. Halberstam, N. Cohen, P. Slimovich, L. Rossetti, H. Shamoon, *Diabetes*, 45 (1996) 659.
- [6] N. D Chasteen, *Biological Magnetic Resonance Vol.3*, Plenum Press New York, (1981) 54.
- [7] *Vanadium: Inorganic & Coordination Chemistry*, Elizebeth M Page, Sherilyn A Wass, University of Reading, Reading UK.
- [8] E. P. Copeland, I. A. Kahwa, J. T. Mague, G. L McPherson, *J. Chem Soc. Dalton Trans.* (1997) 2849.
- [9] B. N. Figgis, J. Lewis, *Prog. Inorg. Chem.* 6 (1964) 37.
- [10] J Slebin, *Chem. Rev.* 65 (1965) 153.
- [11] S. Bhattacharya, T.Ghosh, *Ind. J. of Chemistry*, 38A (1999) 601.
- [12] G. R. Hausan, T. A. Kabanos, A. D. Kkeramidas, D. Mentzafos and A. Terzis, *Inorg. Chem.* 31 (1992) 2587.
- [13] K. B. Pandeya, Om Prakash, R. P. Singh, *J. Ind. Chem. Soc. LX* (1983) 531.
- [14] H. Kon, N E. Sharpless, *J. Chem. Phy.* 42 (1965) 906.
- [15] H. Kon, N E. Sharpless, *J. Chem. Phy.* 70 (1966) 105.

- [16] D. Kivelson, S. K. Lee, *J. Chem. Phys.*, 41 (1964) 1896.
- [17] F. A. Walker, R. L. Carlin, P. H. Rieger, *J. Chem. Phys.* 45 (1966) 4181.
- [18] D. Kivelson, *J. Chem Phys.*, 33 (1960) 1094.
- [19] John G. Reynolds, Shawn C. Sendlinger, Ann M. Murray, John C. Huffman and George Christou. *Inorg. Chem.* 34 (1995) 5745.
- [20] S. S. Dodward, R. S. Dhamnaskar, P. S. Prabhu, *Polyhedron* 8 (1989) 1748.
- [21] N. Raman, Y. P. Raja, A. Kulandaisamy, *Indian Acad. Sci. (Chem Sci.)* 113, (2001) 183.
- [22] T Ma, T. Kojima, Y. Matsuda, *Polyhedron* 19 (2000) 1167.
- [23] Y. Dong, R. K. Narla, E. Udbeck, F. M. Uckun, *J. Inorg. Biochem.* 78 (2000) 321.
- [24] C. Tsiamis, B. Voulgaropoulos, D. Christos, G. P. Voustas, C. A. Kavounis, *Polyhedron*, 19 (2000) 2003.
- [25] S. N. Rao, D.D Mishra, R. C. Maurya, N. N. Rao, *Polyhedron* 16 (1997) 1825.



Chapter 5

SYNTHESES AND SPECTRAL CHARACTERIZATION OF MANGANESE(II) COMPLEXES OF SOME ACID HYDRAZONES

5.1. Introduction

The synthesis, structural investigation and reactions of transition metal complexes of transition metal complexes of Schiff bases have received renewed attention in recent years, because of their biological, analytical and catalytic activities. Compounds of this type have biological activities as antitumor, antiviral and antifungal agents. They usually show an NNS coordinating mode. However there is very little information about ONO or NNO coordinating modes in bibliography [1].

Manganese is an essential trace element typical deficiency symptoms in human beings are growth disorder, bone deformations, abnormalities in membrane formation and defects in connective tissues. The amount of manganese in a grown man is only 10-20 mg, in comparison with 3-4 g of iron. Plants and many bacteria also require minute amount of manganese for healthy existence. In its divalent form manganese can be an enzyme activator or alternatively, the active site of metalloprotein [2-3].

When manganese in relevant physiological oxidation state +2, +3, +4 with normal coordination of oxygen and nitrogen atom from the protein, it forms paramagnetic centers: Manganese(II) high spin electronic configuration (five unpaired electron), manganese(III) (h.s) (four unpaired electrons) and manganese(IV) high spin with three unpaired electron. And hence these type

systems can be easily studied by different physical methods like EPR, electronic spectroscopy and magnetic studies. EPR spectroscopy is very sensitive and informative for manganese(II) and for polynuclear complexes in which the manganese ion are in different oxidation state. Electronic spectroscopy particularly informative in the case of manganese(III) and manganese(IV), where charge transfer spectra are more important.[4]. The oxygen evolving complex (OEC) of photosystem-II is a tetrameric manganese cluster with di(μ -oxo) dimanganese as its key structural feature. [5]. This mixture of tetrameric manganese(IV) complexes has become one of the interesting research area in coordination chemistry. In the course of investigation complexes of different oxidation state and also mixed valence complexes were obtained [6].

In the present work we report four manganese(II) complexes of different acid hydrazones like 2-hydroxyacetophenone nicotinic acid hydrazone (H_2L^2), 2-methoxybenzaldehyde nicotinic acid hydrazone(HL^3), salicylaldehyde nicotinic acid hydrazone (H_2L^5) and 2-hydroxyacetophenone benzoic acid hydrazone (H_2L^6) and their spectral characterization and tentative structural assignments.

5.2. Experimental

5.2.1. Materials

Manganese(II) acetate dihydrate was Analar grade and used with out further purification. All the solvents were dried using standard methods before use.

5.2.2. Synthesis of $Mn(HL^2)_2$

The complex $Mn(HL^2)_2$ was prepared by the following method. Manganese(II) acetate hydrate (1 mmol) was dissolved in ethanol. To the stirred solution of hydrazone (1 mmol) and the heterocyclic base 1, 10-phenanthroline (1 mmol) in ethanol the metal salt solution was added. . Resultant homogeneous brown solution was continued to stirring for 4 hrs. The product formed was filtered and washed with hot ethanol, followed by ether, and dried *in vacuo*.

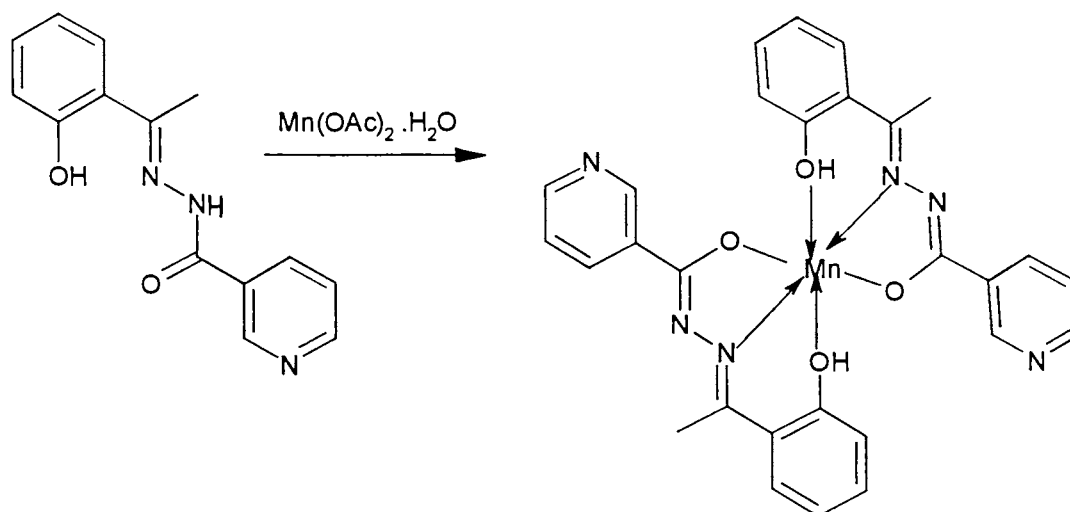


Fig. 1. Scheme of synthesis of $\text{Mn(HL}^2)_2$ complexes

5.2.3. Synthesis of MnL^3_2

The complex MnL^3_2 was prepared by the following method. Manganese(II) acetate hydrate (1 mmol) was dissolved in ethanol. To the stirred solution of hydrazone (2 mmol) in ethanol, the metal salt solution was added. A resultant homogeneous reddish brown solution was refluxed for 12 h. The product formed was filtered and washed with hot ethanol, followed by ether, and dried *in vacuo*.

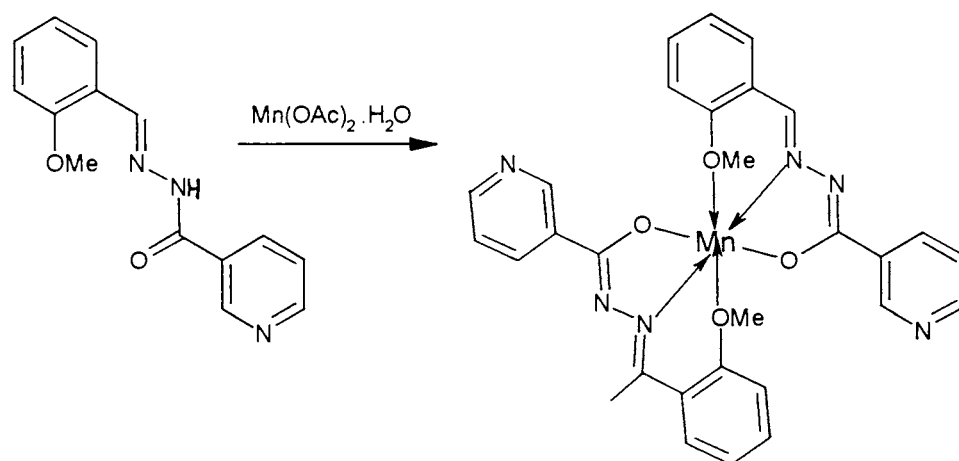


Fig. 2. Scheme of synthesis of MnL^3_2

5.2.4. Syntheses of $Mn(HL^5)_2$ and $Mn(HL^6)_2$

The complexes $Mn(HL^5)_2$ and $Mn(HL^6)_2$ were prepared by the following method. Manganese(II) acetate hydrate (1 mmol) was dissolved in ethanol. To the stirred solution of hydrazone (2 mmol) in ethanol the metal salt solution was added. Resultant homogeneous brown solutions were continued to stirring for 4-6 h. The products formed were filtered and washed with hot ethanol, followed by ether, and dried *in vacuo*.

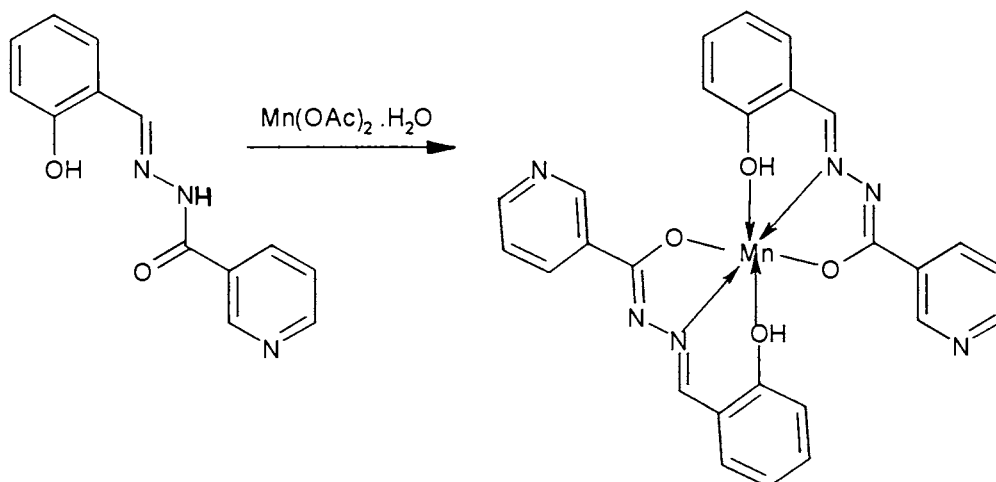


Fig. 3. Scheme of synthesis of $Mn(HL^5)_2$

5.3. Results and discussion

5.3.1. Syntheses of the complexes

The ligands were found to coordinate as monoanionic L^- on complexation to manganese(II). The complex, $Mn(HL^2)_2$ was found to be readily formed from manganese acetate solution in ethanol by the ligand in presence of heterocyclic base, 1,10-phenanthroline. But the yield was very low and from the elemental analysis the heterocyclic base was not present in the complexes. The elemental analysis of the complexes, $Mn(HL^5)_2$ and $Mn(HL^6)_2$ were in agreement with the empirical formulas suggested for the compounds. The formation of MnL^3_2 was

found to be difficult. All the compound are sparingly soluble in water, ethanol and methanol and soluble in DMF and DMSO Conductivity measurement in DMF shows the complexes to be nonconductors.

Table 1. Colours, empirical formula and elemental analyses of manganese(II) complexes

| Compound | Colour | Analytical data found (calculated) | | |
|-----------------------------|----------------|------------------------------------|-------------|------------------|
| | | C % | H % | N % |
| H_2L^2 | Pale yellow | 66.12 (65.85) | 5.24 (5.13) | 16.95 (16.46) |
| $Mn(HL^2)_2$ | Reddish orange | 59.76 (59.68) | 4.30 (4.29) | 14.26 (14.91) |
| MnL^3_2 | Reddish orange | 59.82 (59.62) | 4.89 (4.29) | 14.68 (14.91) |
| $Mn(HL^5)_2 \cdot C_2H_5OH$ | Reddish orange | 58.11 (57.83) | 3.91 (4.51) | 15.10 (14.45) |
| $Mn(HL^6)_2$ | Brown | 63.62 (64.17) | 4.51 (4.32) | 9.53 (10.01) |

5.3.2. Magnetic moment measurements

The magnetic measurements were done using VSM, and calculations were made using computed values for pascal constants for diamagnetic corrections. The values suggested spin only values for mononuclear complexes having d^5 configuration with poor orbital contribution. The room temperature magnetic measurements were found to be ~ 5.8 BM corresponding to five unpaired electrons. For manganese(II) d^5 systems it is orbitally single degenerate and hence no orbital contribution to the magnetic moment is expected. However μ_{eff}

$\mu_{s.o.}$, some of the magnetic moment must have been quenched by field of the ligand [7].

5.3.3. Electron paramagnetic resonance spectral studies

The spin Hamiltonian used to represent the EPR of the manganese(II) is given by *Ingram* [8].

$$H = g \beta H_s + D \{S_z^2 - 1/3 S(S+1)\} + E (S_x^2 - S_y^2)$$

Where H is the magnetic field vector, D is the axial zero field splitting term and E is the rhombic zero field splitting parameter. If D and E are very small compared to $g \beta H_s$, five epr transitions are expected with a g value ~ 2.0 given by Bra-ket notation

$$|+5/2 \rangle \leftrightarrow | +3/2 \rangle, | +3/2 \rangle \leftrightarrow | +1/2 \rangle, | +1/2 \rangle \leftrightarrow | -1/2 \rangle, | -1/2 \rangle \leftrightarrow | -3/2 \rangle \text{ and } | -3/2 \rangle \leftrightarrow | -5/2 \rangle$$

If D is large, the only one transition between $|+1/2 \rangle \leftrightarrow |-1/2 \rangle$ will be observed. If D or E is very large, the lowest doublet has effective g values $g_{\parallel} \sim 2.0$, $g_{\perp} \sim 6.0$. for $D \neq 0$ and $E = 0$), but for $D = 0$ and $E \neq 0$, middle Kramer's doublet has anisotropic g values of 4.29. Depending upon the values of A and D, the number of lines appear in the spectra are 6, 24, or 30 [9].

The EPR parameters observed for the frozen DMF solution are presented in the Table 2. Electron paramagnetic resonance spectra of the complexes in solution at liquid nitrogen temperature gave six peak correspond to $+5/2, \dots, -5/2$ correspond to $m=0$. in addition to this axial field spectrum a pair of low intensity forbidden lines lying between each of the two main hyperfine line is observed in solution spectra. These forbidden lines correspond to $m=+1$ or -1 due to the mixing of nuclear hyperfine levels by zero field splitting factor of the Hamiltonian. The forbidden lines are themselves split by spin-spin interaction of the sextuplet state [10]. The average separation of the forbidden hyperfine doublet is ~ 24 G. The observed g values are very close to the free electron spin value, 2.0023 which is consistent with the typical manganese (II) and also suggestive of the absence of spin orbital coupling in the ground state 6A_1 without any sextet

term of higher energy. The A_{iso} values are found to be ~ 96 G, which are consistent with the distorted octahedral structure for manganese(II) species.[9,11-13]

Table 2. EPR parameters and magnetic susceptibility of manganese(II) complexes

| Compound | g_{iso} | A_{iso} | μ_{eff} BM |
|-----------------------------|-----------|-----------|----------------|
| $Mn(HL^2)_2$ | 2.00169 | 95.0 | 5.78 |
| $Mn(L^3)_2$ | 2.00448 | 94.4 | 5.64 |
| $Mn(HL^5)_2 \cdot C_2H_5OH$ | 1.99767 | 94.4 | 5.92 |
| $Mn(HL^6)_2$ | 2.00448 | 96.0 | 5.88 |

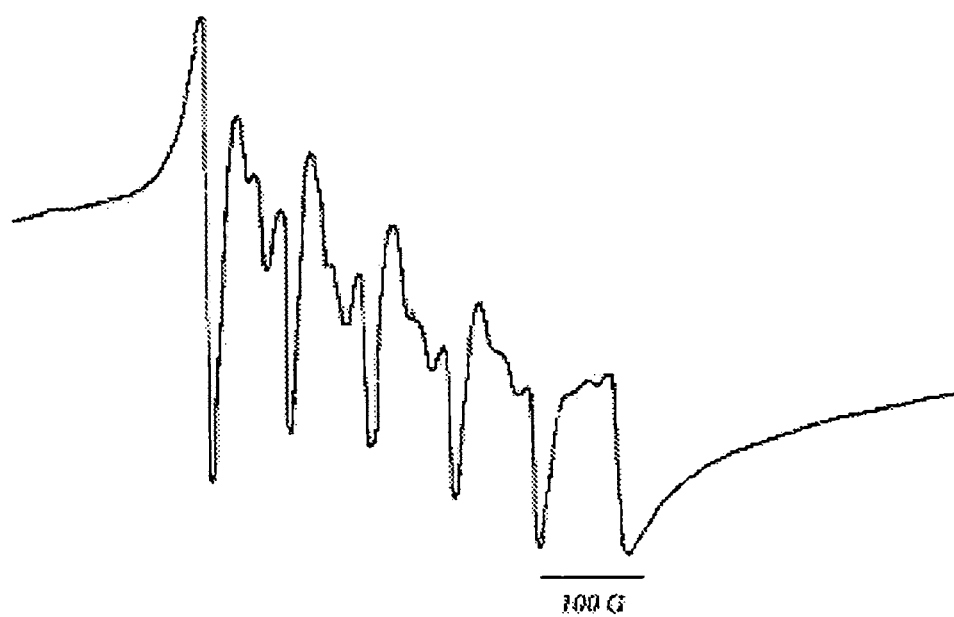


Fig. 4. Solution state EPR spectrum of MnL^3_2 at 77 K

5.3.4. Infrared spectral studies

The coordination sites of the ligands while complexation were assigned on the basis of the comparative infrared spectral analyses of the ligand and the complexes. The coordination takes place through the phenol oxygen or methoxy group, azomethine nitrogen and oxygen from the hydrazide moiety, by enolisation followed by deprotonation.

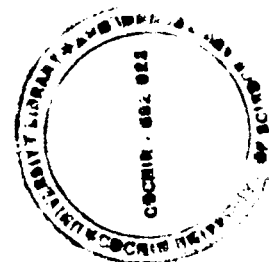
Compound, H_2L^2 , H_2L^3 , H_2L^5 and H_2L^6 show a band 3100 cm^{-1} , which is due NH stretching vibration. These bands are absent in complexes, which suggests enolisation of the carbonyl group, followed by deprotonation. IR spectra of complexes show sharp band around 1530 cm^{-1} due to newly formed N=C bond indicating the coordination of hydrazones take place in the form of enol rather than as keto form. Further proof for the complexation for enol oxygen is obtained from the appearance of a new band $\sim 439\text{ cm}^{-1}$ which is assignable for the $\nu(\text{Mn-N})$ for the complexes. The lowering of the band approximately 1610 cm^{-1} (C=N) by $15\text{-}10\text{ cm}^{-1}$ is explicit evidence for coordination of the hydrazone through the azomethine nitrogen. Which is supported by the new band at $523\text{-}501\text{ cm}^{-1}$ in the complexes, which are assigned to Mn-N. The increase in (N-N) in the spectra of complexes is due to the increase in the double bond character offsetting the loss of electron density via donation to metal and is a confirmation of the coordination of the ligand through azomethine nitrogen. On the coordination of the OH group to the metal lowers the OH stretching frequency by $20\text{-}35\text{ cm}^{-1}$. The spectrum of the complexes exhibit a symmetric shift in the position of the band in the region $1600\text{-}1350\text{ cm}^{-1}$ due to C=C and C=N vibrational modes and their mixing patterns are different from those present in ligands spectra [14-15].

R
546.302
SRE

Table 3. Selected IR frequencies of ligands and manganese(II) complexes (cm⁻¹)

| Compound | $\nu_{C=N}$ | $\nu_{N=N}$ | $\nu_{N=C}$ | ν_{C-O} | ν_{Mn-N} | ν_{Mn-O} |
|--|-------------|-------------|-------------|---------------|--------------|--------------|
| H ₂ L ² | 1603 | 1001 | 1523 | | | |
| Mn(HL ²) ₂ | 1594 | 1026 | 1530 | 1347, 1424 | 515 | 443 |
| HL ³ | 1611 | 998 | 1513 | | | |
| Mn(L) ₂ | 1598 | 1027 | 1521 | 1363, 1422 | 501 | 444 |
| H ₂ L ⁵ | 1609 | 1010 | 1510 | | | |
| Mn(HL ⁵) ₂ C ₂ H ₅ OH | 1595 | 1037 | 1522 | 1352, 1469 | 523 | 432 |
| H ₂ L ⁶ | 1620 | 1002 | 1530 | | | |
| Mn(HL ⁶) ₂ | 1600 | 1028 | 1536 | 1344, 1469 | 518 | 437 |

G 8644



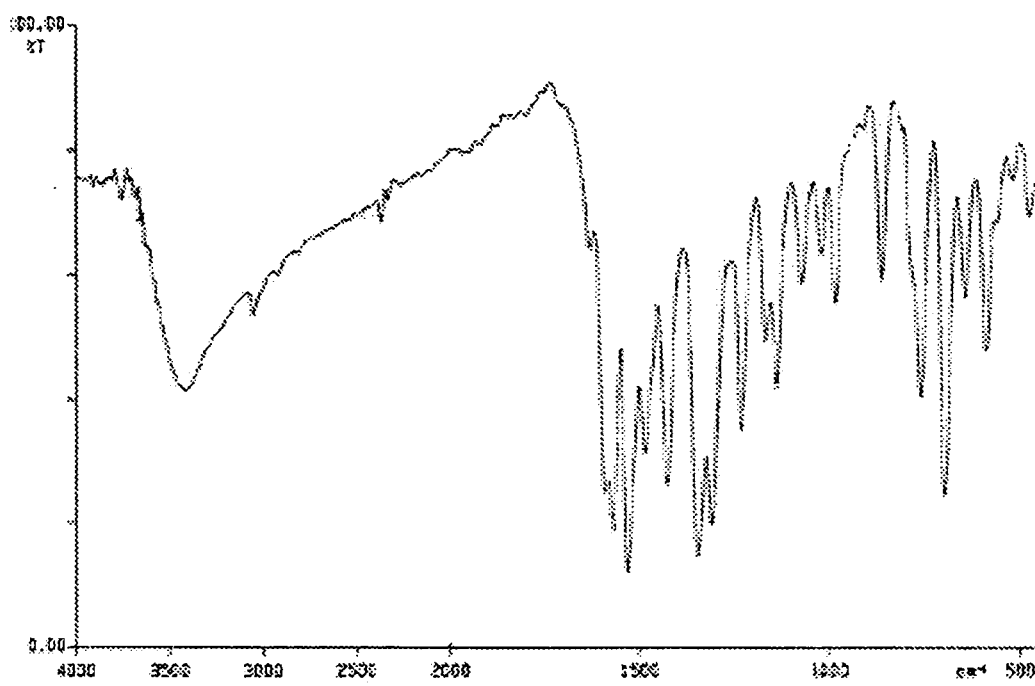
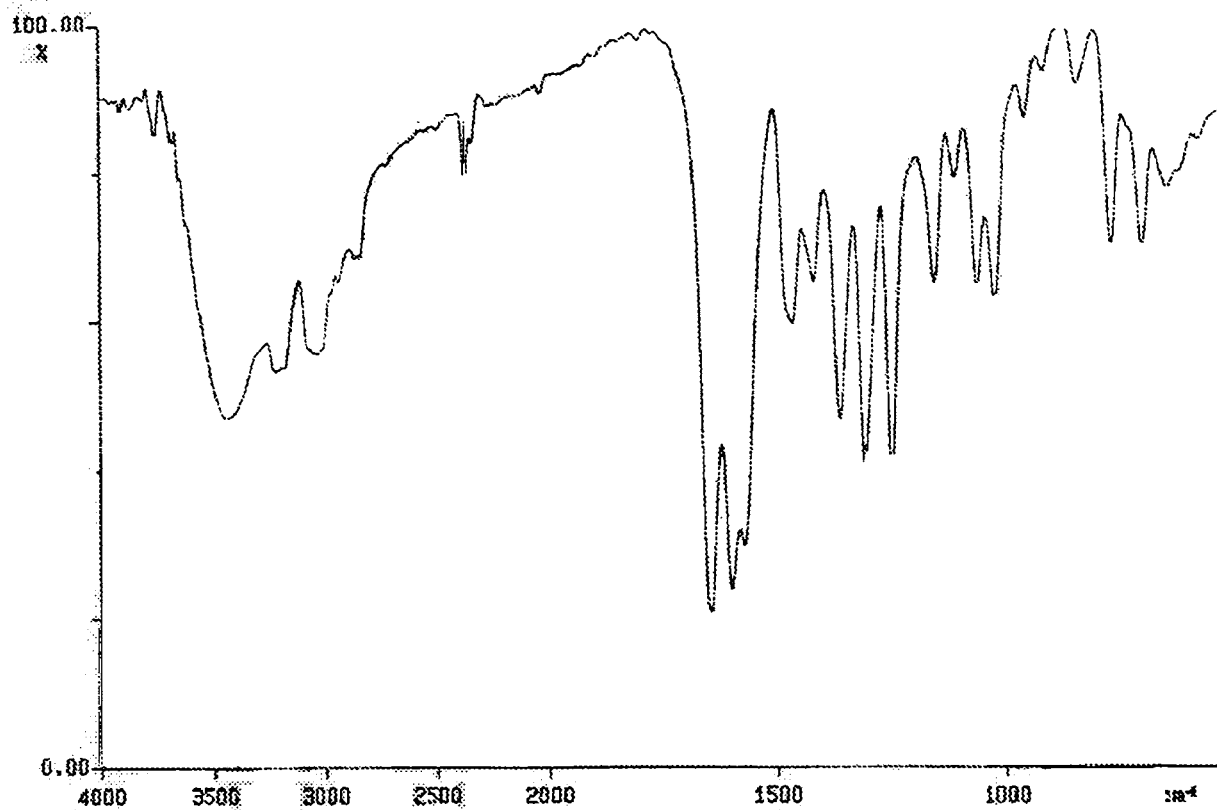


Fig. 5. IR spectrum of $Mn(HL^2)_2$ and $Mn(HL^6)_2$

5.3.5. Electronic spectral analyses

The six coordinated high spin manganese(II) are d^5 system and the d-d transitions for the complexes are doubly forbidden. Thus the intensities of the transitions from the ground state to the state of four-fold multiplicity are very weak and the peaks appear as shoulders. The significant absorption bands of the spectra recorded in solid state are presented in the Table 4. The d-d bands are correspond to ${}^6A_{1g}-{}^4T_{1g}({}^4G)$, ${}^6A_{1g}-{}^4E_{2g}({}^4G)$, ${}^4A_{1g}-{}^4E_g$ and ${}^4A_{1g}-{}^4T_{1g}(P)$ are observed with very weak intensities, suggest octahedral geometry for all the compounds[9].

Table 4. Electronic spectral assignments of manganese(II) complexes

| Compound | ${}^6A_{1g}-{}^4T_{1g}({}^4G)$ | ${}^6A_{1g}-{}^4E_{2g}({}^4G)$ | ${}^4A_{1g}-{}^4E_g$ | ${}^4A_{1g}-{}^4T_{1g}(P)$ |
|-----------------------------|--------------------------------|--------------------------------|----------------------|----------------------------|
| $Mn(HL^2)_2$ | 19088 | 23809 | 28974 | 32121 |
| $Mn(L^3)_2$ | 19494 | 22767 | 28833 | 31078 |
| $Mn(HL^7)_2 \cdot C_2H_5OH$ | 18985 | 22987 | 28096 | 31445 |
| $Mn(HL^8)_2$ | 18115 | 23452 | 28974 | 31746 |

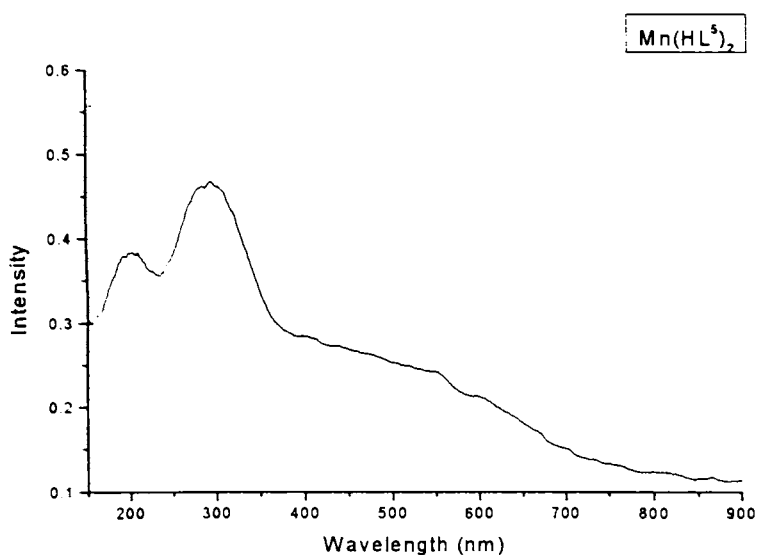


Fig. 6. Electronic spectrum of $Mn(HL^5)_2$

5.3.6. *Biological activity studies*

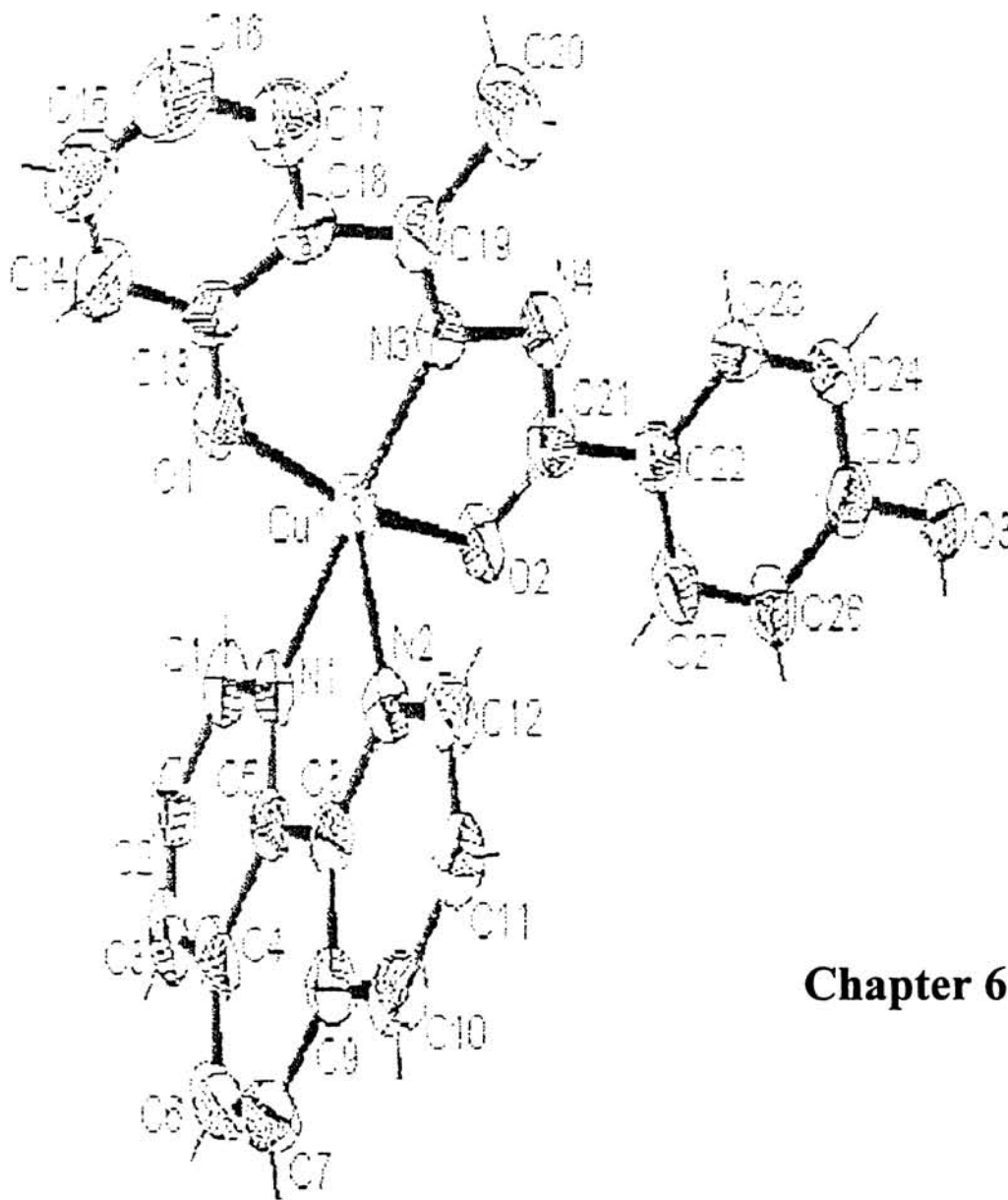
All the synthesized complexes were tested for their antimicrobial activity. The antimicrobial agent may be either bacteriostatic or bactericidal. The effectiveness of an antimicrobial agent in sensitivity testing is based on the size of the zones of inhibition. When the test substances are introduced on to a lawn of bacterial culture by disc diffusion method. The disc diffusion method was used for screening for the antimicrobial property of the test samples. The active diameter around the discs was below 8 mm. All the four manganese(II) complexes were showed no or little activity against both the Gram positive and Gram negative bacteria. Surprisingly we observed enhanced growth of microorganisms over the discs, instead of activity for two of the compounds $\text{Mn}(\text{HL}^6)_2$ and $\text{Mn}(\text{L}^3)_2$.

Concluding remark

An interesting series of binary complexes manganese(II) have been synthesized by the reaction of manganese(II) acetate dihydrate and four different acid hydrazones in appropriate conditions and characterized by analytical and different spectral techniques, like IR, far IR, EPR and UV-Vis spectral studies and magnetic studies. All the compounds are paramagnetic. EPR studies of all compounds gave axial spectra. The spectra indicate all the complexes have a distorted octahedral geometry. The coordination takes place through the phenolic/methoxy oxygen, azomethine nitrogen and oxygen from the hydrazide moiety. All electronic transitions were assigned. The values are consistent with distorted octahedral structure.

References

- [1] F. H-Ureña, N. A. I-Cabeza, M. N. M-Carretero, A. L. P-Chamorro, *Acta Chim. Slov.* 47 (2000) 481.
- [2] E. Frieden, *Biochemistry of essential Ultratrace Elements* Plenum, New York (1984).
- [3] V. L. Scramm, F. C. Wedler, *Manganese in metabolism and Enzyme function*, Academic Press, Orlando, FL, USA (1986).
- [4] Karl Wieghardt, *Angew. Chem. Int. Ed. Engl.* 28 (1989) 1153.
- [5] V. K. Yachandra, K. Sauer, M. P. Klein, *Chem Rev.* 96 (1996) 2927.
- [6] Blandin, R. Davydov, C. Philonze, M. F. Charlot, S. Styring, B. Akermark, J. J. Girerd, A. Boussac, *J. Chem. Soc. Dalton Trans.* (1997) 4069.
- [7] R. L. Carlin, *Magnetochemistry*, Springer, Berlin, Heidelberg (1986) 346.
- [8] D. J. E. Ingram, *Spectroscopy at Radio and microwave frequencies*, 2nd edition, Butterworth (1967).
- [9] B. S. Garg, M. R. P. Kurup, S. K. Jain, Y. K. Bhoon, *Transition Met. Chem.* 13 (1988) 91.
- [10] W. Linert, F. Renz, R. Boca, *J. Coord. Chem.* 40 (1996) 293.
- [11] J. E. Drumheller, R. S. Rubins, *Phys. Rev.* 133 (1964) 1099.
- [12] R. Singh, I. S. Ahuja, C. L. Yadava, *Polyhedron* 1 (1982) 327.
- [13] B. Bleany and R. S. Rubins, *Proc. Phys. Soc. London*, 77, 103, 1961.
- [14] E. W. Aincough, A. M. Brodie, A. J. Dobbs, J. D. Ranford, J. M. Waters, *Inorg. Chim. Acta* 267(1998) 27.
- [15] S. C. Chan, L. L. Koh, P-H Leung, J. D Ranford, K. Y. Sim, *Inorg. Chim. Acta* 236(1995) 101.



Chapter 6

**SYNTHESIS, SPECTRAL CHARACTERIZATION AND
MAGNETIC STUDIES OF STUDIES OF TERNARY
NICKEL(II) COMPLEXES WITH SOME ACID
HYDRAZONES AND HETEROCYCLIC BASES**

6.1. Introduction

The synthesis, structural investigation and reaction of Schiff bases and their transition metal complexes have received a renewed attention in recent years. The real impetus towards the developing their coordination chemistry was their physico-chemical properties. The discovery and development of new, more effective cancer medicines is the one of the main goal of present day of medicine and chemical investigation. Recently the discoveries of antitumor effects of inorganic and particularly of metal complexes and their use to cure cancer disease have received increasing attention. Metal chelation is very important process, useful both to remove toxic metals from polluted environment and to afford new chemical features to metal complexes in order to make them suitable for practical purposes, for instance practical application.

Nickel(II) has been chosen since its trace presence is now recognized to be essential for bacteria, plants, animals and human [1], and it is also known that many nickel complexes, coordinately unsaturated, can behave as Lewis acids.

Nickel(II) complexes with N_2O_2 Schiff base ligands derived from salicylaldehyde have long been used as homogeneous catalysts [2-5]

In this chapter we report the syntheses, spectral and magnetic characterization of seven ternary nickel(II) with different acid hydrazones like 2-hydroxyacetophenone nicotinic acid hydrazone (H_2L^2), 2-hydroxyacetophenone 4-hydroxybenzoic acid hydrazone (H_2L^4), salicylaldehyde nicotinic acid hydrazone (H_2L^5) and 2-hydroxyacetophenone benzoic acid hydrazone (H_2L^6), and heterocyclic bases like 2, 2' bipyridine/ 1, 10 phenanthroline, and one binary complexes of dianionic acid hydrazone.

6.2. Experimental

6.2.1 Materials

Nickel(II) acetate dihydrate (Merk) was of Analar grade and used without further purification. All the solvents were dried using standard methods before use.

6.2.2 Syntheses of the complexes

6.2.2.1 Syntheses of NiL^2bipy , NiL^5bipy and NiL^5phen

All the above-mentioned complexes were synthesized using the following general method. Nickel(II) acetate dihydrate (1 mmol) was dissolved in water. To a stirred ethanolic solution of acid hydrazones (2-hydroxyacetophenone nicotinic acid hydrazone (H_2L^2) / salicylaldehyde nicotinic acid hydrazone (H_2L^5)) (1 mmol) and 2, 2'-bipyridine / 1, 10 phenanthroline (1 mmol), nickel solution was added. Resultant homogeneous brown solutions was stirred for 3 h. The products formed were filtered and washed with cold ethanol, followed by ether, and dried *in vacuo* over P_4O_{10} . Unfortunately we are unable to grow single crystals suitable for single crystal XRD for any of these complexes.

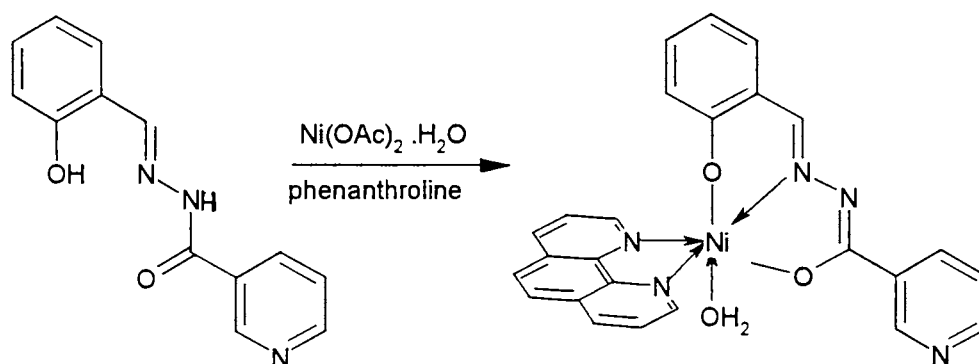


Fig. 1. Scheme of the synthesis of NiL^5phen

6.2.2.2. Synthesis of $\text{NiL}^2\text{H}_2\text{O}$

Nickel(II) acetate dihydrate (1 mmol) was dissolved in water. To a stirred ethanolic solution of 2-hydroxyacetophenone nicotinic acid hydrazone (1 mmol) nickel solution was added. Resultant homogeneous brown solutions were stirred for 3 h. The products formed were filtered and washed with cold ethanol, followed by ether, and dried *in vacuo* over P_4O_{10} .

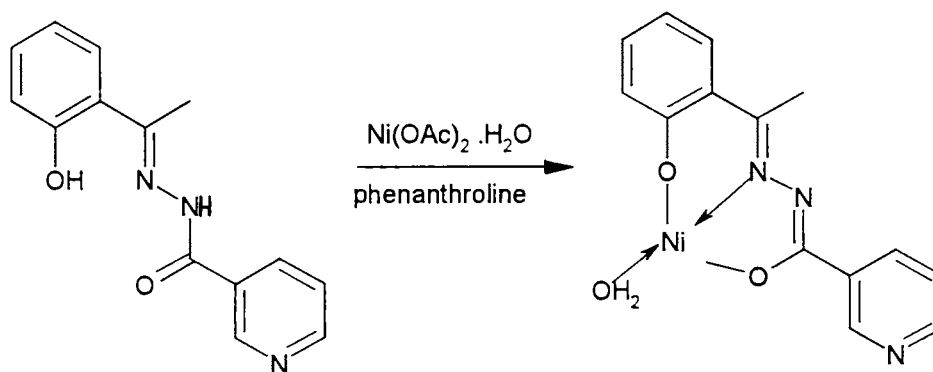


Fig. 2. Scheme of the synthesis of $\text{NiL}^2\text{H}_2\text{O}$

6.2.2.3. Syntheses of NiL^4bipy , NiL^6bipy , NiL^4phen and NiL^6phen

All the above-mentioned complexes were synthesized using the following general method. Nickel(II) acetate dihydrate (1 mmol) was suspended in ethanol. This suspension was added to a stirred ethanolic solution of acid hydrazone (2-hydroxyacetophenone 4-hydroxybenzoic acid hydrazone (H_2L^4)/ 2-hydroxyacetophenone benzoic acid hydrazone (H_2L^6)), (1 mmol) and 2, 2'-bipyridine / 1, 10-phenanthroline (1 mmol) for 1h. Resultant solution was refluxed for 6 h. The product formed was filtered and washed with cold ethanol, followed by ether, and dried *in vacuo* over P_4O_{10} . Unfortunately we are unable to grow single crystals suitable for single crystal XRD for any of these complexes.

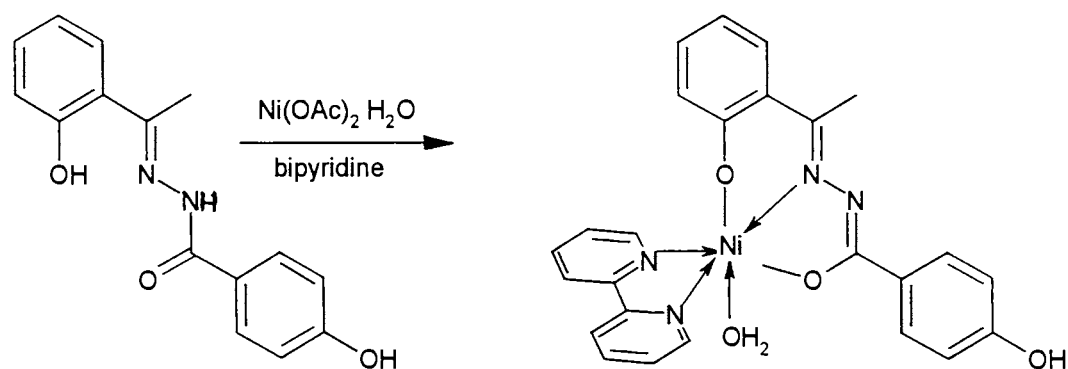


Fig. 3. Scheme of the synthesis of NiL^4bipy

6.3. Results and discussion

3.1. Syntheses of the nickel(II) complexes

The colors and partial elemental analyses complexes are presented in the Table 1. The elemental analyses data are consistent with 1:1:1 ratio of the metal ion : hydrazone : heterocyclic base for the complexes prepared except for $NiL^2 \cdot H_2O$. One or more molecules water are also present in the molecule. The ligand H_2L gets double deprotonated and coordinates as L^{2-} . The complexes are insoluble in most of

the common polar and non polar solvents. They are partially soluble in DMF and DMSO. The conductivity measurements in DMF showed that all the complexes are non electrolytes.

Table 1. Color and partial elemental analyses nickel(II) complexes

| Compound | Color | Analytical data found (calculated) | | |
|--|----------------|------------------------------------|-------------|---------------|
| | | C% | H% | N% |
| NiL ² bipy2H ₂ O | Reddish orange | 56.9 (57.2) | 3.99 (4.60) | 13.92 (13.89) |
| NiL ² H ₂ O | Yellow | 58.86 (59.02) | 4.69 (4.45) | 10.30 (10.56) |
| NiL ⁴ bipyH ₂ O | Reddish orange | 64.28 (64.64) | 4.87 (4.98) | 9.67 (10.01) |
| NiL ⁴ phenH ₂ O | Reddish orange | 65.70 (65.59) | 4.68 (4.89) | 9.29 (9.56) |
| NiL ⁵ bipy2H ₂ O | Reddish orange | 56.97 (56.36) | 3.65 (4.32) | 14.50 (14.29) |
| NiL ⁵ phen2H ₂ O | Reddish orange | 58.50 (58.43) | 4.16 (4.12) | 13.26 (13.62) |
| NiL ⁶ bipyH ₂ O | Orange | 62.61 (61.89) | 4.33 (4.57) | 11.50 (11.55) |
| NiL ⁶ phen2H ₂ O | Reddish orange | 61.33 (61.51) | 3.99 (4.59) | 10.45 (10.63) |

6.3.2. Magnetic moment measurements

The magnetic measurements were done using vibrating sample magnetometer, and calculations were made using computed values for Pascal constants for diamagnetic corrections. The magnetic moment in the polycrystalline state at 300 K of the complexes was found to be 1.18-3.2 BM.

Nickel(II) complexes show diamagnetic behavior consistent with square planar environment or paramagnetic behavior consistent with an octahedral geometry and tetrahedral environment around the metal atom. Five coordinate geometry is quite unusual among the nickel(II). Octahedral nickel(II) has an orbitally nondegenerate 3A_2 ground state and magnetic moments are in the range of 2.8-3.3 BM, which is very close to spin only value 2.8. Tetrahedral nickel(II) has a 3T_1 ground state and magnetic moment are in the range of 4-4.3 BM. Both tetrahedral and octahedral have two unpaired electrons, but tetrahedral having higher magnetic moments. Nyholm had suggested an inverse relationship exists between magnetic moments and the distortion from tetrahedral geometry.

The magnetic moment value of four coordinated $NiL^2 \cdot H_2O$ is 1.18 BM which is very low compared to the reported values for the tetrahedral complexes. Such low value exists in literature. Though square planar nickel(II) complexes are diamagnetic, there are some reports on weakly paramagnetic nickel(II) complexes having low spin [6]. To explain this phenomenon equilibrium between spin free and spin paired configuration is suggested. The anomalous low moments could be due to equilibrium in the solid state between the square planar and tetrahedral structures [7] or could be due to a partial population of spin triplet state close to the idealized ground state $^1A_{1g}$ for D_{4h} symmetry [8-9]. The low values reported for nickel(II) complexes, which are thought to be arises from quenching of orbital contribution to the magnetic moment due to distortion D_{3h} symmetry or due to strong in plane π bonding and axial ligation as has been found in the some other nickel(II) complexes [10-12].

As the consequences of interaction among nickel atom with the free electron pairs of the heteroatoms of the neighboring molecules, which leads to extension of coordination number can also leads to the paramagnetism of the square planar nickel(II) complexes [13]. The paramagnetic property of four coordinate nickel(II) systems are also because of the spin cross over phenomenon. By molecular orbital calculation, it has been found that for planar paramagnetic nickel(II) splitting of the

highest occupied molecular orbital is small and contribution of the spin free configuration to ground state should be apparent [14]. This paramagnetic behavior is because of the equilibrium between diamagnetic spin paired ground state and low lying triplet state [15]. Unfortunately, our attempts to prepare single crystals of the compound $\text{NiL}^2 \cdot \text{H}_2\text{O}$ have so far been unsuccessful; hence the confirmation of the geometry of the compound was based on the electronic spectra of the compound.

Table 2. The magnetic moment and predicted structure of the comopounds

| Compound | μ_{eff} BM | Proposed geometry |
|--|-----------------------|-------------------|
| $\text{NiL}^2 \text{bipy} \cdot 2\text{H}_2\text{O}$ | 2.76 | Pseudo octahedron |
| $\text{NiL}^2 \cdot \text{H}_2\text{O}$ | 1.18 | Square planar |
| $\text{NiL}^4 \text{bipy} \cdot \text{H}_2\text{O}$ | 3.10 | Pseudo octahedron |
| $\text{NiL}^4 \text{phen} \cdot \text{H}_2\text{O}$ | 3.21 | Pseudo octahedron |
| $\text{NiL}^5 \text{bipy} \cdot 2\text{H}_2\text{O}$ | 2.91 | Pseudo octahedron |
| $\text{NiL}^5 \text{phen} \cdot 2\text{H}_2\text{O}$ | 3.04 | Pseudo octahedron |
| $\text{NiL}^6 \text{bipy} \cdot \text{H}_2\text{O}$ | 2.71 | Pseudo octahedron |
| $\text{NiL}^6 \text{phen} \cdot 2\text{H}_2\text{O}$ | 2.57 | Pseudo octahedron |

6.3.3. Infrared spectral analyses

Coordination is expected through the phenolic oxygen, azomethine nitrogen and enolated carbonyl group. Compound H_2L^1 , H_2L^2 , H_2L^4 , H_2L^5 and H_2L^6 , show a band around 3400 and 3100 cm^{-1} , which are due to -OH stretching mode and -NH stretching mode of free -OH group and -NH respectively. These bands are absent in

complexes, which suggests deprotonation of the phenolic group indicating the coordination through phenolic oxygen, and enolisation of the carbonyl group, followed by deprotonation. On coordination the azomethine nitrogen shifts to a lower wavenumber by $\sim 20 \text{ cm}^{-1}$. The mode of coordination of carbonyl oxygen is expected upon deprotonation of the ligand. The spectral band of -NH disappears in the complex, which indicates the enolisation followed by deprotonation and the coordination through the carbonyl oxygen. Another band which is considered to be sensitive to this coordination, is the -N=N which shifts to a higher wavenumber in complex, due to the increase in the double bond character of -N=N bond. A newly formed C-O bond as the result of the enolisation gives two bands at ~ 1360 and $\sim 1470 \text{ cm}^{-1}$. The IR spectra show a sharp band at $\sim 1500 \text{ cm}^{-1}$ indicates the newly formed -N=C, confirming the coordination of hydrazone takes place in the form of enolate rather than as keto form. The spectrum of the complexes exhibit a symmetric shift in the position of the band in the region $1600\text{-}1350 \text{ cm}^{-1}$ due to -C=C and -C=N vibrational modes and their mixing patterns are different from those present in ligands spectra.

In the case of the octahedral complexes, the nitrogen atoms of the heterocyclic bases occupy the fourth and fifth positions. The heterocyclic ring breathing is observed in the finger print region, $1400\text{-}600 \text{ cm}^{-1}$. And the sixth position is occupied by water molecule. A broad band at $\sim 3500 \text{ cm}^{-1}$ conforms the presence of water molecule in the coordination sphere [16].

Table 3. Selected IR frequencies of ligands and nickel(II) complexes (cm^{-1})

| Compound | $\nu_{\text{C=N}}$ | $\nu_{\text{N=C}}$ | $\nu_{\text{C-O}}$ | $\nu_{\text{Ni-O}}$ | $\nu_{\text{Ni-N}}$ |
|--------------------------------------|--------------------|--------------------|--------------------|---------------------|---------------------|
| H_2L^2 | 1603 | | | | |
| NiL^2bipy | 1593 | 1526 | 1357, 1466 | 518 | 490, 247 |
| $\text{NiL}^2\text{H}_2\text{O}$ | 1597 | 1534 | 1344, 1470 | 353 | - |
| H_2L^4 | 1610 | | | | |
| $\text{NiL}^4\text{bipyH}_2\text{O}$ | 1602 | 1497 | 1368, 1437 | 510, 353 | 492, 258 |
| $\text{NiL}^4\text{phenH}_2\text{O}$ | 1599 | 1500 | 1367, 1437 | 353 | 248 |
| H_2L^5 | 1609 | | | | |
| $\text{NiL}^5\text{bipyH}_2\text{O}$ | 1602 | 1520 | 1359, 1447 | 344 | 482, 253 |
| $\text{NiL}^5\text{phenH}_2\text{O}$ | 1602 | 1517 | 1345, 1457 | 356 | 487, 254 |
| H_2L^6 | 1609 | | | | |
| $\text{NiL}^6\text{bipyH}_2\text{O}$ | 1589 | 1508 | 1364, 1430 | 520, 355 | 457, 248 |
| $\text{NiL}^6\text{phenH}_2\text{O}$ | 1590 | 1504 | 1362, 1436 | | |

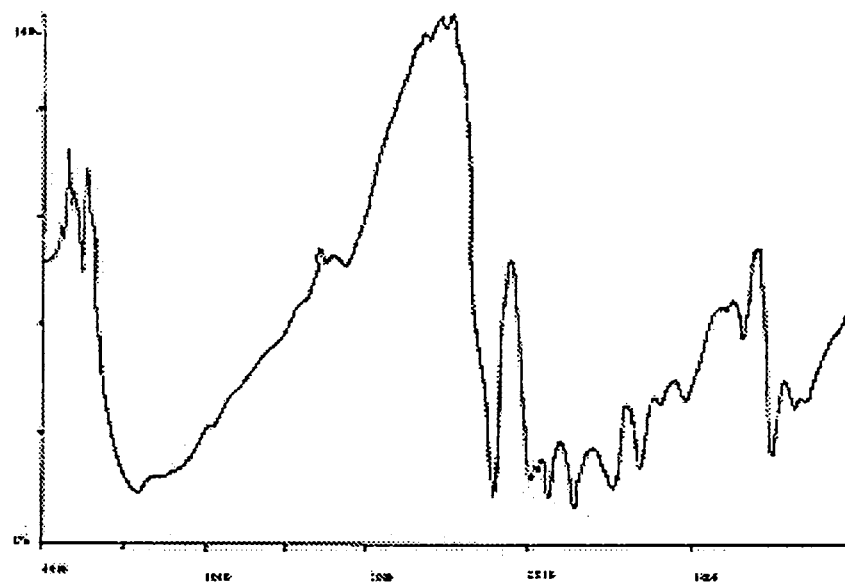


Fig. 4. IR spectrum of $\text{NiL}^4 \text{bipy} \cdot \text{H}_2\text{O}$

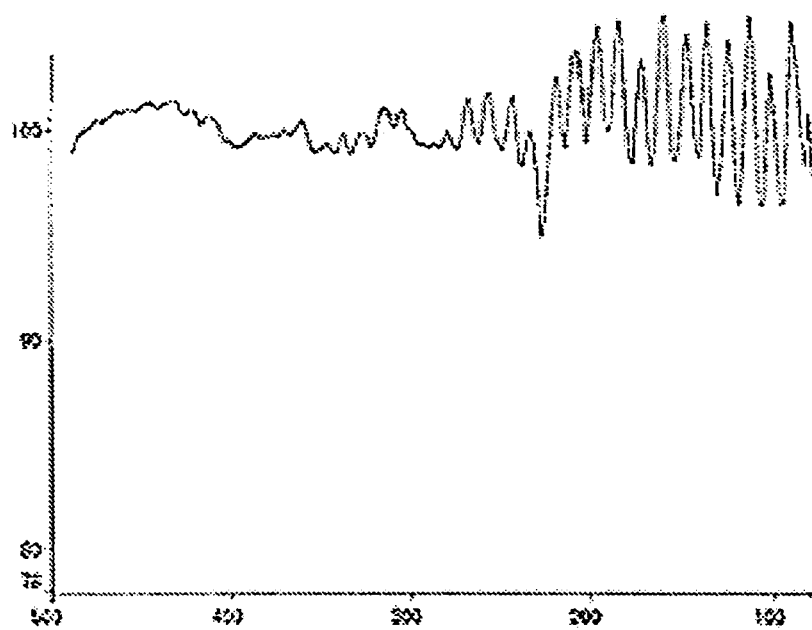


Fig. 5. Far IR spectrum of the H_2L^4

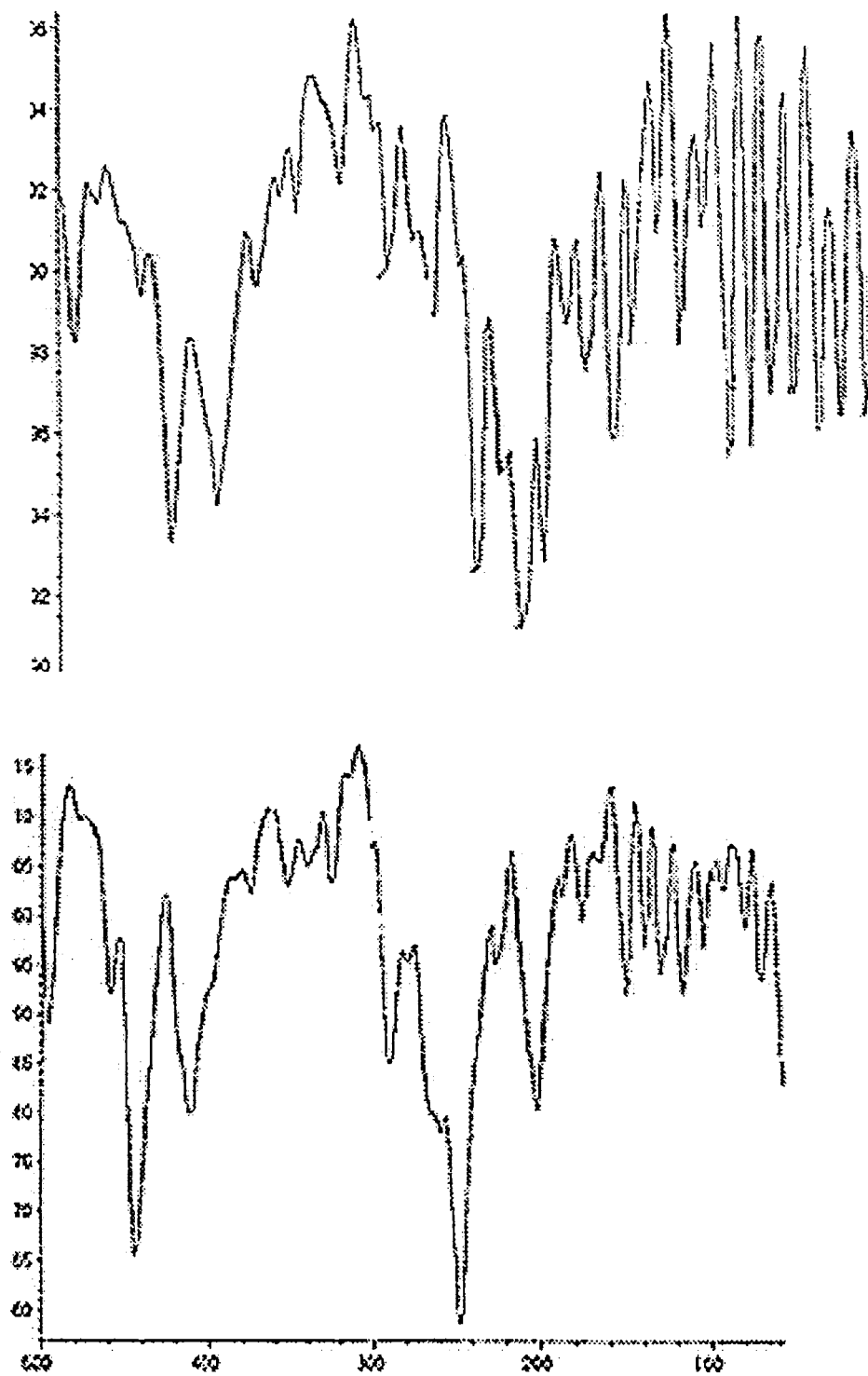


Fig. 6. Far IR spectrum of $\text{NiL}^4 \text{bipy} \cdot \text{H}_2\text{O}$ and $\text{NiL}^2 \text{H}_2\text{O}$

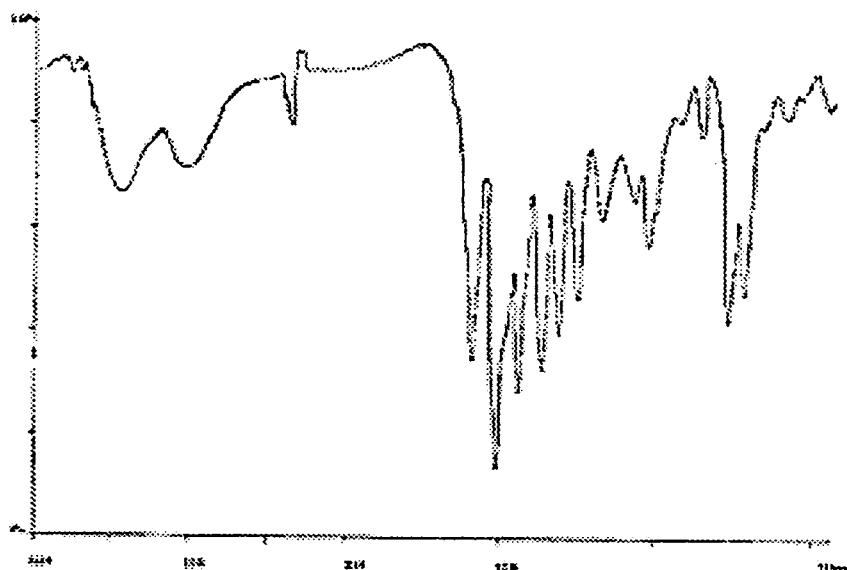


Fig. 7. IR spectrum of $\text{NiL}^6 \text{bipyH}_2\text{O}$

6.3.4. Electronic spectral analyses

The electronic spectra of the complexes were recorded in solid state and in DMF solution. All the complexes show $\pi \rightarrow \pi^*$ transition at $40000\text{-}35714 \text{ cm}^{-1}$ and $n \rightarrow \pi^*$ at ~ 30000 and $\sim 27000 \text{ cm}^{-1}$. The slight shift observed in these values of the complexes from the ligands is due to complexation. The bands observed in the range of $25000\text{-}18000 \text{ cm}^{-1}$ are assignable to the charge transfer (CT) bands [17-18].

For the compound $\text{NiL}^2 \cdot \text{H}_2\text{O}$, absence of peaks at $\sim 15000 \text{ cm}^{-1}$ indicate absence of tetrahedral symmetry. For tetrahedral geometry the likely spin allowed transitions for the $3d^8$ nickel(II) complexes are ${}^3\text{T}_1(\text{F}) \rightarrow {}^3\text{T}_2$, ${}^3\text{T}_1(\text{F}) \rightarrow {}^3\text{A}_2$, ${}^3\text{T}_1(\text{F}) \rightarrow {}^3\text{T}_1(\text{P})$. In most nickel(II) complexes with this stereochemistry, the ${}^3\text{T}_1(\text{F}) \rightarrow {}^3\text{A}_2$ transition occurs in the range $7000\text{-}9000 \text{ cm}^{-1}$, and the ${}^3\text{T}_1(\text{F}) \rightarrow {}^3\text{T}_1(\text{P})$ transition is found around $14000\text{-}16000 \text{ cm}^{-1}$ [20]. All these bands are absent in the case of

$\text{NiL}^2\cdot\text{H}_2\text{O}$ and there is no band at $\sim 24000\text{ cm}^{-1}$, which rules out the possibility of the tetrahedral – square planar equilibrium in this compound [8]. The low energy band of this complex is broad and split in two components (at ~ 9000 and $\sim 7200\text{ cm}^{-1}$) indicating tetragonal distortion. The magnetic moment ($\sim 3\text{ BM}$) lie in the region expected for octahedral complexes. The electronic spectrum of the compounds be assigned assuming that the stereochemistry pseudo-octahedral [16, 20].

Table 4. Electronic spectral assignment of the nickel(II) complexes (cm^{-1})

| Compound | $\pi\rightarrow\pi^*$ | $n\rightarrow\pi^*$ | CT | ${}^3\text{T}_{2g}\leftarrow{}^3\text{A}_{2g}$ | ${}^3\text{T}_{1g}\leftarrow{}^3\text{A}_{2g}$ | ${}^3\text{T}_{1(\text{P})}\leftarrow{}^3\text{A}_{2g}$ |
|--------------------------------------|-----------------------|---------------------|-----------------|--|--|---|
| NiL^2bipy | 40000 | 29850, 28571 | 20000, 18518 | 9009 | - | 13385 |
| $\text{NiL}^2\text{H}_2\text{O}$ | 35741 | 28571, 26455 | 18348 | | - | - |
| $\text{NiL}^4\text{bipyH}_2\text{O}$ | 37037 | 30303, 28818 | 18415 | 7462 | 11765 | - |
| $\text{NiL}^4\text{phenH}_2\text{O}$ | 35417 | 29418, 28985 | 18518 | | 10416 | - |
| $\text{NiL}^5\text{bipyH}_2\text{O}$ | 35714 | 30303, 28571 | 18182 | 7692 | 11764 | 13166 |
| $\text{NiL}^5\text{phenH}_2\text{O}$ | 39804 | 30303, 28571 | 19804, 18182 | 7792 | 11740 | 13385 |
| $\text{NiL}^6\text{bipyH}_2\text{O}$ | 37258 | 27027 | 25000, 17857 | 7201 | 10926 | 12287 |
| $\text{NiL}^6\text{phenH}_2\text{O}$ | 37567 | 29980, 27895 | 23580, 19345 | 7320 | 11080 | 12342 |

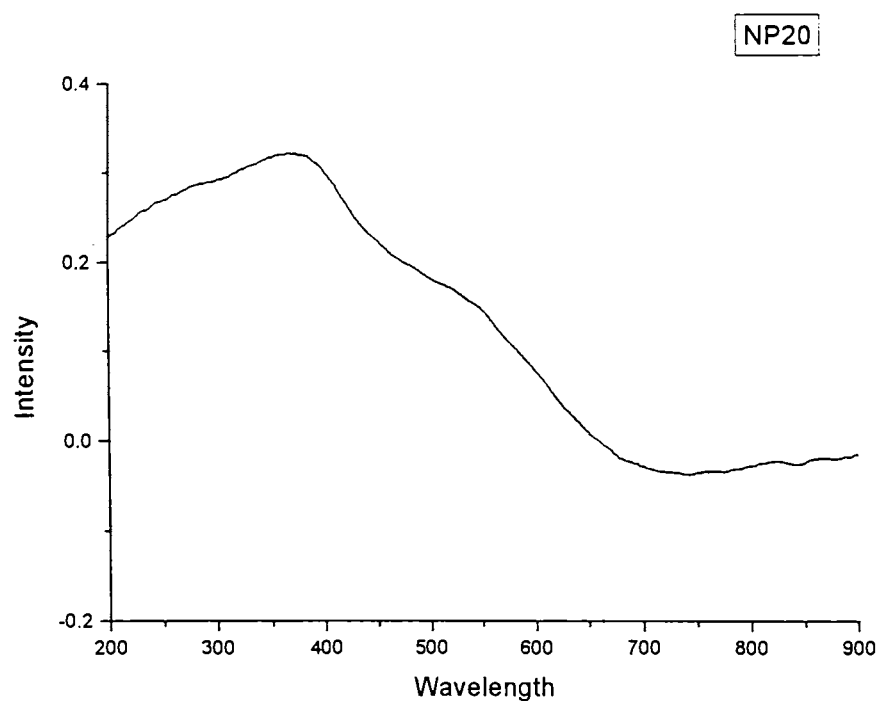


Fig. 8. The electronic spectrum of $\text{NiL}^2 \cdot \text{H}_2\text{O}$

6.3.5. *Biological activity studies*

All the synthesized complexes were tested for their antimicrobial activity. The antimicrobial agent may be either bacteriostatic or bactericidal. The effectiveness of an antimicrobial agent in sensitivity testing is based on the size of the zones of inhibition. When the test substances are introduced on to a lawn of bacterial culture by disc diffusion method. The disc diffusion method was used for screening for the antimicrobial property of the test samples. The active diameter around the discs was below 8 mm. All the eight nickel(II) complexes were showed no or little activity against both the Gram positive and Gram negative bacteria.

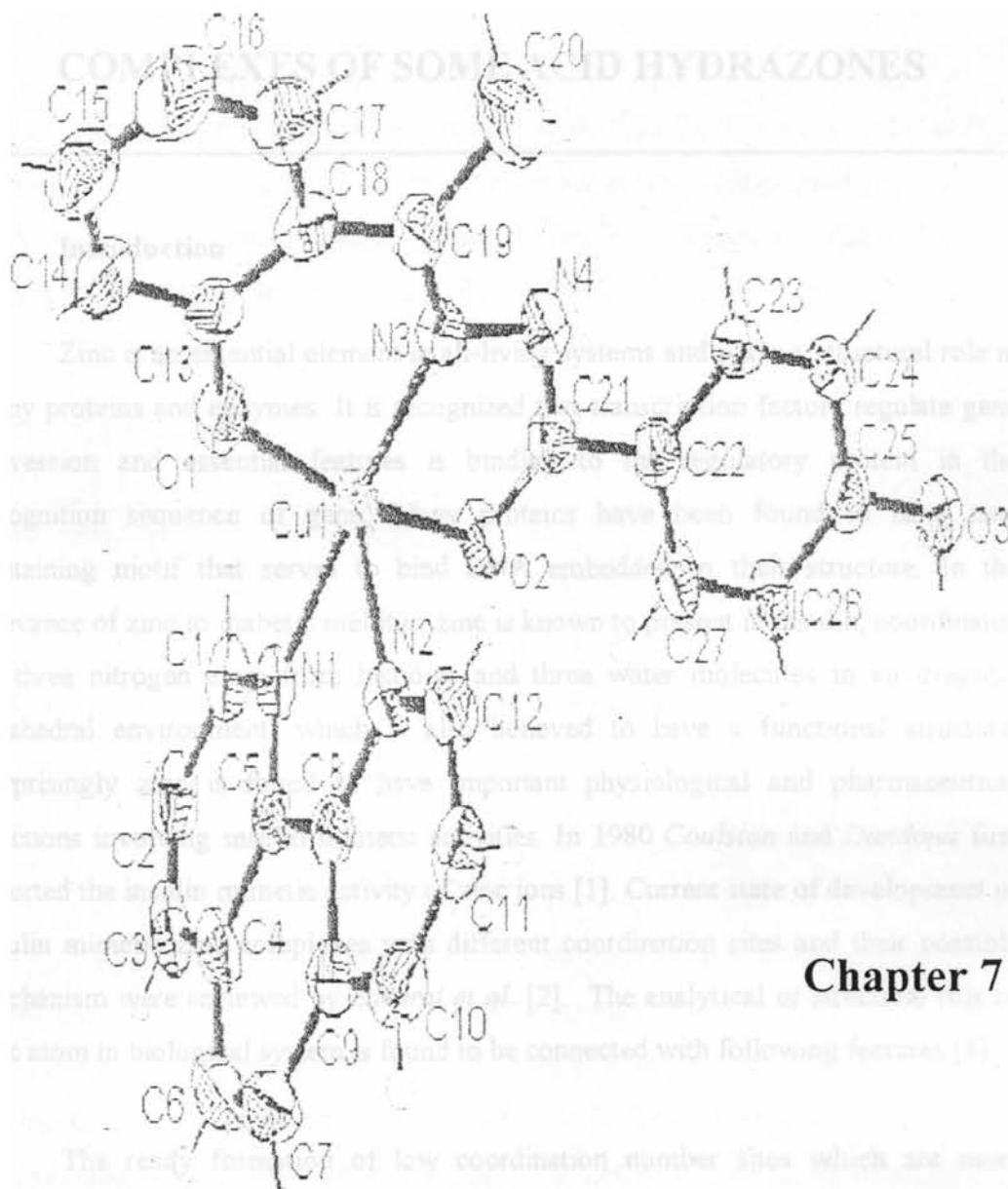
Concluding remark

An interesting series of heterocyclic adduct of nickel(II) complexes have been synthesized by the reaction of nickel(II) acetate with some hydrazones in presences of heterocyclic bases like 2,2'-bipyridine and 1,10-phenanthroline and characterized by analytical and different spectral techniques, like IR, far IR, and UV-Vis spectral studies and magnetic studies. The coordination geometry around nickel(II) in all complexes except for $NiL^2 \cdot H_2O$ are octahedral with one dibasic tridentate ligand L^2 , and one bidentate heterocyclic base. A water molecule occupies the sixth position. The coordination takes place through the deprotonated hydroxyl group azomethine nitrogen and oxygen from the hydrazide moiety. All electronic transitions were assigned. The values are consistent with pseudo-octahedral structure. All the compounds are paramagnetic. The paramagnetic property of four coordinated nickel(II) system is because of the spin cross over phenomenon.

Reference

- [1] M. A. Halcrow, G. Cristou, *Chem. Rev.* 94 (1994) 2421.
- [2] C. Gosden, K. P. Healy, D. Pletcher, *J. Chem. Soc., Dalton Trans.* (1978) 972.
- [3] K. P. Healy, D. Pletcher, *J. Organomet. Chem.* 186 (1980) 401.
- [4] C. Gosden, J. B. Kerr, D. Pletcher, R. Rosas, *J. Electroanal. Chem. Interfacial Electrochem.* 117 (1981) 101.
- [5] C. E. Dahm, D. G. Peters, *J. Electroanal. Chem. Interfacial Electrochem.* 406 (1996) 119.
- [6] M. Mathew, G. J. Palenic, G. R. Clark, *J. Inorg. Chem.* 12 (1973) 346.
- [7] R. H. Holm, M. J. O. Conner, *Inorg. Chem.* 14 (1971) 408.
- [8] P. Bindu, M. R. P. Kurup, *Ind. J. Chem.* 36A (1997) 1094.
- [9] J. C. Donini, Hellebone, A. B. P. Lever, *J. Am. Chem. Soc.*, 93 (1971) 6455.
- [10] R. D. Bereman, G. D. Shields, *Inorg. Chem.*, 18 (1979) 946.
- [11] S. Balasubramanian, C. N. Krishnan, *Polyhedron*, 5 (1986) 669.
- [12] M. A. Ali, S. E. Livingstone, D. J. Phillips, *Inorg. Chim. Acta*, 6 (1972) 39.
- [13] R. Pestorek, Z. Travnicek, E. Kvapilova, Z. Sindelar, F. Brezina, J. Marec, *Polyhedron*, 18 (1998) 151.

- [14] R. A. Eittah, M. Hamed, S. El. Makabaty, *Trans. Met. Chem.* 8 (1983) 198.
- [15] S. K. Jain, B. S. Garg, Y. K. Bhoon, *Trans. Met. Chem.* 12 (1987) 73.
- [16] A. Sreekanth, S. Sivakumar, M. R. P. Kurup, *J. Mol. Struct.* 655 (2003) 47.
- [17] B. S. Garg, M. R. P. Kurup, S. K. Jain, Y. K. Bhoon, *Transition Met. Chem.* 16 (1991) 111.
- [18] N. C. Kasuga, K. Sekino, C. Koumo, N. Shimada, M. Ishikawa, K. Nomiya, *J. Inorg. Biochem.* 84 (2001) 55.
- [19] R. L. Dutta, A. Syamal, *Elements of Magnetochemistry*, 2nd edn. Affiliated East-West Press, Pvt. Ltd (1993).
- [20] C. Spinu, A. Kriza, *Açta Chim. Slov.* 47 (2000) 179.



SYNTHESIS, SPECTRAL CHARACTERIZATION AND BIOLOGICAL INVESTIGATIONS OF ZINC(II) COMPLEXES OF SOME ACID HYDRAZONES

7.1. Introduction

Zinc is an essential element in all-living systems and plays a structural role in many proteins and enzymes. It is recognized that transcription factors regulate gene expression and essential features is binding to the regulatory protein in the recognition sequence of gene. Many proteins have been found to have zinc containing motif that serves to bind DNA embedded in their structure. In the relevance of zinc to diabetic mellitus, zinc is known to present in insulin, coordinated by three nitrogen atom from histidine and three water molecules in an irregular octahedral environment. which is also believed to have a functional structure. Surprisingly zinc is found to have important physiological and pharmaceutical functions involving insulin mimetic activities. In 1980 *Coulston* and *Dandona* first reported the insulin mimetic activity of zinc ions [1]. Current state of development of insulin mimetic zinc complexes with different coordination sites and their possible mechanism were reviewed by *Sakurai et al.* [2]. The analytical or structural role of zinc atom in biological system is found to be connected with following features [3].

- The ready formation of low coordination number sites which are more strongly acidic than high coordination number sites.
- The easy deformation of geometry of the ligand in the coordination sphere with subsequent change in coordination number from four to five to six.
- Relatively rapid exchange of ligand in the complexes.

- Absence of redox chemistry.

This chapter consists of the syntheses of four zinc(II) complexes of four different acid hydrazones and their characterization using different spectral techniques, like electronic spectra, IR spectra and ^1H NMR spectra. The hydrazones used for the syntheses are H_2L^1 , H_2L^2 , H_2L^5 and H_2L^6 .

7.2. Experimental

7.2.1 Materials

Zinc(II) acetate dihydrate (S. D. Fine) was of Analar grade and used without further purification. All the solvents were dried using standard methods before use.

7.2.2 Syntheses of the complexes

The complexes $\text{ZnL}\cdot\text{H}_2\text{O}$, where L is the dianion of different acid hydrazone, were prepared as follows. To a hot ethanolic solution of H_2L (1 mmol), hot ethanol solution of zinc(II) acetate dihydrate (1 mmol) in ethanol was added. Resultant homogeneous yellow solution was stirred for 2-6 h. The yellow product formed was filtered and washed with hot ethanol, followed by ether, and dried *in vacuo* over P_4O_{10} .

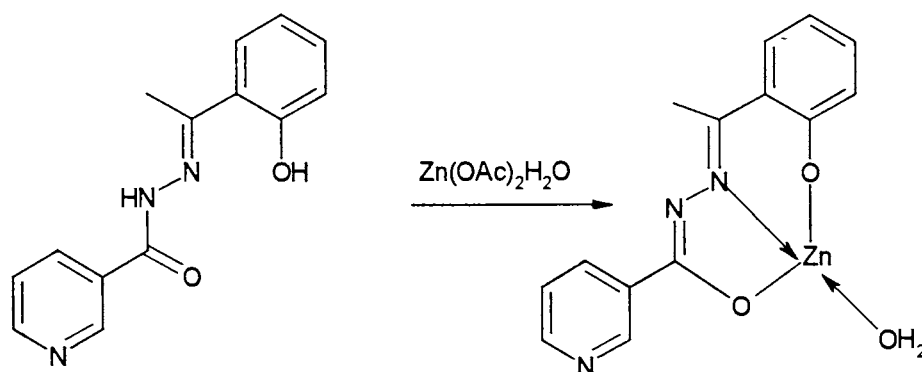


Fig. 1. Scheme of the synthesis of zinc(II) complexes

7.3. Results and discussion

7.3.1. Syntheses of the zinc(II) complexes

The colors, elemental analyses, stoichiometries complexes are presented in the Table 1. The elemental analyses data are consistent with the general empirical formula $\text{ZnL} \cdot \text{H}_2\text{O}$ for the all complexes. The ligand H_2L gets deprotonated and coordinated as L^{2-} . The fourth position is occupied by one molecule of water. The complexes are insoluble in most of the common polar and non polar solvents. They are partially soluble in DMF and DMSO. The conductivity measurements in DMF showed that all the complexes are non-electrolytes. All the compounds are diamagnetic in nature.

Table 1. Colours, empirical formula and elemental analyses of zinc(II) complexes

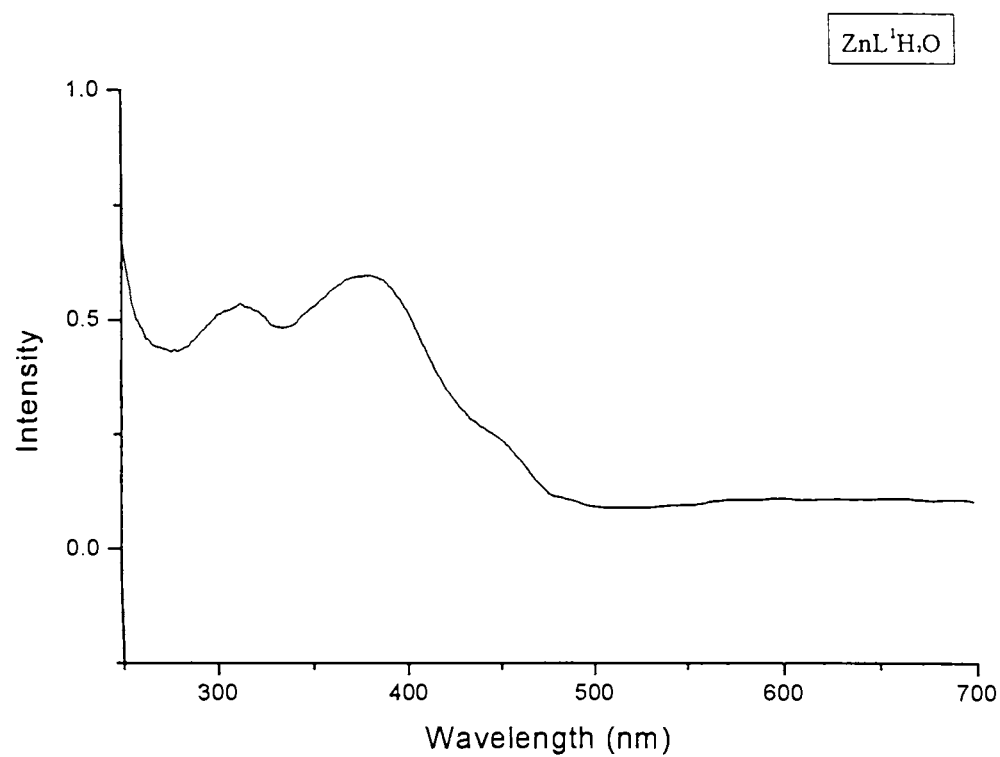
| Compound | Colour | Analytical data found (calculated) | | |
|-----------------------------------|---------------|------------------------------------|-------------|------------------|
| | | C % | H % | N % |
| ZnL ¹ H ₂ O | Bright yellow | 52.28 (51.87) | 3.76 (3.94) | 8.71 (9.21) |
| ZnL ² H ₂ O | Bright yellow | 49.95 (50.33) | 3.89 (3.76) | 12.48 (12.87) |
| ZnL ⁵ H ₂ O | Bright yellow | 48.39 (48.95) | 3.44 (3.63) | 13.02 (12.85) |
| ZnL ⁶ H ₂ O | Bright yellow | 53.67 (54.02) | 4.20 (4.32) | 8.35 (8.20) |

7.3.2. Electronic spectral studies

The electronic spectra of the all complexes were recorded in solid state. The spectra showed $\pi \rightarrow \pi^*$ transition and $n \rightarrow \pi^*$ transitions at ~ 35000 and ~ 32000 cm^{-1} . The complexes showed there is no appreciable absorption at ~ 21000 cm^{-1} which is in accordance with d^{10} electronic configuration. The moderately intense bands at ~ 25000 cm^{-1} , are assigned to LMCT of zinc(II) complexes [4].

Table 2. Selected infrared frequencies of the zinc(II) complexes.

| Compound | $\pi \rightarrow \pi^*$ | $n \rightarrow \pi^*$ | LMCT |
|-----------------------------------|-------------------------|-----------------------|--------------|
| ZnL ¹ H ₂ O | 33300 | 26317 | 22222 |
| ZnL ² H ₂ O | 32459 | 29429, 26110 | 20000, 23122 |
| ZnL ³ H ₂ O | 34210 | 25316 | 20480 |
| ZnL ⁶ H ₂ O | 31134 | 28166 | 21876 |

Fig. 2. Electronic spectrum of ZnL¹H₂O

7.3.3. IR spectral studies

The coordination sites of the ligands while complexation were assigned on the basis of the comparative infrared spectral analyses of the ligand and the complexes. The coordination takes place through the deprotonated phenolic oxygen, azomethine nitrogen and oxygen from the hydrazide moiety, by enolisation followed by deprotonation. The presence of water molecule in the coordination sphere is confirmed by a broad peak at $\sim 3400\text{ cm}^{-1}$, in the spectrum of the complexes.

Compound, H_2L^1 , H_2L^2 , H_2L^5 and H_2L^6 show a sharp band $\sim 3100\text{ cm}^{-1}$, which is due NH stretching vibration. These bands are absent in complexes, which suggests enolisation of the carbonyl group, followed by deprotonation. IR spectra of complexes show sharp band $\sim 1525\text{ cm}^{-1}$ due to newly formed N=C bond indicating the coordination of hydrazones take place in the form of enol rather than as keto form. Further proof for the complexation for enol oxygen is obtained from the appearance of a new band $\sim 565\text{ cm}^{-1}$ which is assignable for the $\nu(\text{Zn-O})$ for the complexes. The lowering of the band approximately 1610 cm^{-1} (C=N) by $\sim 20\text{ cm}^{-1}$, is explicit evidence for coordination of the hydrazone through the azomethine nitrogen, which is supported by the new band at $\sim 455\text{ cm}^{-1}$ in the complexes which are assigned to Zn-N. The increase in (N-N) in the spectra of complexes is due to the increase in the double bond character offsetting the loss of electron density via donation to metal and is a confirmation of the coordination of the ligand through azomethine nitrogen. The loss of OH proton indicated by the absence of the band at $\sim 3400\text{ cm}^{-1}$ in the complexes. The spectrum of the complexes exhibit a symmetric shift in the position of the band in the region $1600\text{-}1350\text{ cm}^{-1}$ due to C=C and C=N vibrational modes and their mixing patterns are different from those present in ligands spectra. Presence of a broad band at $\sim 3450\text{ cm}^{-1}$ confirms the presence of water molecule in the coordination sphere [5].

Table 3. Selected IR frequencies of ligands and manganese(II) complexes (cm^{-1})

| Compound | $\nu_{\text{C=N}}$ | $\nu_{\text{N=N}}$ | $\nu_{\text{N=C}}$ | $\nu_{\text{C-O}}$ | Zn-O | Zn-N |
|----------------------------------|--------------------|--------------------|--------------------|--------------------|------|------|
| H_2L^1 | 1620 | 1001 | 1523 | | | |
| $\text{ZnL}^1\text{H}_2\text{O}$ | 1594 | 1024 | 1534 | 1344, 1431 | 554 | 459 |
| H_2L^2 | 1603 | 998 | 1513 | | | |
| $\text{ZnL}^2\text{H}_2\text{O}$ | 1598 | 1025 | 1524 | 1354, 1431 | 572 | 467 |
| H_2L^5 | 1609 | 1010 | 1510 | | | |
| $\text{ZnL}^5\text{H}_2\text{O}$ | 1595 | 1034 | 1518 | 1348, 1459 | 586 | 448 |
| H_2L^6 | 1615 | 1002 | 1530 | | | |
| $\text{ZnL}^6\text{H}_2\text{O}$ | 1600 | 1033 | 1541 | 1343, 1449 | 556 | 454 |

7.3.4. ^1H NMR spectral studies

The spectra were recorded at 500 MHz. The signals at $\delta \sim 13$ ppm and $\delta \sim 11$ ppm which represent OH and NH respectively in uncomplexed ligands are absent in complexes, which is an evidence for the coordination of the ligands as doubly deprotonated anions.

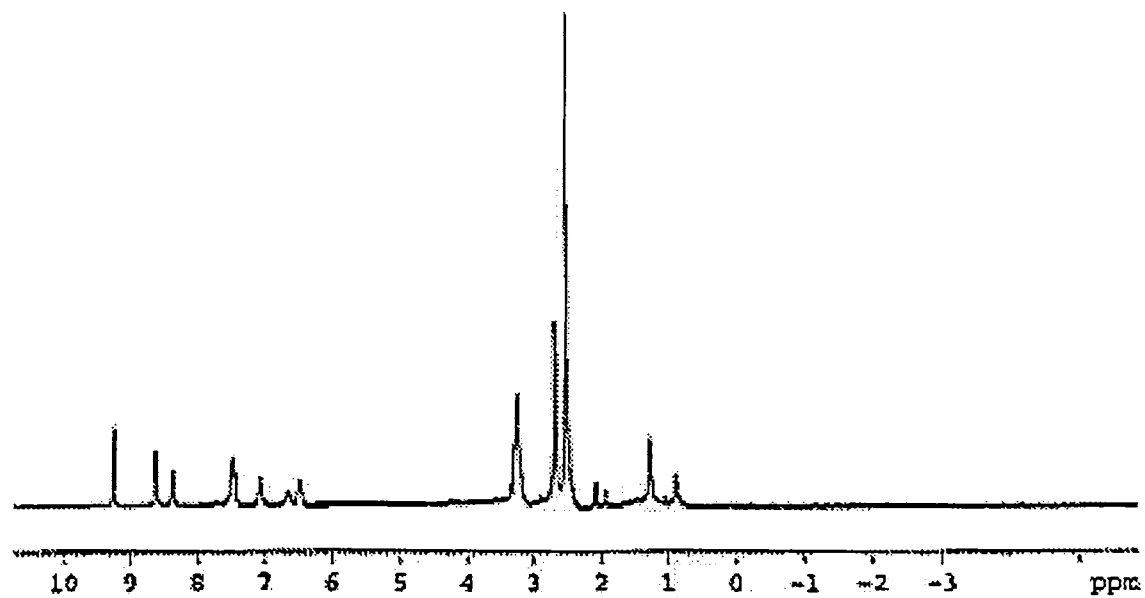


Fig. 3. ^1H NMR spectrum of $\text{ZnL}^2\text{H}_2\text{O}$

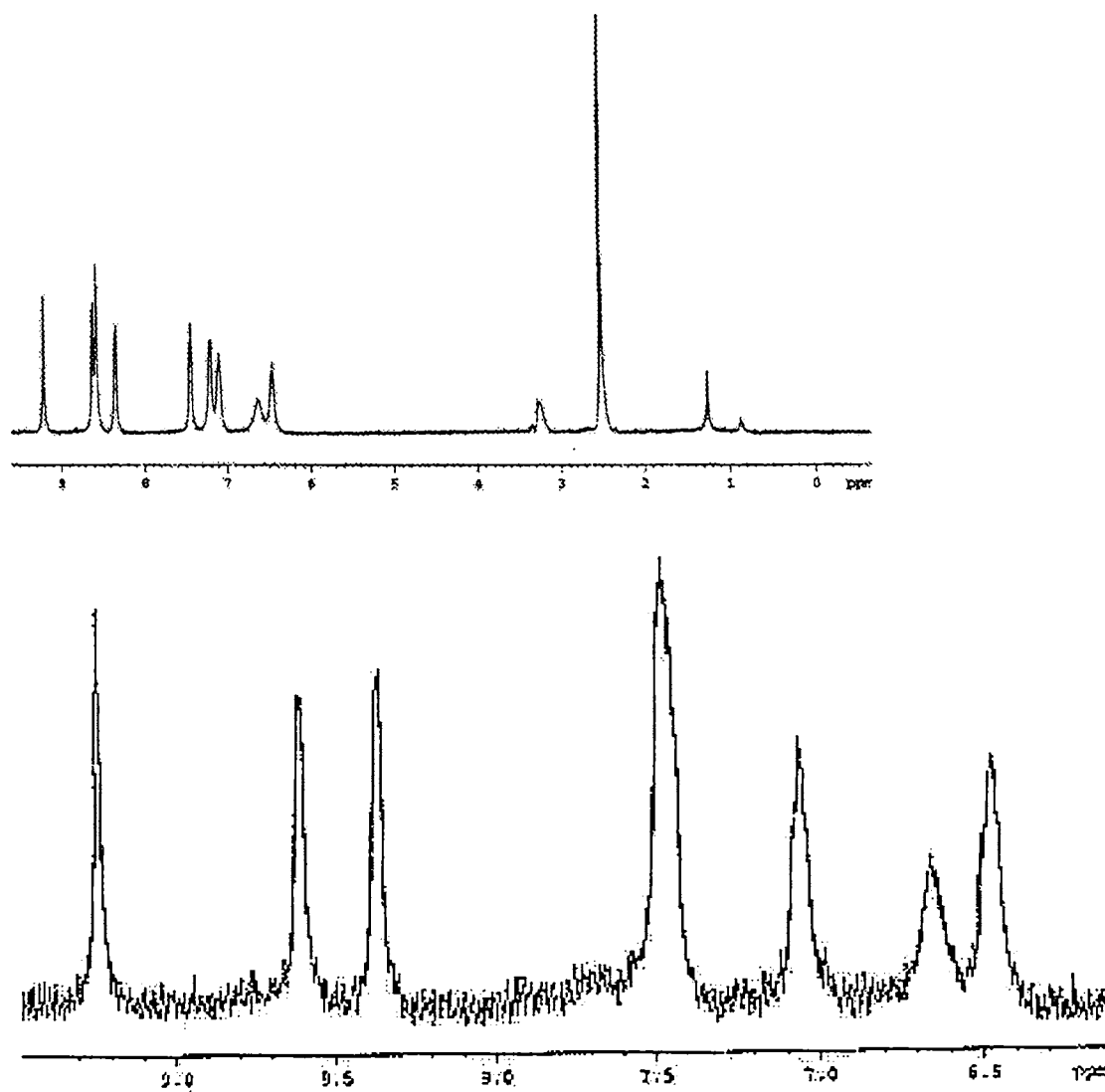


Fig. 4. ^1H NMR spectrum of $\text{ZnL}^5\text{H}_2\text{O}$

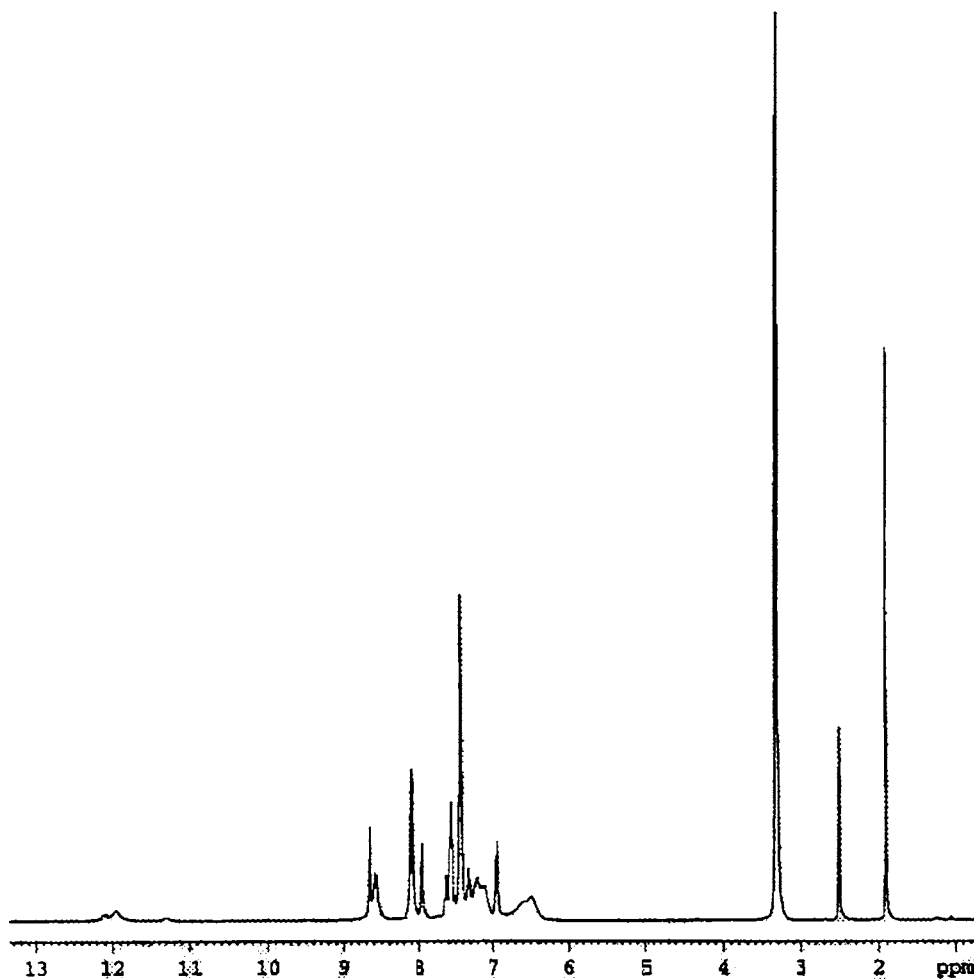


Fig. 5. ^1H NMR spectrum $\text{ZnL}^6\text{H}_2\text{O}$

7.3.6. *Biological activity studies*

All the synthesized complexes were tested for their antimicrobial activity. The antimicrobial agent may be either bacteriostatic or bactericidal. The effectiveness of an antimicrobial agent in sensitivity testing is based on the size of the zones of inhibition. When the test substances are introduced on to a lawn of bacterial culture by disc diffusion method. The disc diffusion method was used for screening

for the antimicrobial property of the test samples. The active diameter around the discs was below 8 mm. All the four zinc(II) complexes showed no or little activity against both the Gram positive and Gram negative bacteria.

Concluding Remark

Four zinc(II) complexes were synthesized using zinc(II) acetate and four different acid hydrazones namely salicylaldehyde benzoic acid hydrazone (H_2L^1), 2-hydroxyacetophenone nicotinic acid hydrazone (H_2L^2), salicylaldehyde nicotinic acid hydrazone (H_2L^3) and 2-hydroxyacetophenone benzoic acid hydrazone (H_2L^4) and characterized by different spectral analyses like infrared, 1H NMR and electronic spectral analyses. All the compounds were screened for biological activities and found to be inactive against all the *Gram Positive* and *Gram Negative* bacteria.

References

- [1] L. Coulston, P. Dandona, *Diabetes*, 29 (1980) 665.
- [2] H. Sakurai, Y. Kojima, Y. Yoshikawa, K. Kawabe, H. Yasui, *Coord. Chem. Rev.* 226 (2002) 187.
- [3] R. P. J. Williams, *Endeavour, New. Ser.* 8 (1984) 2.
- [4] A. Sreekanth, S. Sivakumar, M. R. P. Kurup, *J. Mol. Struct.* 655 (2003) 47.
- [5] G. C. Percy, D. A. Thornton, *J. Inorg. Nuclear Chem.* 34 (1972) 3351.

SUMMARY AND CONCLUSION OF THE WORK

The thesis entitled “*Synthesis, spectral characterization, structural studies and biological investigations of transition metal complexes of some acid hydrazones*” deals with the syntheses and the spectral characterization of six substituted acid hydrazones and their coordination compounds of different transition metals like copper(II), oxovanadium(IV), manganese(II), nickel(II) and zinc(II). It also discusses the biological screening tests for all the acid hydrazones and the complexes with five microorganisms. The thesis is divided in to seven chapters.

Chapter 1.

This chapter deals with the brief review on acid hydrazones and their structural and stereochemical properties and different coordination modes. This also gives a brief account of their transition metal complexes and objectives of the present studies. Various techniques used to elucidate the bonding structure and stereochemistry of the ligands and the complexes prepared are also included in this chapter.

Chapter 2.

This chapter deals with the syntheses and spectral characterization of six acid hydrazones derived from different acid hydrazide and ketones/aldehydes, namely

Salicylaldehyde benzoic acid hydrazone (H_2L^1)

2-Hydroxyacetophenone nicotinic acid hydrazone (H_2L^2)

2-Methoxybenzaldehyde nicotinic acid hydrazone (HL^3)

2-Hydroxyacetophenone 4-hydroxybenzoic acid hydrazone (H_2L^4)

Salicylaldehyde nicotinic acid hydrazone (H_2L^5)

2-Hydroxyacetophenone benzoic acid hydrazone (H_2L^6)

All these acid hydrazones have substitution at the second position of the ketonic/aldehydic part. Complete NMR assignments for one hydrazone was made using COSY homonuclear and HMQC heteronuclear correlation techniques. Single crystal X-ray crystal studies for H_2L^2 were done, and the compound crystallizes into an orthorhombic lattice with a non-centrosymmetric space group $Pca2_1$ with two crystallographically unique molecules in an asymmetric unit.

Chapter 3.

This chapter deals with the detailed preparative and physicochemical studies of two new heterocyclic base adducts of copper(II) complexes of general formula $CuLB$, where L is the dianion of 2-hydroxyacetophenone 4-hydroxybenzoic acid hydrazone (H_2L^4) and B is the heterocyclic base, 2, 2' bipyridine (bipy) or 1, 10 phenanthroline (phen), have been synthesized and characterized by different physicochemical methods. The molar conductivity measurements in DMF solution indicate the non-electrolyte nature of both complexes. The electronic and IR spectroscopic data indicate that the complexes have square pyramidal geometry with one dibasic tridentate ligand L^{2-} , and one bidentate heterocyclic base. The coordination takes place through the deprotonated hydroxyl group, azomethine nitrogen and oxygen from the hydrazide moiety. The magnetic susceptibility values at room temperature are consistent with the spin only value for monomeric copper(II) species without any copper-copper interactions. EPR studies of all compounds gave axial spectra. Simulation of EPR spectra gave the correct values for g and A for each compound. The g values indicate that the unpaired electron resides in the $d_{x^2-y^2}$ orbital. The crystal and molecular structure of CuL^4phen was

determined by single crystal X-ray diffraction method. The compound crystallizes into monoclinic lattice with space group $P2_1/c$. Investigations on antimicrobial activities showed that they are moderately active against *Gram negative* bacteria. The electrochemical analysis showed that the Cu(II)/Cu(I) system is reversible.

Chapter 4.

This chapter deals with syntheses, spectral characterization and biological investigation of oxovanadium(IV) complexes. An interesting series of heterocyclic adduct of oxovanadium(IV) complexes have been synthesized by the reaction of vanadium(IV) oxide acetylacetonate with some hydrazones in presences of heterocyclic base, 2,2'-bipyridine and characterized by analytical and different techniques, like IR, far IR, EPR and UV-Vis spectral studies and magnetic studies. The acid hydrazones used for the syntheses are H_2L^1 , H_2L^2 , H_2L^4 and H_2L^5 . the magnetic measurement showed all the complexes are paramagnetic and the values lie at ~ 1.7 BM, suggest mononuclear oxovanadium(IV) with no vanadium vanadium interactions. The EPR spectra indicate the presence of free electron in the d_{xy} orbital. The coordination geometry around oxovanadium(IV) in all complexes are octahedral with one dibasic tridentate ligand L^{2-} , and one bidentate heterocyclic base. The coordination takes place through the deprotonated hydroxyl group, azomethine nitrogen and oxygen from the hydrazide moiety. And the oxygen of the oxovanadium species occupies the sixth position of the octahedron. All electronic transitions were assigned. The values are consistent with distorted octahedral structure. All the compounds are paramagnetic. EPR studies of all compounds gave axial spectra and the bonding parameters are calculated for all the compounds. The antimicrobial studies showed all the complexes are moderately active against all the microorganisms under study.

Chapter 5.

An interesting series of binary complexes manganese(II) have been synthesized by the reaction of manganese(II) acetate dihydrate and four different acid hydrazones namely H_2L^2 , H_2L^3 , H_2L^5 and H_2L^6 , in appropriate conditions and characterized by analytical and different spectral techniques, like IR, far IR, EPR and UV-Vis spectral studies and magnetic studies. All the compounds are paramagnetic and the magnetic moment were ~ 5.9 BM, which are consistent with the mononuclear high spin manganese(II) central metal ion without any manganese manganese interactions. EPR studies of all compounds gave axial spectra The spectra indicate all the complexes have a distorted octahedral geometry The coordination takes place through the phenolic/methoxy oxygen, azomethine nitrogen and oxygen from the hydrazide moiety. All electronic transitions were assigned. The values are consistent with distorted octahedral structure. All the four manganese(II) complexes were showed no or little activity against both the *Gram positive* and *Gram negative* bacteria.

Chapter 6.

An interesting series of heterocyclic adduct of nickel(II) complexes have been synthesized by the reaction of nickel(II) acetate with some hydrazones in presences of heterocyclic bases like 2,2'-bipyridine and 1,10-phenanthroline and characterized by analytical and different spectral techniques, like IR, far IR, and UV-Vis spectral studies and magnetic studies. The coordination geometry around nickel(II) in all complexes except for $Ni(II)L^2.H_2O$ are octahedral with one dibasic tridentate ligand L^{2-} , and one bidentate heterocyclic base. A water molecule occupies the sixth position. The coordination takes place through the deprotonated hydroxyl group azomethine nitrogen and oxygen from the hydrazide moiety. All electronic transitions were assigned. The values are consistent with pseudo-octahedral structure. All the compounds are paramagnetic The paramagnetic property of four coordinated nickel(II) system is because of the spin cross over

phenomenon. Antimicrobial studies showed that all the eight nickel(II) complexes were showed no or little activity against both the *Gram positive* and *Gram negative bacteria*.

Chapter 7.

An interesting series zinc(II) complexes have been synthesized by the reaction of zinc(II) acetate with some hydrazones and characterized by analytical and different spectral techniques, like ^1H NMR, IR, far IR, and UV-Vis spectral studies. All complexes square planar with one dibasic tridentate ligand L^{2-} and one water molecule in the coordination sphere. The coordination takes place through the deprotonated hydroxyl group azomethine nitrogen and oxygen from the hydrazide moiety. All electronic transitions were assigned. Antimicrobial studies showed that all the four zinc(II) complexes were showed no or little activity against both the *Gram positive* and *Gram negative bacteria*.